MONOGRAPH

No. 34

2009

Jukka Seppälä

Fluorescence properties of Baltic Sea phytoplankton

MONOGRAPHS of the

Boreal Environment Research

34

Jukka Seppälä

Fluorescence properties of Baltic Sea phytoplankton

Yhteenveto: Itämeren kasviplanktonin fluoresenssiominaisuudet

The publication is available in the internet:
www.enviroment.fi/publications

Contents

List of original articles and author's contribution

I Seppälä J, Balode M (1998) The use of spectral fluorescence methods to detect changes in the phytoplankton community. *Hydrobiologia* 363: 207-217

II Babichenko S, Leeben A, Poryvkina L, Shalapyonok A, Seppälä J (2001) Variability of *Chlorella* sp. fluorescence in response to different nitrogen conditions. *International Journal of Remote Sensing* 22: 403-414

III Raateoja M, Seppälä J, Kuosa H (2004) Bio-optical modeling of primary production in SW Finnish coastal zone, Baltic Sea: fast repetition rate fluorometry in Case 2 waters. *Marine Ecology Progress Series* 267: 9-26

IV Raateoja M, Seppälä J, Ylöstalo P (2004) Fast repetition rate fluorometry is not applicable to studies of filamentous cyanobacteria from the Baltic Sea. *Limnology and Oceanography* 49: 1006-1012

V Seppälä J, Ylöstalo P, Kuosa H (2005) Spectral absorption and fluorescence characteristics of phytoplankton in different size fractions across the salinity gradient in the Baltic Sea. *International Journal of Remote Sensing* 26: 387-414

VI Seppälä J, Ylöstalo P, Kaitala S, Hällfors S, Raateoja M, Maunula P (2007) Ship-of-opportunity based phycocyanin fluorescence monitoring of the filamentous cyanobacteria bloom dynamics in the Baltic Sea. *Estuarine, Coastal and Shelf Science* 73: 489-500

VII Seppälä J, Olli K (2008) Multivariate analysis of phytoplankton spectral *in vivo* fluorescence: estimation of phytoplankton biomass during a mesocosm study in the Baltic Sea. *Marine Ecology Progress Series* 370: 69-85

Article I. Seppälä planned the experiment, collected field samples, carried out analyses onboard, analysed the data and wrote the article. Balode counted phytoplankton samples, and commented the taxonomic part of the article.

Article II. Experiments were planned and carried out together by all authors, Seppälä participating especially in the *Chlorella* experiment. Babichenko, Leeben and Poryvkina wrote the article, with contributions from Seppälä and Shalapyonok in the interpretation of fluorescence data.

Article III. Raateoja and Seppälä planned and carried out the experiment and analysed the data together. Seppälä was responsible for Chl*a* analyses, spectral and radiometric measurements. Raateoja was responsible for productivity and variable fluorescence measurements and primary production modelling. Raateoja wrote the article, with contributions from Seppälä especially in the spectral part. Kuosa contributed in the algal ecological part of the article.

Article IV. Seppälä, Raateoja, and Ylöstalo planned and carried out the experiment together. Seppälä was responsible for cultures, and spectrofluorometric measurements, Raateoja was responsible for FRRF measurements, and Ylöstalo was responsible for absorption measurements. Data was analysed and article was written together, Raateoja having main responsibility.

Article V. Seppälä and Ylöstalo planned and carried out the experiment together. Seppälä was responsible for analyses, except Kuosa carried out picophytoplankton counts. Data was analysed together by Seppälä and Ylöstalo. Seppälä wrote the article, with substantial contributions from Ylöstalo. Kuosa contributed in the taxonomical parts of the article.

Article VI. Seppälä planned the experiment together with Ylöstalo, Raateoja and Kaitala. Ylöstalo performed the initial instrument tests together with Seppälä. Seppälä performed the reference measurements with cultures. Seppälä, Maunula, Ylöstalo and Raateoja did onboard PC-fluorometer maintenance. Hällfors counted phytoplankton samples, and commented the taxonomic part of the article. Seppälä analysed the data and wrote the article with contributions from Kaitala, Ylöstalo and Raateoja.

Article VII. Seppälä planned the experiment, collected field samples, carried out analyses, analysed the data and wrote the article. Olli counted phytoplankton samples, and commented the taxonomic part of the article.

Abbreviations

Symbol	Definition	Units
Chl$a$	Chlorophyll a	
Chl$b$	Chlorophyll b	
Chl$c$	Chlorophyll c	
APC	Allophycocyanin	
PC	Phycocyanin	
PE	Phycoerythrin	
PEC	Phycoerythrocyanin	
PBS	Phycobilisome	
PSI	Photosystem I	
PSII	Photosystem II	
RCII	Reaction centre of PSII	
DCMU	3-[3,4-dichlorophenyl]-1,1-dimethylurea	
POC	Particulate organic carbon	
PON	Particulate organic nitrogen	
POP	Particulate organic phosphorus	
[Chl$a$]	Chl$a$ concentration	mg m^{-3}
d	Diameter of spherical cells	µm
c_i	Intracellular Chl$a$ concentration	kg m^{-3}
λ	Wavelength	nm
q	Light quantum	
E_0	Irradiance	µmol q m^{-2} s^{-1}
PAR	Photosynthetically active radiation (λ = 400-700 nm)	µmol q m^{-2} s^{-1}
c	Velocity of light quanta in vacuum	3×10^{10} cm s^{-1}
h	Planck's constant	6.625×10^{-34} Js
ε	Energy of light quantum	J
F	Fluorescence	µmol q m^{-3} s^{-1} , but often dimensionless
$F(\lambda)$	Spectral fluorescence	dimensionless
$F(\lambda_{ex/em})$	Fluorescence detected using excitation λ = ex and emission λ = em	dimensionless
I , $I(\lambda_{ex})$	Absorption, at excitation λ = ex	µmol q m^{-3} s^{-1}

Symbol	Definition	Units
Φ_F	Quantum yield of fluorescence	Emitted quanta (absorbed quanta)$^{-1}$
k_f	Rate constant of Chl$a$ excited state decay due to fluorescence	s^{-1}
k_d	Rate constant of Chl$a$ excited state decay due to thermal emission	s^{-1}
k_s	Rate constant of Chl$a$ excited state decay due to spill-over	s^{-1}
k_p	Rate constant of Chl$a$ excited state decay due to photochemistry	s^{-1}
R	Chl$a$ specific fluorescence	µmol q s^{-1} mg^{-1}, or dimensionless
$a_p(\lambda)$	Spectral absorption coefficient for particles	m^{-1}
$a_{ph}(\lambda)$	Spectral absorption coefficient for phytoplankton	m^{-1}
$a_{nap}(\lambda)$	Spectral absorption coefficient for non-phytoplankton particles	m^{-1}
$a_{PS}(\lambda)$	Spectral absorption coefficient for photosynthetically usable light of phytoplankton	m^{-1}
$a_{PSII}(\lambda)$	Spectral absorption coefficient for PSII	m^{-1}
$a_{PSI}(\lambda)$	Spectral absorption coefficient for PSI	m^{-1}
$a_{PP}(\lambda)$	Spectral absorption coefficient for photoprotective pigments	m^{-1}
$a*_{ph}(\lambda)$	Spectral Chl$a$-specific absorption coefficient for phytoplankton	m^2 (mg Chl$a$)$^{-1}$
$\bar{a}_{ph}*$	Spectrally averaged Chl$a$-specific absorption coefficient for phytoplankton	m^2 (mg Chl$a$)$^{-1}$
$a_{PSII}*(\lambda)$	Chl$a$-specific absorption coefficient of PSII	m^2 (mg Chl$a$)$^{-1}$
$\bar{a}_{PSII}*$	Spectrally averaged Chl$a$-specific absorption coefficient for PSII	m^2 (mg Chl$a$)$^{-1}$
$a_{sol}*(\lambda)$	Theoretical spectral Chl$a$-specific absorption coefficient of phytoplankton material in solution	m^2 (mg Chl$a$)$^{-1}$
$Q_a*(\lambda)$	Specific absorption efficiency	dimensionless
$Q_a(\lambda)$	Efficiency factor for light absorption	dimensionless
ρ'	Absorption index	dimensionless
F_0	Minimum fluorescence of dark-acclimated cells	dimensionless
F_M	Maximum fluorescence of dark-acclimated cells	dimensionless
F_V	($F_M - F_0$), variable fluorescence of dark-acclimated cells	dimensionless
$F_V/F_M, \Phi_P^{max}$	Maximum quantum yield of PSII photochemistry	dimensionless
F_S	Steady state fluorescence in actinic light	dimensionless
F_M'	Maximum fluorescence in actinic light	dimensionless
$(F_M'-F_S)/F_M'$	Photochemical efficiency in actinic light	dimensionless
n_{PSII}	Number of photosynthetic units	q (mg Chl$a$)$^{-1}$
σ_{PSII}	Effective PSII absorption cross section of dark-acclimated cells	Å^2 q^{-1} or m^2 q^{-1}
σ_{PSII}'	Absorption cross section in ambient light	Å^2 q^{-1} or m^2 q^{-1}
$\bar{\sigma}_{PSII}^{opt}$	Spectrally averaged optical cross-section of PSII	m^2 q^{-1}
EEM	Excitation-emission fluorescence matrix	
FRRF	Fast repetition rate fluorometry	
PAM	Pulse amplitude modulation	
mp	Match-point wavelength in the no-overshoot method to determine $a_{PSII}(\lambda)$	
sc	Scaling factor between $a_{PS}(\lambda)$ and $a_{PSII}(\lambda)$ at $\lambda = mp$	

Symbol	Definition	Units
PCA	Principal component analysis	
PCR	Principal component regression	
PLS	Partial least squares	
n	Number of analytes	
l	Number of samples	
m	Number of wavelengths	
f	Number of factors in PCA	
R	Matrix (*l by m*) of spectral responses	
C	Matrix (*l by n*) of analyte concentrations	
K	Matrix (*n by m*) of calibration constants in **K**-matrix approach	
P	Matrix (*m by n*) of calibration constants in **P**-matrix approach	
$\mathbf{E}_k$	Error matrix (*l by m*) in **K**-matrix approach	
$\mathbf{E}_r$	Error matrix (*l by n*) in **P**-matrix approach	
$\mathbf{F}, \mathbf{F}_R, \mathbf{F}_C$	Matrices (*f by m*) of factors in PCA and PLS	
$\mathbf{S}, \mathbf{S}_R, \mathbf{S}_C$	Matrices (*l by f*) of scores in PCA and PLS	

Fluorescence properties of Baltic Sea phytoplankton

Jukka Seppälä

Department of Biological and Environmental Sciences, Faculty of Biosciences, University of Helsinki, Finland

To obtain data on phytoplankton dynamics (abundance, taxonomy, productivity, and physiology) with improved spatial and temporal resolution, and at reduced cost, traditional phytoplankton monitoring methods have been supplemented with optical approaches. Fluorescence detection of living phytoplankton is very sensitive and not disturbed much by the other optically active components. Fluorescence results are easy to generate, but interpretation of measurements is not straightforward as phytoplankton fluorescence is determined by light absorption, light reabsorption, and quantum yield of fluorescence - all of which are affected by the physiological state of the cells. In this thesis, I have explored various fluorescence-based techniques for detection of phytoplankton abundance, taxonomy and physiology in the Baltic Sea.

In algal cultures used in this thesis, the availability of nitrogen and light conditions caused changes in pigmentation, and consequently in light absorption and fluorescence properties of cells. The variation of absorption and fluorescence properties of natural phytoplankton populations in the Baltic Sea was more complex. Physical environmental factors (e.g. mixing depth, irradiance and temperature) and related seasonal succession in the phytoplankton community explained a large part of the seasonal variability in the magnitude and shape of Chlorophyll *a* (Chl*a*)-specific absorption. Subsequent variations in the variables affecting fluorescence were large; 2.4-fold for light reabsorption at the red Chl*a* peak and 7-fold for the spectrally averaged Chl*a*-specific absorption coefficient for Photosystem II. In the studies included in this thesis, Chl*a*-specific fluorescence varied 2-10 fold. This variability in Chl*a*-specific fluorescence was related to the abundance of cyanobacteria, the size structure of the phytoplankton community, and absorption characteristics of phytoplankton.

Cyanobacteria show very low Chl*a*-specific fluorescence. In the presence of eukaryotic species, Chl*a* fluorescence describes poorly cyanobacteria. During cyanobacterial bloom in the Baltic Sea, phycocyanin fluorescence explained large part of the variability in Chl*a* concentrations. Thus, both Chl*a* and phycocyanin fluorescence were required to predict Chl*a* concentration.

Phycobilins are major light harvesting pigments for cyanobacteria. In the open Baltic Sea, small picoplanktonic cyanobacteria were the main source of phycoerythrin fluorescence and absorption signal. Large filamentous cyanobacteria, forming harmful blooms, were the main source of the phycocyanin fluorescence signal and typically their biomass and phycocyanin fluorescence were linearly related. It was shown that for reliable phycocyanin detection, instrument wavebands must match the actual phycocyanin fluorescence peak well. In order to initiate an operational ship-of-opportunity monitoring of cyanobacterial blooms in the Baltic Sea, the distribution of filamentous cyanobacteria was followed in 2005 using phycocyanin fluorescence.

Various taxonomic phytoplankton pigment groups can be separated by spectral fluorescence. I compared multivariate calibration methods for the retrieval of phytoplankton biomass in different taxonomic groups. During a mesocosm experiment, a partial least squares regression method gave the closest predictions for all taxonomic groups, and the accuracy was adequate for phytoplankton

bloom detection. This method was noted applicable especially in the cases when not all of the optically active compounds are known.

Variable fluorescence has been proposed as a tool to study the physiological state of phytoplankton. My results from the Baltic Sea emphasize that variable fluorescence alone cannot be used to detect nutrient limitation of phytoplankton. However, when combined with experiments with active nutrient manipulation, and other nutrient limitation indices, variable fluorescence provided valuable information on the physiological responses of the phytoplankton community. This thesis found a severe limitation of a commercial fast repetition rate fluorometer, which couldn't detect the variable fluorescence of phycoerythrin-lacking cyanobacteria. For these species, the Photosystem II absorption of blue light is very low, and fluorometer excitation light did not saturate Photosystem II during a measurement.

This thesis encourages the use of various *in vivo* fluorescence methods for the detection of bulk phytoplankton biomass, biomass of cyanobacteria, chemotaxonomy of phytoplankton community, and phytoplankton physiology. Fluorescence methods can support traditional phytoplankton monitoring by providing continuous measurements of phytoplankton, and thereby strengthen the understanding of the links between biological, chemical and physical processes in aquatic ecosystems.

Itämeren kasviplanktonin fluoresenssiominaisuudet

Jukka Seppälä

Department of Biological and Environmental Sciences, Faculty of Biosciences, University of Helsinki, Finland

Optiset automaattilaitteet tarjoavat kustannustehokkaan sekä ajallisesti ja paikallisesti hyvin kattavan tavan seurata planktonlevien määrää, levälajiston koostumusta, levätuotantoa, ja leväsolujen fysiologista tilaa. Elävien planktonlevien fluoresenssiin perustuva mittausmenetelmä on hyvin tarkka ja muut optisesti aktiiviset veden ainesosat eivät häiritse mittausta. Fluoresenssimittausten tulosten tulkintaa hankaloittaa kuitenkin planktonlevien fluoresenssin voimakkuuteen vaikuttavat leväsolujen valon absorption määrä, fluoresoidun valon uudelleenabsorptio, ja fluoresenssin kvanttisaanto. Nämä tekijät vaihtelevat planktonleväsolujen fysiologisen tilan muuttuessa. Tässä väitöskirjatyössä olen selvittänyt erilaisten fluoresenssimenetelmien käyttöä planktonlevien määrän, levälajiston vaihtelun ja fysiologisen tilan mittaamisessa Itämerellä.

Leväviljelmiä käyttäen havaitsin, että typen saatavuus ja valaistus vaikuttivat leväsolujen pigmentaatioon, sekä absorptio- ja fluoresenssiominaisuuksiin. Itämeressä luonnon planktonleväyhteisöjen absorptio- ja fluoresenssiominaisuuksien vaihtelu oli mutkikkaampaa. Fysikaaliset ympäristötekijät (sekoittuvan vesikerroksen syvyys, auringon säteilyn määrä, ja lämpötila) ja

kasviplanktonyhteisöjen vuosisukkessio selittivät suuren osan *a*-klorofyllin spesifisen absorption voimakkuudesta ja spektraalisesta vaihtelusta. Tutkimuksissani Itämerellä planktonlevien *a*-klorofyllin spesifinen fluoresenssi vaihteli 2-10 – kertaisesti, ja fluoresenssin määrä ei siis tarkasti kuvaa planktonlevän biomassan määrää. Havaittua vaihtelua selittivät syanobakteerien osuus planktonlevien biomassasta, planktonleväyhteisöjen kokojakauma ja planktonlevien absorptio-ominaisuudet.

Elävien syanobakteerien sisältämän *a*-klorofyllin fluoresenssi on hyvin alhainen. Muiden planktonlevien läsnäollessa *a*-klorofyllin fluoresenssia ei voikaan käyttää syanobakteerien esiintymisen selvittämiseen. Syanobakteerikukintojen aikaan Itämerellä fykosyaniinin fluoresenssi selitti suuren osan *a*-klorofyllin pitoisuuksien vaihtelusta. Tutkimukseni mukaan, luotettavan arvion saaminen Itämeren levämäärästä kesäaikaan vaatiikin *a*-klorofyllin fluoresenssin lisäksi fykosyaniinin fluoresenssin mittaamista.

Fykobiliinit ovat syanobakteerien tärkeimmät fotosynteettiset pigmentit. Avoimella Itämerellä fykoerytriinin fluoresenssin ja absorption määrä liittyi pienikokoisten syanobakteerien esiintymiseen. Fykosyaniinin fluoresenssi oli puolestaan peräisin isoista rihmamaisista syanobakteereista, jotka muodostavat haitallisia kukintoja. Solulaskentojen perusteella arvioidun rihmamaisten syanobakteerien biomassan ja fykosyaniinin fluoresenssin välille saatiin lineaarinen riippuvuussuhde. Väitöskirjatyössäni fykosyaniinin fluoresenssin operatiivinen havainnointi Itämerellä aloitettiin vuonna 2005, ja sen avulla voidaan arvioida syanobakteerikukinnan kehitystä aika- ja tilaskaalalla, mikä ei aikaisemmin ole ollut mahdollista.

Taksonomisia planktonleväryhmiä voidaan tunnistaa fluoresenssisormenjälkien avulla. Väitöskirjatyössäni vertailin monimuuttujamenetelmien soveltuvuutta spektraalisten aineistojen tulkinnassa. Ekosysteemikokeen aikana, tilastollinen korrelaatiomenetelmä (PLS, partial least squares) osoittautui paremmaksi kuin perinteisemmät regressiomenetelmät. Eri leväryhmien erottelu PLS menetelmällä onnistui hyvin ja menetelmän avulla saadaan luotettava kuva eri leväryhmien vuosisukkessiosta ja leväkukinnoista.

Fluoresenssin kvanttisaannon muutosten avulla voidaan tutkia planktonlevien fysiologista tilaa. Tulokseni osoittivat, että Itämerellä tämä menetelmä yksinään ei anna luotettavaa kuvaa planktonlevien ravinnerajoitteisuudesta. Yhdistettynä aktiivisiin ravinnemanipulaatiokokeisiin, ja muihin ravinnerajoitteisuuden indikaattoreihin, menetelmä tarjoaa kuitenkin arvokasta tietoa planktonleväyhteisön fysiologisesta vasteesta ravinnelisäyksiin. Työssä havaittiin lisäksi, että yleisesti käytössä oleva kaupallinen FRR fluorometri ei sovellu Itämeren kukintoja muodostavien rihmamaisten syanobakteerien fysiologian tutkimiseen niiden erikoisen pigmentaation vuoksi. Väitöskirjatyöni osoitti elävien planktonlevien fluoresenssimittausten olevan hyödyllisiä silloin kun halutaan jatkuvatoimisesti havainnoida planktonlevien määrää, syanobakteerien määrää, taksonomisten leväryhmien esiintymistä ja planktonleväsolujen fysiologista tilaa. Automatisoidut fluoresenssimenetelmät tukevat kustannustehokkaasti perinteistä planktonleväseurantaa ja niiden avulla voidaan saada entistä tarkempaa tietoa vesiekosysteemien toiminnan syy-seuraussuhteista.

Asiasanat: *a*-klorofylli, fykosyaniini, pigmentit, planktonlevä, syanobakteeri, Itämeri, spektraalinen fluoresenssi, spektraalinen absorptio, leväfysiologia, ravinnerajoitteisuus, valoakklimaatio, monimuuttujakalibrointi

1 Introduction

The surface of the Earth is largely covered by water (70.8%). Tiny phytoplankton cells, for the most part too small to observe by human eye, populate all illuminated aquatic systems. The first photosynthetic organisms evolved 3.2-2.4 Ga ago. Photosynthesis in the proterozoic ocean, approximately 2.3-2.2 Ga ago, turned the atmosphere oxygenic (Falkowski 2006). Currently, the contribution of phytoplankton to the global carbon fixation, i.e. primary production, is roughly 40-50% (Falkowski & Raven 2007).

Phytoplankton production is the basis of the aquatic food-webs. Seasonal, vertical and horizontal dynamics of phytoplankton, their taxonomic and functional diversity, and their role in nutrient and energy cycles (local and global) are the key topics for ecological aquatic studies. Detection of phytoplankton biomass is approached by various methods. The existing technologies for phytoplankton monitoring range from traditional microscopy to automated discrimination and counting of micrometer–size phytoplankton particles by flow-cytometry, and to observations of ocean colour from space and subsequent calculation of bulk phytoplankton biomass (Cullen et al. 1997, Schofield et al. 1999).

Observing the distribution of phytoplankton is not only an issue for aquatic sciences, but there are increasing societal needs for this information. Aquatic ecosystems are severely threatened by human actions like increased use of resources (e.g. fish), transformation or destroying of natural habitats, pollution by toxic chemicals, and nutrient loads (Vitousek et al. 1997, Elmgren 2001, Lotze et al. 2006). Increase in the frequency of harmful algal blooms in coastal areas and lakes, due to increased eutrophication, has prompted public concern. These blooms impede the use of water bodies for recreation, fisheries, and as drinking water supply (Anderson el al. 2002). Requirements for the understanding of phytoplankton dynamics in a global scale, and related capacity of carbon fixation, have arisen due to the expected global warming and subsequent need to identify the global carbon sources and sinks. Oceans have been major sinks for anthropogenic CO_2 emissions (Raven & Falkowski 1999) and currently there is a debate whether CO_2 sequestration should be enhanced by management actions.

To protect and recover aquatic ecosystems, wise policy decisions for management require high-quality information on the state of environment. The observing systems for oceans, coastal seas, and large lakes need to cover wide areas with sufficient spatial and temporal resolution. Furthermore, the operations must be cost-efficient and involve quick processing of the data. Such requirements are not easily met by traditional methods of water sampling and laboratory analysis. Optical approaches for the detection of phytoplankton, relying on the specific optical signatures of phytoplankton pigments, have been increasingly utilized (Cullen et al. 1997, Schofield et al. 1999, Babin et al. 2005). Optical instruments measuring fluorescence, absorption or scattering signals of phytoplankton can provide large amounts of data. Consequently, a very important, and non-trivial, step is relating the measured optical quantities to the desired products, like the biomass, taxonomy or productivity of phytoplankton.

Fluorometric detection of living phytoplankton has been carried out for more than 40 years (Lorenzen 1966). Various instrumental, methodological and cell physiological aspects have been widely studied. This thesis assesses fluorescence methods for the detection of living phytoplankton in the Baltic Sea. Specifically, I will explore the information content of the fluorometric signal measured with different techniques, and evaluate the limitations and potential of various methods for environmental monitoring. While focusing on the detection of the phytoplankton by fluorescence methods, two key issues must be kept in mind. These are agreeably expressed by Falkowski and Kiefer (1985) "*We should keep in mind that the information obtained by these measurements is fluorescence, not chlorophyll or productivity per se* ", and by Maxwell and Johnson (2000) "*Because it is so easy to generate data with chlorophyll fluorescence, it is also easy to generate large amounts of meaningless data*".

To provide some background, I briefly review the pigmentation of various phytoplankton groups, especially for those groups present in my study area, the Baltic Sea. This is followed by the theoretical basics in light absorption and fluorescence by phytoplankton. Then, to put fluorescence detection of phytoplankton into perspective, I will shortly describe the most common phytoplankton detection methods.

1.1 Phytoplankton pigments

Fluorescence properties of phytoplankton cells depend on the pigmentation of the cell. These pigments have two main functions. First, chlorophylls, phycobilins and some carotenoids harvest light energy for photosynthesis. Secondly, some carotenoids act as photoprotectants and prevent photooxidation. Additionally, phycobilins in cyanobacteria may serve as nitrogen storage.

Chlorophyll *a* (Chl*a*) is present in all photosynthetic organisms (except in anaerobic photosynthetic bacteria), and has a central role in photosynthesis. Accessory chlorophylls are found in most taxonomic groups (Table 1) except in cyanobacteria (blue-green algae) and Eustigmatophyceae (Rowan 1989). As an exception to these rules, Prochlorophytes (subdivision of Cyanobacteria) contain either Chl*a* and Chl*b* or divinyl-Chl*a* and divinyl-Chl*b* (Ting et al. 2002). Chlorophyll *b* (Chl*b*) is present in higher plants, in green algae (Chlorophyta), and euglenophytes. Three different forms of chlorophyll *c* exist (Chlc_1, Chlc_2, Chlc_3), and the taxonomic groups containing these pigments are commonly grouped as Chromophyta. Each chlorophyll pigment has various degradation products, which are sometimes present in natural samples due to grazing or the senescence of cells. Pheophytin *a*, a typical degradation product of Chl*a*, plays a role also in the photosynthetic electron transport chain (Falkowski & Raven 2007).

Several hundreds of different carotenoids are known. In phytoplankton, some carotenoids, like β,β-carotene, are found in most taxonomic groups, while some are diagnostic taxonomic markers (Jeffrey & Vesk 1997, Table 1). Zeaxanthin is considered as a marker of marine cyanobacteria (Jeffrey & Vesk 1997), and it is also the main carotenoid for picocyanobacteria (*Synechococcus* sp.) isolates from the Baltic Sea (J. Seppälä & F. Pollehne, unpublished). For filamentous cyanobacteria, which are abundant in the Baltic Sea, zeaxanthin is present in *Anabaena lemmermannii* and *Aphanizomenon* sp., but not in *Nodularia spumigena* (Schlüter et al. 2004). Other carotenoids specific for filamentous cyanobacteria include echinonene and myxoxanthophyll. Alloxanthin is considered as a taxonomic marker of Cryptophyta (Rowan 1989), but in the Baltic Sea it is present also in *Dinophysis norvegica* (Dinophyta) (Meyer-Harms & Pollehne 1998) and in phototrophic ciliate *Mesodinium rubrum* (Eker-Develi et al. 2008; also know as *Myrionecta rubra*, Crawford & Lindholm 1997). Peridinin and diadinoxanthin are the major carotenoids for dinophytes. Haptophytes can be divided into four sub-groups by their pigmentation, and the main carotenoids include diatoxanthin, diadinoxanthin, fucoxanthin and 19´-hexanoyloxyfucoxanthin (Jeffrey & Vesk 1997). The pigmentation of Chrysophyceae is rather similar to haptophytes. Violaxanthin is the most important carotenoid in Eustigmatophyceae (Owens et al. 1987). For euglenophytes diatoxanthin and diadinoxanthin are the major carotenoids (Bjørnland 1982, Jeffrey & Vesk 1997). Lutein is the most important carotenoid for chlorophytes, while neoxanthin, zeaxanthin, antheraxanthin and violaxanthin are present in the most cases as well (Rowan 1989).

There are four different groups of phycobiliproteins: allophycocyanin (APC), phycocyanin (PC), phycoerythrin (PE), and phycoerythrocyanin (PEC). The number and type of different phycobilin chromophores present in each phycobiliprotein varies (Rowan 1989). In cyanobacteria, APC and PC are always present, though sometimes at low quantities. PE is present in several taxonomical cyanobacterial groups, while PEC is more or less limited to the strains that form heterocysts (Bryant 1982). The strains with both PE and PEC present are not known. In cryptophytes, either PE or

Table 1. Pigmentation of the major algal divisions/classes present in the Baltic Sea. For carotenoids only major taxonomically significant pigments are shown. (+) indicates that pigment is of minor importance, or found only in a few species/strains. Note that the table is compiled from the sources (Rowan 1989, Jeffrey & Vesk 1997) covering all aquatic environments as only few studies are available for species isolated from the Baltic Sea.

Pigment	Cyanobacteria	Cryptophyta	Dinophyta	Haptophyta	Chrysophyta	Eustigmatophyceae	Euglenophyta	Chlorophyta
Chl$a$	+	+	+	+	+	+	+	+
Chl$b$							+	+
Chlc_1				+	+			
Chlc_2		+	+	+	+			
Chlc_3				+	(+)			
Alloxanthin		+	(+)					
Antheraxanthin								+
19´-Butanoyloxyfucoxanthin				+	+			
Diadinoxanthin			+	+	+		+	
Diatoxanthin			(+)	+	+		+	
Echinenone	+							
Fucoxanthin				+	+			
19´-Hexanoyloxyfucoxanthin				+				
Lutein								+
Peridinin			+					
Myxoxanthophyll	+							
Neoxanthin							+	+
Violaxanthin					+	+		+
Zeaxanthin	+					(+)	+	+
Allophycocyanin	+							
Phycocyanin	+	(+)						
Phycoerythrin	(+)	(+)	(+)					
Phycoerythrocyanin	(+)							

PC is present, but never both (Rowan 1989). PE or PC is also present in the ciliate *Mesodinium rubrum*, and in a few dinoflagellates (Vesk et al. 1996).

Pigmentation of phytoplankton may contain a lot of taxonomic information. Pigment chemotaxonomy is the common name for approaches that use diagnostic pigments (or the related optical signals) in the identification or quantification of different taxonomic groups.

Pigments are not freely distributed in the phytoplankton cells, but are bound to specific proteins and located within the thylakoid membranes. For eukaryotes, these membranes are in the chloroplasts, and for cyanobacteria they are dispersed in the cytoplasm. There are two physically and functionally separated photosystems in the cell, photosystem I (PSI) and photosystem II (PSII), with different pigment-protein complexes.

The reaction centre of PSII (RCII) contains Chl*a* and pheophytin *a*. RCII is closely associated with two chlorophyll-proteins, CP47 and CP43, containing Chl*a* and β,β-carotene, which also play a role in light-harvesting (Green & Durnford 1996, Falkowski & Raven 2007). In eukaryotic algae, chlorophyll-carotenoid proteins form light harvesting antennas for PSII and composition of these proteins vary between taxonomic groups (Green & Durnford 1996, Table 2). In cyanobacteria, phycobiliproteins locate in phycobilisomes (PBS) and harvest light for PSII (Sidler 1994). The reaction centre for PSI contains Chl*a* and β,β-carotene. Light energy for photosynthesis is captured by antenna pigments, further transferred to Chl*a* in chlorophyll-proteins (which harvest light as well), and finally transferred to reaction centres, where the subsequent photochemical reactions take place (Falkowski & Raven 2007).

Table 2. Light harvesting antenna pigment complexes for PSII in the major algal groups (from Green & Durnford 1996).

Algal group	Light harvesting antenna for PSII
Cyanobacteria	Phycobilisomes
Cryptophyta	Alloxanthin - Chl*a/c*; phycobiliproteins
Dinophyta	Peridinin - Chl*a/c*
Haptophyta	Fucoxanthin - Chl*a/c*
Chrysophyta	Fucoxanthin - Chl*a/c*
Eustigmatophyceae	Violaxanthin/vaucheriaxanthin - Chl*a*
Euglenophyta	Diadinoxanthin/diatoxanthin/neoxanthin - Chl*a/b*
Chlorophyta	Lutein/neoxanthin/zeaxanthin/violaxanthin - Chl*a/b*

1.2 Light absorption by phytoplankton pigments

Depending on wavelength, electromagnetic radiation can be divided into different categories, like ultraviolet-radiation, visible light and infrared-radiation. Photosynthetically active radiation (PAR) extends from 400 to 700 nm. The energy of light quantum, photon, (ε) is inversely proportional to its wavelength (λ),

$$\varepsilon = h \, c \, \lambda^{-1} \tag{1}$$

where h is Planck's constant (6.625×10^{-34} Js), and c is velocity of the photons in vacuum (3×10^{10} cm s^{-1}).

In the absorption of light, the energy of a quantum is transferred to a molecular entity (Braslavsky 2007). Absorption depends on wavelength and the possible electron states of the absorbing molecule. Based on the distribution of these energy levels, a molecule has an absorption spectrum with wavelength regions characterised by high and low absorption corresponding to the likelihood of light absorption.

The photosynthetic pigments of phytoplankton have evolved to harvest sunlight efficiently (Kiang et al. 2007). Various pigments are complementary in light harvesting, and thus they are characterized by different spectra. All chlorophylls have high absorption in the blue spectral region. As summarized by Rowan (1989), in acetone Chl*a*, Chl*b* and Chl*c* have absorption peaks at 430 nm, 455-460 nm and 440-450 nm, respectively (Fig. 1a). In the red region Chl*a* and Chl*b* show peaks at 660-665 nm and 645-648 nm, respectively, and absorb more efficiently than Chl*c* (with different forms having peaks at 625-630 nm). Most carotenoids have three absorption peaks in the PAR region and typically these are positioned at the blue, green or yellow region of spectra (sometimes extending to the UV). The phycobiliproteins, depending on the phycobilin chromophores, absorb in the blue-green to orange regions.
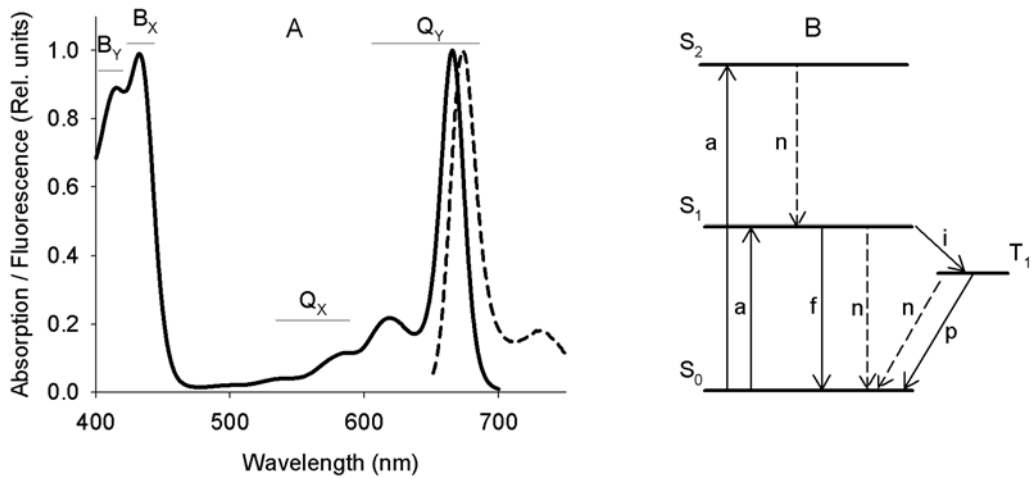
Figure 1. (A) Absorption spectrum of Chl*a* in ethanol (solid line) with absorption peaks corresponding to excited states at blue range (B_Y and B_X) and at red range (Q_X and Q_Y). Fluorescence spectra of Chl*a* (dashed line) corresponds the light emission from the lowest exited state (Q_Y), and has a mirror shape of Q_Y absorption band. (B) A simplified presentation of the energy level diagram showing the absorption (a) of quantum, and corresponding formation of excited states (S_0-S_1 and S_0-S_2 transients). Higher excited states decay to S_1 (n, non-radiative decay). Competing processes for S_1 decay include fluorescence (f), non-radiative decay, and intersystem crossing (i), where triplet state (T_1) is formed, followed by non-radiative decay or phosphorescence (p).

   The proteins binding the pigments in cells modify their absorption properties and absorption peaks are shifted towards longer wavelengths. For Chl*a*, *in vivo* absorption peaks are at 435–440 nm and at 673–679 nm (Lohrenz et al. 2003, Johnsen & Sakshaug 2007). For carotenoids the absorption peaks can be shifted towards the red by up to 90 nm compared to the absorption of extracted pigments in solvents (Anderson & Barrett 1986). For each pigment, the exact position of the *in vivo* absorption maxima varies between phytoplankton groups (Table 3) and these can be estimated indirectly e.g. using the derivative analysis or Gaussian decomposition approach (Lohrenz et al. 2003). Absorption properties of the individual pigment-protein complexes can be measured, provided they are carefully separated physically (e.g. Jovine et al. 1995).

   In the cells, pigments are not uniformly distributed but they are in discrete packages, in the pigment-protein complexes located in the chloroplast membranes (or in the photosynthetic membranes in cyanobacteria). The pigments partly shade each other and the actual absorption efficiency is less than if the pigments were uniformly distributed. This package effect is more pronounced for highly pigmented particles, e.g. for cells grown in low light with a high cellular pigment content. Larger cells tend to have a stronger package effect than small cells (Kirk 1994).

1.3 Fluorescence properties of living phytoplankton

1.3.1 Principles of fluorescence

When a pigment absorbs a light quantum, one electron is raised from a ground state (S_0) to a higher energy level, electron state (S_1, S_2, …) (Fig. 1b). The energy differences between the ground and excited states correspond to the maxima in absorption spectra. Light absorption is very rapid with a timescale of 10^{-15} s. The higher excited states decay quickly (approx. $<10^{-12}$ s) to the lowest excited state (S_1), the excess energy being released as heat. The S_1 decay processes include fluorescence (emission of a new photon within 10^{-9} – 10^{-7} s), non-radiative decay (releasing heat in

Table 3. *In vivo* light absorption by pigments harvesting light for PSII, and their corresponding fluorescence emission maximum (compiled from Bryant 1982, Anderson & Barrett 1986, Johnsen et al. 1994a, Johnsen et al. 1994b, Sidler 1994, Lohrenz et al. 2003). Accessory chlorophylls and carotenoids do not have own *in vivo* fluorescence emission, but transfer the energy to Chl*a*.

	Absorption peaks (nm)	Fluorescence emission maximum (nm)
Chl*a*	435-440, 620-635, 672-676	682
Chl*b*	465-470, 650	
Chl*c*	455-465, 590, 625-643	
Alloxanthin	488[a]	
Diadinoxanthin	440-490	
Fucoxanthin	515-545	
Peridinin	440-540	
PE	490-575	570-580
PEC	570-595	625-635
PC	615-640	635-645
APC	620-655	660-675

[a] For alloxanthin only a peak wavelength is given

$10^{-7} - 10^{-5}$ s), and intersystem crossing (triplet formation at the timescale $10^{-10} - 10^{-8}$ s). The latter is sometimes accompanied by the emission of a photon, known as phosphorescence (at timescale 10^{-3}-10^2 s). Fluorescence emission (change from S_1 to S_0) is a spectral mirror image of absorption corresponding to the change from S_0 to S_1 (Lakowicz 1999, Fig. 1a). The energy of fluorescence emission is typically less than the absorption, thus emission occurs at longer wavelengths than absorption (Stokes shift) and the remaining energy is released as thermal emission (Owens 1991, Lakowicz 1999).

The quantum yield of fluorescence (Φ_F) relates the amount of photons emitted (F) to the amount of photons absorbed (I),

$$\Phi_F = F\, I^{-1} \tag{2}$$

Alternatively, Φ_F may be expressed using the rate constants for the different excited state decay processes,

$$\Phi_F = k_f (k_f + k_d)^{-1} \tag{3}$$

where k_f and k_d are the rate constants for the excited state decay as fluorescence and non-radiative processes (including e.g. thermal emission and triplet formation), respectively.

In chlorophyll pigments, light absorption leading to the higher electron states corresponds to absorption bands Q_X in the red, and B_X and B_Y in the blue (Falkowski & Raven 2007). These states rapidly decay to the lowest excited state S_1 corresponding to the Q_Y band (centred at 625-670 nm, depending on the pigment and solvent, Rowan 1989, see Fig. 1a). Chlorophyll fluorescence arises only from Q_Y, and fluorescence emission is red-shifted by 5-10 nm. For pure Chl*a*, Φ_F varies from 0.23 to 0.32 depending on the organic solvent used (Udenfriend 1962). Fluorescence of carotenoids is very weak with quantum yields in the order from 0.0001 to 0.00001 (Frank et al. 1997). In contrast, phycobiliproteins are highly fluorescent with quantum yield from 0.51 to 0.98 (Oi et al. 1982).

1.3.2 Energy transfer

Pigments do not exist isolated in the living phytoplankton cell, and this has consequences for light absorption and excitation energy transfer. Antenna pigments absorb light at their specific wavelengths. Pigments in the reaction centres participate in the light harvesting as well, but their quantitative share is minor due to the low amount of pigment involved (Owens 1991). The absorbed light energy is efficiently transferred towards Chl*a* in the reaction centres. This transfer of energy may take place by resonance when emission and absorption lines of the energy donor and acceptor overlap (Förster transfer) or by an exchange mechanism when the orbitals of donor and acceptor overlap (Dexter transfer) (Clegg 2006). Because the excitation transfer from accessory chlorophylls and carotenoids in the antenna to Chl*a* is very rapid (10^{-12} s), the fluorescence quantum yield of these antenna pigments is very low and thus their fluorescence cannot be efficiently detected.

In the phycobilisomes, energy is transferred by Förster transfer (Sidler 1994). Energy flows from the short-wavelength absorbing PE (absorption maxima at 490-575 nm / fluorescence emission maxima at 570-580 nm) or PEC (570-595 nm / 625-635 nm) to PC (615-640nm / 635-645 nm) and further to the long wavelength absorbing APC (620-655 nm / 660-675 nm) (Mimuro 1990, Sidler 1994). From APC the light energy is transferred to Chl*a* in photosystem reaction centres. Energy transfer in phycobilisomes is very efficient (>95%). Due to high fluorescence quantum yield, however, fluorescence of various phycobilins can be efficiently detected.

1.3.3 *In vivo* fluorescence of phytoplankton cells

Most (approx. >90%) of the Chl*a* fluorescence arises from PSII, with maximum emission around 682 nm. First, there are often more Chl*a* and accessory pigments in PSII than in PSI. Secondly, in PSII, the excitation energy may travel back and forth in Chl*a* pigments located in the antenna or in the reaction centre, due to overlap between absorption and fluorescence maxima (approx. 5-10 nm). The primary source of PSII fluorescence are Chl*a* pigments in the antenna that are more than hundred times more numerous than Chl*a* pigments in the reaction centre. The absorption maximum of PSI reaction centre Chl*a* is around 700 nm, and its fluorescence takes place at longer wavelengths. The received excitation energy of PSI reaction centre can thus not be easily returned to antenna Chl*a* with its absorption maxima around 675 nm. The fluorescence yield of PSI is very low as the decay of the excited state by photochemistry and non-radiative processes is rapid (Owens 1991, Falkowski & Raven 2007).

The fluorescence quantum yield of Chl*a in vivo* is lower than *in vitro* and varies from 0.005 to 0.05 (Babin 2008). In living cells, photochemistry competes efficiently for the energy from excited state decay with a relatively high rate constant, k_p. Some energy may be directed to PSI (spill-over, with rate constant k_s). If photosynthesis is not possible, when all reaction centres are inactive or closed (k_p is zero), the maximum fluorescence yield can be expressed with the following rate constants,

$$\Phi_F = k_f \left(k_f + k_d + k_s \right)^{-1} \tag{4a}$$

If all the reaction centres are open, i.e. ready to receive energy from an excited state, fluorescence yield is at minimum,

$$\Phi_F = k_f \left(k_f + k_d + k_s + k_p \right)^{-1} \tag{4b}$$

For whole cells, Φ_F must be expressed as the sum of open and closed photosynthetic units,

$$\Phi_F = f\, k_f (k_f + k_d + k_s + k_p)^{-1} + (1 - f)\, k_f (k_f + k_d + k_s)^{-1} \tag{4c}$$

where f is a fraction of open reaction centres.

Similarly, if all reaction centres are open, the maximum quantum yield of PSII photochemistry ($\Phi_P{}^{max}$) can be calculated as

$$\Phi_P{}^{max} = k_p (k_f + k_d + k_s + k_p)^{-1} \tag{5}$$

Non-photochemical fluorescence quenching is a common term for processes where the excess excitation energy is converted to heat (energy-dependent quenching, state transition quenching and photoinhibitory quenching) (Falkowski & Raven 2007). While energy-dependent non-photochemical quenching protects PSII from photoinhibition, photoinhibitory non-photochemical quenching takes place during severe light stress and is maybe more related to photodamage (Müller et al. 2001).

1.3.4 Variable fluorescence

Fluorescence is the product of quantum yield and rate of light absorption (I, Eq. 2). When minimum (F_0) and maximum (F_M) fluorescence are measured, $\Phi_P{}^{max}$ can be calculated as follows:

$$F_0 = k_f (k_f + k_d + k_s + k_p)^{-1}\, I \tag{6a}$$

$$F_M = k_f (k_f + k_d + k_s)^{-1}\, I \tag{6b}$$

$$(F_M - F_0)\, F_M{}^{-1} = k_p (k_f + k_d + k_s + k_p)^{-1} = \Phi_P{}^{max} \tag{6c}$$

F_M - F_0 is called the maximum variable fluorescence (F_V), and F_V/F_M is used as an estimate of photochemical efficiency of PSII. Measurement of F_0 is obtained when the cells have been dark acclimated long enough (15-30 min) to open all the reaction centres, and when all non-photochemical quenching mechanisms are relaxed. Closing the reaction centres, and subsequent measurement of F_M can be carried out in different ways. One possibility is to block the electron transport chain using specific chemicals, like DCMU (3-[3,4-dichlorophenyl]-1,1-dimethylurea). Drawback of this technique is that after the chemical treatment cells are no longer viable. A nonintrusive way for closing reactions centres is to expose them to saturating light. Single turnover technique uses short (microseconds) intense light flashes that ultimately cause single closure of PSII reaction centres. Fast Repetition Rate fluorometry (FRRF) is a typical single turnover technique used in oceanography and was also utilized in this thesis. Multiple turnover technique uses relatively long (milliseconds) saturating light pulse that produces several photosynthetic events (turnovers). Pulse amplitude modulation (PAM) fluorometry is commonly used for multiple turnover measurements. These two light treatments affect different parts of the electron transport chain, and consequently the measured F_M values are slightly different (Kolber et al. 1998, Kromkamp & Forster 2003, Suggett et al. 2003). Typically, for healthy algal cells F_V/F_M is close to 0.65 (single turnover) or 0.7-0.8 (multiple turnover). The resulting F_V/F_M can be used in the calculation of the rate of photosynthesis or as an index of physiological status of the cells (Kromkamp & Forster 2003, Suggett et al. 2003). When fluorescence is measured with a standard laboratory or field fluorometer with continuous light supply the resulting fluorescence signal is somewhere between F_0 and F_M.

1.3.5 *In vivo* Chl*a* fluorescence and the estimation of phytoplankton biomass

For decades, *in vivo* Chl*a* fluorescence has been used to estimate phytoplankton biomass. Currently, a wide range of instruments are available with different optical and mechanical configurations. The method was first described by Lorenzen (1966), and he already listed some potential limitations of the method, including factors affecting Chl*a*-specific fluorescence (R), which is the ratio between fluorescence intensity (F) and concentration of extracted Chl*a* ([Chl*a*]),

$$R = F[\text{Chl}a]^{-1} \tag{7}$$

The potential of the *in vivo* fluorescence technique to provide a continuous record of phytoplankton abundance was acknowledged in follow-up studies (e.g. Flemer 1969, Platt 1972), but the results were considered only semi-quantitative. The reasons for the variability between extracted Chl*a* values and *in vivo* fluorescence readings were explored in more detail, and identified as changes in ambient light conditions, physiological diel rhythms, nutrient stress, species composition, and the presence of humic material (Flemer 1969, Kiefer 1973a, Kiefer 1973b, Loftus and Seliger 1975). The effects of temperature were considered minor (Lorenzen 1966, Kiefer 1973a). Kiefer (1973a) noted that the presence of Chl*a* degradation products had only a minor effect on the variability of R.

In the early studies, the observed variations in R were 2 to 4-fold for single species, while up to 10-fold changes were observed for natural samples (Kiefer 1973a, Loftus and Seliger 1975). The larger variation in the field samples was due to additive effects of species composition and cell physiology. Later, Vincent (1983) demonstrated that R varied 50-fold between different species, and he further pointed out the dependency of the fluorescence on the optical setup of the instruments.

In Eq (6) fluorescence intensity is related to light absorption and the quantum yield of fluorescence. Additional terms are needed to fully describe the measured fluorescence signal ($F(\lambda_{ex/em})$ with units: µmol q m^{-3} s^{-1}), detected at given excitation (*ex*) and emission (*em*) wavelengths. Intracellular reabsorption of the fluoresced light can be described by the specific absorption efficiency ($Q_a{}^*(\lambda_{em})$, also index of package effect, see 4.1.2.2.). $Q_a{}^*(\lambda_{em})$ ranges from 0 (all reabsorbed) to 1 (no reabsorption). Several instrumental factors are required if fluorescence is measured in physical units. Omitting these instrumental factors, for clarity, $F(\lambda_{ex/em})$ can be expressed in relative units as:

$$F(\lambda_{ex/em}) = I(\lambda_{ex})\, Q_a{}^*(\lambda_{em})\, \Phi_F \tag{8}$$

Light absorption can be expressed as a product of irradiance (E_0; µmol q m^{-2} s^{-1}), Chl*a* concentration ([*Chla*]; mg m^{-3}), the number of photosynthetic units (n_{PSII}; q (mg Chl*a*)$^{-1}$), and spectrally averaged optical cross-section of PSII ($\overline{\sigma}_{PSII}{}^{opt}$; m^2 q^{-1}) weighted by irradiance spectra (i.e. by the excitation spectra of the instrument) (Falkowski & Kiefer 1985, Babin 2008). Thereafter, $F(\lambda_{ex/em})$ may be calculated as:

$$F(\lambda_{ex/em}) = E_0\, [\text{Chl}a]\, n_{PSII}\, \overline{\sigma}_{PSII}{}^{opt}\, Q_a{}^*(\lambda_{em})\, \Phi_F \tag{9}$$

Eq. 9 describes the rate of light absorption by PSII. The Chl*a*-specific absorption coefficient for PSII ($\bar{a}_{PSII}{}^*$; m^2 (mg Chl*a*)$^{-1}$), can be represented as:

$$\overline{a}_{PSII}{}^* = n_{PSII}\, \overline{\sigma}_{PSII}{}^{opt} \tag{10}$$

and it can be calculated from the spectrally resolved Chl*a*-specific absorption coefficient of PSII ($a_{PSII}{}^*(\lambda)$; m^2 (mg Chl*a*)$^{-1}$), the spectral irradiance of the fluorometer ($E_0(\lambda)$; µmol q m^{-2} s^{-1}), and the integrated irradiance ($E_0(PAR)$; µmol q m^{-2} s^{-1}):

$$\bar{a}_{PSII}^* = (\int_{\lambda=400}^{700} a_{PSII}^*(\lambda)\, E_0(\lambda)\, \mathrm{d}\lambda)\, (E_0(PAR))^{-1} \tag{11}$$

When the excitation light of the fluorometer is considered constant, the obtained fluorescence per the irradiance of fluorometer can be expressed as:

$$F(\lambda_{ex/em})\, E_0^{-1} = [\mathrm{Chl}a]\, \bar{a}_{PSII}^*\, Q_a^*(\lambda_{em})\, \Phi_F \tag{12}$$

Without accounting for the large natural variability of physiological variables in the Eq. 9 or Eq. 12, fluorescence intensity serves only as a semi-quantitative proxy for Chl*a* concentration. Only when the physiological variability is considerably less than the variability in biomass, reliable Chl*a* estimations may be achieved. Typically, conversion from fluorometer readings to Chl*a* concentrations is done using a frequent *in situ* calibration, where water samples are collected for analytical Chl*a* measurements.

1.3.6 Phycobilin fluorescence

In contrast to eukaryotic algae, cyanobacterial PSII contains only a minor fraction of the total cellular Chl*a* (Bryant 1986, Johnsen & Sakshaug 1996) and no accessory Chl or photosynthetic carotenoids. For cyanobacteria most (80-90%) of the Chl*a* is located in the non-fluorescing PSI, and consequently a specific feature for cyanobacteria is a very low Chl*a*-specific *in vivo* fluorescence when compared to that of eukaryotic algae (Campbell et al. 1998). In natural phytoplankton communities, even a low variability in the abundance of eukaryotes, with high Chl*a*-specific fluorescence, will mask the variability in the abundance of cyanobacteria. Therefore Chl*a* *in vivo* fluorescence describes cyanobacterial distribution poorly.

Phycobilins are the major light harvesting pigments in cyanobacterial PSII. These pigments are not widely abundant in other phytoplankton groups (Table 1). The fluorescence of phycobilins can be used to estimate their concentration, and allows the monitoring of cyanobacteria, similar to how *in vivo* Chl*a* fluorescence can be used to detect bulk Chl*a* concentration. The type and amount of phycobilin pigment in cyanobacterial cells varies between cyanobacterial groups and the fluorescence wavelengths monitored must be selected accordingly.

In waters where blue and green light is efficiently absorbed e.g. by humic material (i.e. yellowish/reddish lake and coastal waters), PC absorbing in the orange-red spectral regions is typically the major phycobiliprotein. In oligotrophic oceanic waters blue light penetrates deep into the water column, and consequently phycourobilin-rich PE with absorption maximum at 495-500 nm is the most beneficial for light harvesting. In coastal waters where green light penetrates deepest (e.g. the open Baltic Sea), it is more advantageous to have phycoerythrobilin-rich PE (absorption maxima 540–575 nm) (Wood et al. 1998). Differently coloured cyanobacteria share the light resource in the intermediate water-types (Stomp et al. 2007). Due to variability in cyanobacterial pigmentation, there is no single instrumental setup for phycobilin fluorescence detection, but the method must be optimized separately for the each water-body and cyanobacterial group. The method of measuring phycobilin fluorescence as an index for cyanobacterial distribution was proposed long ago (Yentsch & Yentsch 1979), and the potential of this method for cyanobacteria detection has been reported several times (e.g. Watras & Baker 1988, Lee et al. 1994). However, the operational use of phycobilin fluorometers has not been widespread, and results from long-term monitoring are scarce (but see e.g. Izydorczyk et al. 2005). Instruments have been available from several manufacturers, and with several optical configurations, while the assessment of their performance has been rarely reported (but see Brient et al. 2008).

There are no reports where, to best of my knowledge, pigment-specific fluorescence of phycobilins has been studied *in vivo*. One reason is that practical analytical methods for quantitative estimation of phycobilin concentrations are not available. Several analytical methods have been proposed, but the overall extraction efficiency of phycobilins is typically low for field samples with several cyanobacteria species (with variable extraction efficiency) and phycobilins present (Simis et al. 2005). Consequently, conversion from the phycobilin fluorescence signal to the biomass of cyanobacteria is further complicated as the phycobilin content of cyanobacterial cells varies, especially in response to light and nitrogen conditions (Bryant 1986).

1.3.7 Spectral fluorescence of phytoplankton

A whole fluorescence excitation emission matrix (EEM) describes 3-way data (excitation wavelength × emission wavelength × signal intensity) with contributions from all the fluorescing compounds present in a sample. EEMs show the location and intensity of the emission and excitation peaks for all the fluorophores having fluorescence in the selected spectral window. The EEM–method is also called two-dimensional fluorescence spectroscopy or total luminescence spectroscopy. The measurement is done by incrementing excitation wavelengths stepwise while measuring spectral emission for each excitation wavelength, or vice versa. Typically, the EEMs are visualized using surface or contour plots.

Light harvesting accessory pigments, with the exception of phycobilins, do not have their own *in vivo* fluorescence, but transfer energy to Chl*a*. Consequently, *in vivo* fluorescence emission spectra of phytoplankton show only responses of Chl*a* and phycobilins. To measure emission spectra, emission wavelengths are scanned using a constant excitation wavelength. In excitation spectra, excitation wavelengths are scanned while emission remains constant. Then, the excitation spectra correspond to the spectral absorption of those antenna pigments that transfer light energy to the pigment whose emission is measured. Thus, an excitation spectrum measured at the Chl*a* emission maximum around 682 nm contains information on the absorption properties of PSII antenna pigments.

The Chl*a* red absorption peak located at 670-680 nm cannot be efficiently detected if the emission is measured at the Chl*a* fluorescence maximum at 682 nm, because the excitation and emission wavelengths are too close each other and the excitation band will partly overlap with Chl*a* emission. The red Chl*a* peak can best be measured by detecting fluorescence at wavelengths >710 nm because Chl*a* emission extends towards the far-red (see Fig. 1a). Chl*a* emission is rather low at >710 nm compared to that at 682 nm, and therefore instrument settings must be changed to improve sensitivity, e.g. by increasing emission slit width.

The spectral shape of fluorescence is influenced by the spectral properties of lamp, mirrors, filters, monochromators, and detector. Excitation spectra can be corrected using a quantum counter, a medium with constant quantum yield independent of excitation wavelength. Correction for emission spectra is more difficult and involves a calibrated light source or both the quantum counter and a scatterer. Alternatively, emission spectra may be corrected by comparing with a known emission spectrum (Lakowicz 1999).

Quantum corrected far-red excitation spectra provide the shape of absorption by pigments harvesting light for PSII (Neori et al. 1988). As fluorescence is measured in relative units, these spectra also lack a physical unit. When these spectra are scaled one-to-one against corresponding Chl*a*–specific absorption, so that no overshoot takes place at longer wavelengths (~540-700 nm), approximation of PSII light absorption coefficient is obtained in real units (m^2 (mg Chl*a*)$^{-1}$) (for more details, see 4.1.2.1.). This method assumes that i) photoprotective pigments do not absorb at ~540-700 nm, ii) transfer of energy from photosynthetic accessory pigments to Chl*a* is close to 100%, and iii) scaling is dependent mainly on the pigmentation of PSII antenna (Johnsen &

Sakshaug 2007). In the measurements of the quantum yield of photosynthesis and in bio-optical modelling of photosynthesis, it is important to separate light absorption by photosynthetic and non-photosynthetic pigments (Sakshaug et al. 1991, Raateoja & Seppälä 2001). For such applications, quanta corrected and scaled far-red Chl*a* excitation spectra may serve as a proxy of light harvesting by PSII or by all photosynthetic pigments, the latter assuming similar pigment composition of PSI and PSII antenna (Sakshaug et al. 1997).

As noted above, spectral fluorescence contains information on the pigmentation of PSII antennae. The major taxonomic phytoplankton groups differ in PSII antenna pigmentation (Table 2) and thus have different spectral properties; *in vivo* excitation and emission maxima for major PSII pigments are listed in Table 3. Yentsch and Yentsch (1979), Vincent (1983), and Yentsch and Phinney (1985) examined the group-specific excitation and emission spectra, and suggested that exciting Chl*a* using a few specific wavelengths of accessory pigments gains some level of taxonomic information on the phytoplankton population. Yentsch and Phinney (1985) introduced a "chlorophyll-to-accessory pigment ratio", which is measured as a ratio of fluorescence emission (at 685 nm) after excitation through carotenoids (at 530 nm) and through Chl*a* (at 450 nm). They showed that for green algae this ratio is lower than for other groups due to lack of major carotenoids in PSII antenna. In the study with algal cultures, SooHoo et al. (1986) showed that photoacclimation alters this ratio, and prevents the separation of taxonomic groups using a simple index. Taking advantage of the group-specific differences in the whole spectral domain, identification of phytoplankton species in mixed cultures was demonstrated by Oldham et al. (1985) using EEMs and Fourier-transform-based pattern recognition, but field samples have not been analysed with this method.

Typically, four to five taxonomic groups can be discriminated using spectral fluorescence (Poryvkina et al. 1994, Millie et al. 2002). These include i) Chl*b*-containing groups (Chlorophyta, Euglenophyta), ii) Chl*c*-containing groups without phycobilins (Dinophyta, Haptophyta and Chrysophyta grouped together as Chromophyta), iii) Chl*c*-containing groups with phycobilins (Cryptophyta) and iv) cyanobacterial groups with variable phycobilin pigmentation. All these pigment groups contain several phytoplankton classes and numerous species, and therefore the diversity of pigmentation inside each pigment group is large (Jeffrey & Vesk 1997). Thus, there exists no constant spectral signature for any group. The pigmentation of PSII antenna reflects changes in the environment, especially light and nutrient conditions (e.g. SooHoo et al. 1986, Johnsen & Sakshaug 1996). Adjustment of the pigmentation to environmental conditions may be especially large for cyanobacteria that may use their phycobilins as nitrogen reserves.

Variable fluorescence is an additional error source in the spectral measurements. If the excitation light is strong enough to close a fraction of reaction centres, but not all of them, fluorescence yield varies during spectral measurement as a product of excitation light and PSII light absorption (Babin 2008). This could be avoided using DCMU as an inhibitor of photosynthesis.

Various methods have been used to retrieve taxonomic information from spectral fluorescence, including Fourier-transform-based pattern recognition (Oldham et al. 1985), a similarity index algorithm (Millie et al. 1997, Millie et al. 2002), deconvolution using spectral libraries (Gerhardt & Bodemer 2000, Beutler et al. 2002) and principal component regression (Kaitala et al. 1994, Henrion et al. 1997, Zhang et al. 2006). Theory of spectral discrimination, using multivariate calibration, is more closely reviewed in the Methods section (3.6.1).

In situ measurements of spectral fluorescence can be carried out using standard or modified laboratory spectrofluorometers, though instruments dedicated to automated flow-through measurements have been developed as well (Babichenko et al. 2000). For underwater profiling, spectral instruments have not yet been developed, but instruments utilizing a few excitation wavelengths and detection of emission at one or several wavelengths have been described (Desiderio et al. 1997, Beutler et al. 2002).

1.4 Detection of phytoplankton biomass and taxonomy

The various analytical techniques to estimate the standing crop of phytoplankton differ not only in their principles of measurement, they also characterize phytoplankton biomass differently (Reynolds 2006). There are no universally applicable conversion factors that will make the outcomes of different methods equal. Different important methods, in addition to *in vivo* fluorescence methods, for estimation of phytoplankton biomass and taxonomy are shortly described below, and their advantages and disadvantages are summarised in Table 4.

The most traditional method to estimate phytoplankton biomass is microscopy. Microscopy yields the species composition of the phytoplankton, a cornerstone in understanding the diversity and functioning of aquatic ecosystems. In the Finnish phytoplankton guide (Tikkanen 1986) approximately 800 taxons are described and more recently Guy Hällfors listed >1000 species present in the Baltic Sea (HELCOM 2004). Globally it has been approximated that the number of phytoplankton species is >20000 (Jeffrey & Vesk 1997, Falkowski & Raven 2007). Some species cannot be identified by light microscopy, but electron microscopy or molecular methods are needed. Molecular probes to detect individual taxa have been recently developed (Scholin et al. 2008). As only a small amount of samples can be processed, microscopy is inadequate for applications that require a rapid approximation of phytoplankton biomass and taxonomy and when the number of samples is large.

Electronic counting of aquatic particles was initiated in the late 1960's using Coulter counter (Mulligan & Kingsbury 1968), but it is not possible to distinguish between dead and living particles, and thus phytoplankton biomass estimates for natural samples cannot be directly obtained. In flow cytometry, optical properties of particles in a narrow sample stream are measured. The sample stream is illuminated with a strong light (laser), and fluorescence and light scatter are measured for each individual particle (Yentsch et al. 1983). Forward scatter and side scatter are related to particle size, particle structure and refractive index. Depending on the application, fluorescence of Chl*a*, PE, and PC can be measured. Thus, phytoplankton cells can be discriminated from other particles by their fluorescence properties. Flowcytometry has been an important tool in aquatic sciences mostly because it allows rapid detection, grouping and counting of picophytoplankton cells. Automated *in situ* flowcytometers can be applied to on-line monitoring of phytoplankton biomass, where several particle groups (sometimes up to the species level) can be distinguished (Dubelaar et al. 1999, 2004). To further assist the identification of cells, Sieracki et al. (1998) introduced a combination of flow cytometry and digital imaging (FlowCAM). A system with enhanced resolution and automated image processing has recently been described (Olson & Sosik 2007, Sosik & Olson 2007).

The most widespread method to estimate phytoplankton biomass is the concentration of Chl*a*. However, phytoplankton contains a number of other pigments that are extracted along with Chl*a*. Spectral absorption of other chlorophylls (including their degradation products) is overlapping Chl*a* absorption at the red part of spectrum. Consequently, several methods for simultaneous measurement of Chl*a*, Chl*b* and Chl*c*, or Chl*a* degradation products have been proposed (summarized in Jeffrey & Welschmeyer 1997). These equations, based on measurements at relatively few wavelengths, do not allow definite quantification of all chlorophylls but usually estimates of Chl*a* are considered accurate enough for many applications. More precise spectral methods using multivariate calibration or Gaussian peak analysis have been recently introduced (Moberg & Karlberg 2001, Küpper et al. 2007). For analysis of chlorophylls, fluorometry is more sensitive than spectrophotometry, and the method introduced in the early 1960s (Yentsch & Menzel 1963) has been extensively used in the estimation of Chl*a* concentration. As with spectrophotometry, the presence of other chlorophylls influences Chl*a* determination. Multi-wavelength fluorescence methods have been introduced (summarized in Jeffrey & Welschmeyer 1997) but these are not

Table 4. Comparison of various methods for detection of phytoplankton biomass and taxonomy.

Method	Taxonomic resolution	Sampling	Advantages	Disadvantages
Microscopy	Very high	Discrete samples	Accurate species composition of the phytoplankton biomass.	Very time-consuming and thus a high price per sample. Errors in biomass estimates due to complex or variable cell size. Subsampling errors due to small volumes. Picoplankton requires epifluorescence microscopy. Subjective, and requires a trained person.
Electronic particle counting	Only size- related information	Discrete samples	Rapid and accurate for counting cells in cultures	Does not separate living and dead particles. Problems in determining the volume of non-spherical cells. Counting of small cells (<2 μm) not feasible.
Flowcytometry	Typically <10 groups	Discrete samples Vertical/horizontal/ seasonal profiling	Rapid discrimination of phytoplankton from other particles. Differentiation of picoplankton. May be coupled with digital imaging.	High price of instruments. Need of trained user. Instruments under development.
Molecular probes	Identification of few species	Discrete samples, automation possible	Fast detection of labelled cells, e.g. with flow-cytometry. Possibility to identify species that are difficult to separate by other methods	Probes available for limited number of species. Analytical systems for oceanographic monitoring still under development.
Pigment analysis; spectrophotometry	1-20 pigments; typically 1-3	Discrete samples	Relatively fast, can be partially automated. Simple to perform, methods well established. Low cost per sample.	Inaccurate estimates due to interfering pigments. Several methodological variations. Problems with pigment extraction efficiency.
Pigment analysis; fluorometry and spectrofluorometry	1-12 pigments, typically 1-2	Discrete samples	Relatively fast, can be partially automated. Simple to perform, methods well established. Very sensitive. Low cost per sample.	Inaccurate estimates due to interfering pigments. Only chlorophylls can be analysed. Problems with pigment extraction efficiency.
Pigment analysis; HPLC	Typically approx. 30 pigments	Discrete samples	Accurate determination of major pigments including degradation products. Estimation of phytoplankton class abundances based on signature pigments.	Requires an expensive instrumentation and a trained user. Rather slow. Availability and cost of pigment standards. Problems with pigment extraction efficiency.

Method	Taxonomic resolution	Sampling	Advantages	Disadvantages
Optical: Inherent optical properties (absorption, scattering)	Estimate of Chl$a$, and other pigments or chemotaxonomic groups	Discrete samples Vertical/horizontal/seasonal profiling	Automated devices allow high resolution sampling. Spectral measurements provide information on phytoplankton chemotaxonomy.	Disturbances by other absorbing/scattering components especially in coastal and lake waters. Methodological assumptions and high workload in filter-pad method. Typically requires site specific algorithms. Price of the automated devices is high. Biofouling for automated instruments.
Optical: Apparent optical properties (light attenuation, reflectance)	Estimate of Chl$a$, and other pigments or chemotaxonomic groups	Horizontal/seasonal profiling	Allows high spatial and seasonal resolution. Spectral measurements provide information on phytoplankton chemotaxonomy.	Effects of biofouling, sun-angles, cloudiness, waves, and shading. Applicable only during daytime.
Optical: Ocean colour	Estimate of Chl$a$ and bloom types	Basin-scale images	Global coverage. Spatial and seasonal resolution relevant to oceanic phytoplankton processes.	Information derived only from the surface layer. Requires specific algorithms (including atmospheric corrections) not yet reliable for all optical provinces. Clouds prevent measurements. Small water bodies cannot be efficiently detected.
Optical: *in vivo* Chl$a$ fluorometry	Estimate of Chl$a$	Discrete samples Vertical/horizontal/seasonal profiling	Rapid online information of phytoplankton distribution. Very sensitive. Very low cost per sample.	Semi-quantitative estimate of Chl$a$, as Chl$a$ specific fluorescence is affected by photo-physiology and species composition. Requires frequent calibration with other methods. Biofouling for automated instruments.
Optical: spectral *in vivo* fluorometry	2-6 chemotaxonomic groups	Discrete samples Vertical/horizontal/seasonal profiling	Rapid online information of chemotaxonomic phytoplankton distribution. Low cost per sample.	Photoacclimation affects the spectral signatures of groups. Diversity in the pigmentation inside the chemotaxonomic groups. Lack of commercial equipments with high spectral resolution, suitable for field studies. Biofouling for automated instruments.

widely used. Spectrofluorometric methods, by recording a complete excitation-emission fluorescence matrix, for simultaneous determination of 6 to 12 chlorophyll pigments have been described (Neveux & Lantoine 1993, Moberg et al. 2001, Neveux et al. 2009).

Chromatographic methods are used to separate, identify, and quantify phytoplankton pigments. The identification of group-, class-, and species-specific carotenoids (so-called signature pigments, see Table 1) and developments in high-pressure liquid chromatography (HPLC) boosted the use of chromatographic methods in chemotaxonomic studies (Jeffrey 1997). HPLC is often considered the most reliable method for Chl$a$ determination, especially in the presence of Chl$a$ degradation products. Detection of the signature pigments by HPLC, and the use of constrained pigment ratios for algal classes, allows detection of phytoplankton class abundances (Mackey et al. 1996).

In natural waters, the main optically active constituents are water itself, coloured dissolved organic matter, inorganic particles, detritus, phytoplankton, and other living organisms (Kirk 1994). Their contribution to inherent optical properties varies, and in the open ocean most of the optical variability is due to phytoplankton and related compounds, while in the coastal waters and lakes contributions of dissolved organic matter, phytoplankton and non-algal particulate matter are more complex. Absorption of water constituents can be measured using *in situ* spectrophotometers (Röttgers et al. 2007). Frequently, absorption by phytoplankton pigments is measured using a filter-pad method, where absorption by particulate matter is divided into components of phytoplankton pigments and other particles (e.g. Tassan & Ferrari 1995). The absorption coefficient for phytoplankton is (nonlinearly) related to the Chl$a$ concentration (Bricaud et al. 2004). Using the absorption data, concentrations of major pigments may be estimated or chemotaxonomic information may be derived (e.g. Johnsen et al. 1994b). Additionally, Chl$a$ may be estimated from beam attenuation, scattering and backscattering signals (Sosik 2008).

Diffuse spectral attenuation coefficients for downwelling irradiance, determined from irradiance measurements at several depths, contain the contribution of the optically active constituents and can be used in the estimation of Chl$a$ (Sosik 2008). Water-leaving reflectance can be measured using above-water spectroradiometers operated at fixed platforms or at moving platforms like ships, airplanes, or satellites (Lewis 2008). Ocean colour data recorded using sensors in satellites, typically with low spectral resolution, is used to retrieve Chl$a$ concentrations (Sathyendranath et al. 2001).

1.4.1 Methods applied in the Baltic Sea

Scientific phytoplankton research in the Baltic Sea goes back to the late 19th century. During the first decades, samples for microscopic phytoplankton counts were taken with nets (see review by Finni et al. 2001). Even today, the microscopic identification and counting of phytoplankton cells is an essential method in the phytoplankton monitoring programs.

Data-sets of spectrophotometrically and fluorometrically determined Chl$a$, with various methodological variations, date back to the early 1970s (e.g. Raateoja et al. 2005). Monitoring of the phytoplankton community structure using pigments determined with HPLC has been rather sporadic and limited to short-term studies (e.g. Stoń & Kosakowska 2000, Wänstrand & Snoeijs 2005).

Studies of underwater light distribution have a long history in the Baltic Sea (Jerlov 1968). Spectral light absorption by phytoplankton, and consequent variability in the Chl$a$ specific absorption coefficient has been studied since the mid 1980s (Konovalov et al. 1990) but it has not been a part of continuous monitoring programmes. Detection of surface accumulation of cyanobacterial blooms using satellite imagery goes back to the mid-1970s and the annual bloom distributions have been analysed back to 1979 (Kahru et al. 2007). Currently, Chl$a$ distribution is retrieved from ocean colour provided by several satellites, but the commonly used algorithms are still not well suited for the optically complex waters of the Baltic Sea (Darecki & Stramski 2004).

Experimental studies of phytoplankton distribution using onboard flow-through particle size analyzers and *in vivo* Chl*a* fluorometers started in the mid-1980s (e.g. Kahru & Nômmann 1990). In 1990-91, a flow-through *in vivo* Chl*a* fluorometer was installed onboard passenger ship Georg Ots, commuting between Helsinki and Tallinn (Rantajärvi 2003). The Alg@line project was initiated in 1993 at the Finnish Institute of Marine Research, to maintain and promote these activities, and since then several other merchant ships have been equipped with Chl*a* fluorometers. Studies of the variable Chl*a* fluorescence in measuring phytoplankton productivity commenced in late 1990s (Raateoja 2004).

In vivo spectral fluorescence detection of phytoplankton biomass and community structure was initiated in early 1990s using laser-induced fluorescence (Babichenko et al. 1993), EEMs measured with laboratory spectrofluorometer (Poryvkina et al. 1994), and spectral flow-through fluorescence measurements (Babichenko et al. 1999). This thesis is a continuation of these activities.

2 Objectives

The overall objective of the studies presented in this thesis is to evaluate new instruments and techniques for fluorescence-based detection of phytoplankton biomass and taxonomy, and, to some extent, for measurements of phytoplankton physiological state. My studies have focused on the Baltic Sea, but several findings are applicable to other sea areas and lakes. During the years, the work has included testing of various instruments ranging from the commercially available ones to prototypes, not always producing results suitable for publication. Troubleshooting instrumental faults and detection of methodological limitations are, however, unavoidable during the development phase of such work.

The ultimate goal of these studies has been the development of optical methods to support traditional phytoplankton monitoring and thereby strengthen the understanding of the links between biological, chemical and physical processes. After tests with cultures (II, unpublished results), this has been approached during field cruises (I, V), mesocosm experiment (II, VII), seasonal monitoring campaign (III), and finally using a ship-of-opportunity platform (VI).

As a continuation of preceding work (Poryvkina et al. 1994), my studies started with the differentiation of various taxonomic groups of the Baltic Sea phytoplankton based on their pigmentation and optical properties (I, V, VI, VII, unpublished results). The aim was to identify how many spectral phytoplankton groups can be discriminated for the Baltic Sea. Acclimation of the pigmentation and optical properties of phytoplankton as a response to environmental variables, especially to light and nutrients, was studied in the second phase (II, unpublished results). It was hypothesized that spectral fluorescence (i.e. photosynthetic pigments) is less affected than absorption (i.e. all pigments, including photoprotective ones), and therefore spectral fluorescence methods will be more suitable for chemotaxonomic studies.

Soon it became evident that the specific pigment system of cyanobacteria, exhibiting very low Chl*a* fluorescence, challenges all the Chl*a* fluorescence based detection systems (I, IV, V). Consequently, the importance of phycobilin fluorescence as a marker of cyanobacterial distribution was studied (V, VI). The objective was to evaluate new instruments and develop calibration algorithms to be used on ship-of-opportunity -systems for cyanobacterial detection.

In several studies, the pros-and-cons of the traditional single-wavelength fluorometers for *in vivo* detection of Chl*a* are considered (I, II, V, VI, unpublished data). The subject had previously been vigorously studied, and therefore no major new findings were expected. However, most preceding studies demonstrate the effects of light, nutrients and diel variations on the Chl*a*-specific fluorescence, whereas I expected that much of this variability in the Baltic Sea is due to changes in community structure, specifically related to the abundance of cyanobacteria with very low Chl*a* specific fluorescence.

New methods based on variable fluorescence for the estimation of phytoplankton productivity emerged during my studies. It was soon realized that the information on light absorption by photosynthetic pigments gained from spectral fluorescence measurements could be useful in the evaluation and development of these new techniques (Raateoja & Seppälä 1999). Phytoplankton productivity, taking the absorption by photosynthetic pigments into account, was approached during a monitoring campaign (III). Further, PSII absorption measured by spectral fluorescence was used to verify that some of the new variable fluorescence methods are not applicable to measure productivity of the filamentous cyanobacteria in the Baltic Sea (IV). In later stages of my studies, measurements at several scales were conducted to evaluate whether a variable fluorescence technique could be used to assess nutrient limitation of natural phytoplankton.

The natural variability of the fluorescence and absorption properties of Baltic Sea phytoplankton has been addressed in several studies (I, III, V), with various aims. These studies identified the origins of various optical signals, and provided background information on the optical properties of the Baltic Sea, as compared to other sea areas. Such observations are essential for instrument and algorithm development.

Finally, a long-lasting objective of my studies has been the derivation of chemotaxonomic information from spectral data. After familiarising myself with chemometrics, analysing the power of multivariate calibration in the chemotaxonomic analysis of spectral data became one of the main objectives of my thesis (VII).

3 Material and methods

3.1 Field sampling

Field studies for this thesis were conducted in various sub-basins of the Baltic Sea. The location of the sampling stations and cruise tracks are shown in Fig. 2.
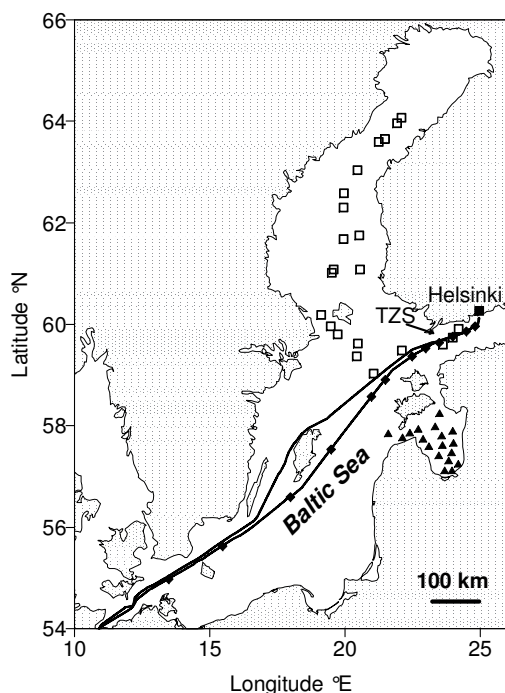

Figure 2. Cruise tracks (continuous line = study VI), sampling stations (triangles = study I, squares = study V), and location of Tvärminne Zoological Station (TZS), which was a site for mesocosm (studies II, VII and UP-III) and laboratory (II, IV) experiments and seasonal monitoring (study III).

In study I, the feasibility of the spectral fluorescence methods to detect bulk changes in the phytoplankton community structure was evaluated. Measurements were carried out in the Gulf of Riga, at the time of cyanobacterial bloom, during a cruise of R/V Marina on 10-13 July 1994. Water samples were taken from 18 stations at fixed depths with Niskin bottles (0, 2.5, 5, 7.5, 10, 15, 20, and 30 m, and a combined sample from 0-10 m). Samples were processed onboard.

Study III concentrates on bio-optical modelling of primary production, and my primary contribution was the quantification of light absorption by the photosynthetic pigments. A bio-optical monitoring campaign was carried out at station "Längden" at the entrance to the Gulf of Finland. The study period lasted from 11 April to 15 November 2000 with 22 sampling days spanning the annual phytoplankton succession with spring bloom, summer minimum, late-summer bloom and autumn periods. Samples (0, 3, 6, 9, 15, and 30 m) were taken at 9:00-10:00 h local time using a Limnos water sampler. Samples were kept in darkness for a few hours until processing at the Tvärminne Zoological Station.

In study V, the phycobilin-related optical signals were investigated. Samples (n=22) were collected during a cruise of R/V Aranda on 12–18 August 2000, after the peak of the cyanobacterial bloom season. The cruise covered the western Gulf of Finland, the northern Baltic Proper, the Åland Sea, and the Gulf of Bothnia. Samples were collected from the ship flow-through system with an inlet at 5 m depth. Processing of samples was conducted on board immediately after sampling. An additional sample was collected by net-haul (0-50 m) using a 200 µm mesh net. From this sample, cyanobacterial filaments were picked for optical measurements.

The operational use of phycocyanin fluorescence in the detection of cyanobacterial blooms in the Baltic Sea was demonstrated in study VI. Ship-of-opportunity data from 9 June to 12 August 2005 was recorded during crossings (n=32) of the cargo ship Finnpartner, commuting between Helsinki and Travemünde (Germany). Water was pumped from the nominal depth of 4 m through the automated measuring system, including fluorometers for Chl$a$ and phycocyanin detection. Discrete water samples were collected at the selected stations using an automated sampler (Isco 3700 R). Depending on the location of the station, samples remained refrigerated between 5 and 36 hours until processing at the Finnish Institute of Marine Research.

3.2 Experimental design of culture and mesocosm experiments

In study II, the effects of nutrient conditions on the fluorescence characteristics of the green alga *Chlorella* sp. (strain TV217) were studied. Batch cultures were grown in modified Erd-Schreiber medium (Hällfors & Hällfors 1992) with or without N addition (N+ and N– respectively). The initial nutrient concentrations for N+ culture were 20 mg NO_3-N L^{-1}, 1 mg NH_4-N L^{-1} and 3 mg PO_4-P L^{-1}. Irradiance was set at 130 µmol q m^{-2} s^{-1} at a 16/8 hours light/dark cycle. Cultures were acclimated to growth conditions for 7 days before inoculation. During the experiment, flasks were shaken continuously. Cultures were sampled for 8 days covering the exponential and stationary growth phase.

The mesocosm experiment of studies II and VII was carried out at Tvärminne Storfjärden between 8 - 28 July 1993. The experiment consisted of eight experimental enclosures (50 m³ each) filled with the surface water of the study site. The natural phytoplankton community was manipulated by various additions of nutrients aiming to induce a series of blooms and by addition of fish aiming to reduce mesozooplankton grazing loss on phytoplankton (Olli et al. 1996). The effect of nutrient status on fluorescence was examined in study II. Three nutrient-enriched units (NP) were observed from experimental day 0 to 10. Mixed water samples (0, 5 and 10 m) were analysed for fluorescence and pigments. Another study (VII) was conducted during this experiment to investigate how multivariate analysis of spectral fluorescence could discriminate phytoplankton biomass in different pigment groups. In study VII four differently manipulated units

were examined from day 7 to 19. The mesocosms were manipulated with nutrient additions (NP), fish (F), and combined nutrient and fish additions (NPF), while one unit received no additions (Control). Details of these manipulations are given in paper VII. Water samples were taken with a Ruttner-type sampler at six depths (0, 2, 4, 6, 8, 10 m) and maintained in darkness for 1-4 hours until measurements were carried out.

Study VII includes comparison of group-specific fluorescence coefficients estimated using linear least squares regression method and fluorescence spectra obtained from pure cultures. For this comparison, I cultured *Synechococcus* sp. (strain CCY9202; Cyanobacteria), *Rhodomonas* sp. (TV22; Cryptophyta), *Thalassiosira pseudonana* (TV5; Chromophyta) and *Chlamydomonas* sp. (TV44; Chlorophyta) in approx. 30 µmol q m^{-2} s^{-1} in a 16/8 h light/dark cycle. Samples for fluorescence measurements were taken during the exponential growth phase.

During a laboratory experiment resolving physiological effects of nutrient limitation on cyanobacteria (P. Ylöstalo, J. Seppälä & M. Raateoja, unpublished), we noted that the commercial FRRF (FAST[tracka], Chelsea Instruments) was inapplicable for detection of variable fluorescence kinetics of the Baltic Sea filamentous species. To demonstrate this, we studied variable fluorescence properties of batch cultures of filamentous cyanobacteria *Nodularia spumigena* (HEM) and *Aphanizomenon* sp. (KAC15) and eukaryotic species *Prymnesium parvum* (KAC39) and *Nannochloris* sp. (TV14) (IV). Cultures were light acclimated at 20 µmol q m^{-2} s^{-1}, and measurements were carried out with cells in the exponential growth phase.

3.3 *In vivo* fluorescence measurements

Various methods and instruments were used to measure fluorescence of living phytoplankton, as summarized in Table 5. In study I, EEM was used to visualize spectral fluorescence of natural phytoplankton communities and the background fluorescence by dissolved organic matter. Additionally, in study VI, EEMs were used to determine whether the optical windows of benchtop field fluorometer using single wavebands were located optimally.

In vivo Chl*a* excitation spectra, resolving the contributions of various light harvesting accessory pigments, were used in all studies. Measurements were carried out at the Chl*a* emission maximum near 682 nm, scanning excitation from 380-400 nm to 660-670nm. Far-red Chl*a* excitation spectra were measured to estimate absorption by PSII (III, IV, V), and for that purpose the excitation spectra were scaled to total phytoplankton absorption spectra (see below). To better separate phycobilin fluorescence from Chl*a* fluorescence, emission spectra at the specific absorption wavelengths of various phycobilins were recorded in study V.

The above-mentioned fluorescence measurements were carried out using a 1-cm quartz cuvette. The number of replicate measurements varied between studies, details are given in the respective papers. Spectra for background fluorescence due to coloured dissolved organic matter and Raman scatter were subtracted. In studies I, IV, and VII, background corrections were obtained by filtering sample aliquots through Whatman GF/F filters (nominal pore size 0.7 µm). In study III, seawater was filtered through 0.4 µm membrane filters (Nuclepore) using low vacuum. Inspection of fluorescence spectra on 30 May 2000 indicated that phycobilin pigments had contaminated the filtrate. It was obvious that cells of the abundant phycoerythrin-containing ciliate *Mesodinium rubrum* had ruptured during filtration and consequently the water-soluble pigments passed the filter. Thereafter in study III, samples were pre-filtered through glass-fibre filters (Whatman GF/F) and no further contamination was observed. Similarly, serial filtration was used in study V. To obtain Chl*a* specific fluorescence, spectra were normalized to corresponding Chl*a* concentrations.

In studies I, III, IV, V, and VII quantum correction of excitation spectra was achieved using Basic Blue 3 (Kopf & Heinze 1984). Oxazine 1 perchlorate was used in study VI. No correction was made in study II. Correction for emission spectra was carried out in study VI using correction

Table 5. Settings of fluorometers in studies I-VII for detection of *in vivo* fluorescence of phytoplankton pigments. Column "DCMU " indicates whether it was added to samples or not. Number of measurements included in each study is indicated (n). Target describes the primary pigments monitored with the given settings.

Study	Excitation [nm]	Emission [nm]	DCMU	n	target	instrument
I	400-640	420-940	no	18	EEM	Shimadzu RFPC5001
I	400-660	682	no	18	Chl*a* exc.spectra	Shimadzu RFPC5001
I	438	682	no	158	Chl*a*	Shimadzu RFPC5001
I	480	682	no	158	Chl*b/c* ->Chl*a*	Shimadzu RFPC5001
I	520	682	no	158	car->Chl*a*	Shimadzu RFPC5001
I	560	580	no	158	PE	Shimadzu RFPC5001
I	630	650	no	158	PC	Shimadzu RFPC5001
I	440	680	no	18	Chl*a* -profiles	Aquatracka, Chelsea Inst.
II	400-670	680	no	34	Chl*a* exc.spectra	Shimadzu RFPC5001
III	380-700	730	yes	132	Chl*a* far-red exc.spectra	Shimadzu RFPC5001
III	440	680	no	21	Chl*a* -profiles	Aquatracka, Chelsea Inst.
IV	380-700	730	yes	4	Chl*a* far-red exc.spectra	Shimadzu RFPC5001
V	380-670	680	yes	66	Chl*a* exc.spectra	Shimadzu RFPC5001
V	380-700	730	yes	66	Chl*a* far-red exc.spectra.	Shimadzu RFPC5001
V	540	550-700	yes	66	PE em. spectra	Shimadzu RFPC5001
V	630	640-700	yes	66	PC em. spectra	Shimadzu RFPC5001
VI	400-660	500-750	no	6	EEM	Varian Cary Eclipse
VI	620	650	no	200000	PC	Turner AU10
VI	460	680	no	200000	Chl*a*	Turner Scufa
VII	400-670	682	no	168	Chl*a* exc.spectra	Shimadzu RFPC5001

spectra supplied by manufacturer. Emission spectra were also recorded in studies I (as a part of EEM) and V, but were not corrected.

In the early studies (I, VII), natural samples were dark-acclimated before measurements to relax non-photochemical fluorescence quenching, and to stabilize fluorescence signal. The rather long dark acclimation period, 1-4 h, was mainly due to logistics of sampling and experiment, while typically dark-period of 15-30 min is required. Later, DCMU (Chem Service Inc. USA) was used to reduce variable fluorescence (III, IV, V). DCMU dissolved in 96% ethanol (2 mmol L^{-1}) was added to the samples (final conc. 20 µmol L^{-1}, and ethanol content <1%), which were subsequently exposed to saturating light for 2-5 minutes to close the reaction centres of PSII.

In study I, rapid screening of the fluorescence of various pigments in the water samples was achieved using fixed waveband fluorescence, combined with an automated sample changer and a microcuvette. The required sample volume was 5-10 mL. In studies I and III, an underwater fluorometer was used for vertical profiling of Chl*a* fluorescence. Finally, in the ship-of-opportunity study (VI), flow-through fluorometers with fixed wavebands were used onboard MS Finnpartner. In the latter application, a continuous flow of water was supplied from the nominal depth of 4 m.

Variable fluorescence in studies III and IV was measured using FRRF (Fast[tracka]). The methodological aspects are given in the respective papers. Additionally, in study IV, the maximum photochemical efficiency at various excitation wavelengths was determined with a bench-top spectrofluorometer (Shimadzu RFPC5001). Several excitation wavelengths from 420 to 590 nm were specifically selected for each species based on their absorption properties. Strictly, minimum fluorescence at dark acclimated state, F_0, is difficult to obtain with this method using a spectrofluorometer with continuous excitation light. Instead, steady state fluorescence, F_S, will be obtained. Maximum fluorescence F_M was obtained after the samples were treated with DCMU (see above). Maximum photochemical efficiency, $(F_M-F_0)\ F_M^{-1}$, was modelled as a function of $(F_M-F_S)\ F_M^{-1}$ measured at various levels of excitation, obtained by placing neutral density filters in the excitation light path. The estimate of $(F_M-F_0)\ F_M^{-1}$ was obtained from the data extrapolated to excitation delivery 0 µmol q m^{-3} s^{-1}.

3.4 Spectral absorption measurements

In vivo absorption of phytoplankton was measured with the filter-pad method using Whatman GF/F filters (II, III, IV, V). Slightly different methods were used in the different studies, due to development of techniques and instruments. All studies used a dual-beam spectrophotometer (Shimadzu 2101-UVPC).

In the experimental study with *Chlorella* sp. (II), filtration volume was adjusted with the help of fluorescence intensity measurements, aiming at constant optical densities on the filter each time. Filters were cut and placed firmly against the wall of a cuvette with some drops of Milli-Q water. An unused wet filter was used as a reference. Spectra were scanned from 750 to 400 nm. Pathlength amplification was corrected for using the wavelength dependent relationship presented by Bricaud and Stramski (1990)

In field studies III and V, samples (250-1000 mL) were measured immediately after filtration (III), or filters were placed onto Petri dishes and stored at –80 ºC for two months (V). Sample and reference filters were placed onto glass microscopy slides and these were placed close to the detector of the spectrophotometer. In study III, a wet blank filter was placed in the reference port. In study V, dry unused filter was placed in the reference port and wet blank filters were measured among samples (for details, see V). Spectra were scanned from 800 to 380 nm. Scattering, assumed wavelength independent, was corrected for by subtracting the average optical density at 780-800 nm (Babin & Stramski 2002). The empirical function presented in Cleveland and Weidemann (1993) was used to correct for pathlength amplification as a function of optical density. In study IV, an integrating sphere accessory was used for absorption measurements (Tassan & Ferrari 1995).

Optical densities were converted to absorption coefficients. In the field studies III and V, total particulate absorption, $a_p(\lambda)$, was decomposed into components of phytoplankton, $a_{ph}(\lambda)$, and non-algal particulate matter, $a_{nap}(\lambda)$. This partitioning was done using the model of Bricaud and Stramski (1990) after some modifications presented in study V. Chl*a*-specific absorption, $a^*_{ph}(\lambda)$, was obtained by normalising the phytoplankton absorption coefficients to Chl*a* concentrations.

To obtain an estimate of light absorption by pigments in PSII (studies III, IV, and V), fluorescence far-red excitation spectra were scaled using the no-overshoot method to $a_{ph}(500\text{-}690)$ resulting in the absorption coefficient of PSII, $a^*_{ps}(\lambda)$ (m^2 (mg Chl*a*)$^{-1}$) (Johnsen & Sakshaug 2007). The scaling factor at the red peak (676 nm) was determined as $a^*_{ps}(676) : a^*_{ph}(676)$. The difference between spectra of $a^*_{ph}(\lambda)$ and $a^*_{ps}(\lambda)$ represent absorption by pigments in PSI and photoprotective carotenoids.

3.5 Other measurements

Chl*a* was quantified using fluorometry. Samples were filtered onto Whatman GF/F filters, and pigments extracted with 96% ethanol for 24 hours. Quantification was carried out with a spectrofluorometer calibrated to Chl*a* standards (I, III, V, VI, VII). In study II, Chl*a* and Chl*b* concentrations in cultures were determined by spectrophotometry using the equations of Jeffrey and Humphrey (1975) and concentrations of total carotenoids by using the equation of Parsons and Strickland (1963). In study II, HPLC was used to quantify Chl*a* and Chl*b* in the mesocosms.

Size-fractionation of phytoplankton samples for Chl*a* and optical measurements was carried out using reverse filtration with 2 and 10 µm (I) or 2 and 20 µm (V) filters. In study VII, subsamples were filtered onto 2 µm membrane filters. Concentrations of Chl*a* and spectral properties for different size-fraction were calculated from the differences between fractions.

Phytoplankton community structure (I, III, V, VI, VII), and cell numbers in culture experiment (II) were determined from samples fixed with Lugol's solution using inverted microscopy (Utermöhl 1958). Cells of picoplankton were counted using epifluorescence microscopy (V, VII). Nutrient concentrations were measured using standard methods (I, V). Underwater spectral downward irradiance was measured using spectral radiometers (LI-1800, LiCor; study III or RAMSES, Trios Gmbh; study IV).

3.6 Statistical methods

Statistical analyses in most studies were limited to Pearson correlations and linear least squares regression. In study VI, multiple regression analysis was used to relate Chl*a* concentration to Chl*a* and PC *in vivo* fluorescence. Study VII dealt with chemometric methods as described below.

3.6.1 Multivariate calibration in spectroscopy

3.6.1.1 Beer's law and least squares methods

According to Beer's law, spectroscopic response (e.g. fluorescence intensity) at a given wavelength is linearly related to the concentration of the analyte and contributions from different analytes are additive (Martens & Næs 1989, Kalivas & Lang 1994). The law is valid for dilute solutions, and in the absence of chemical and physical interferences (e.g. light scattering due to particles, chemical interactions of analytes). Fluorescence properties of living phytoplankton cells are highly variable, depending on their physiological conditions. Thus, strictly, phytoplankton biomass is not linearly related to the fluorescence intensity. However, in study VII, I tested different multivariate calibration techniques to retrieve phytoplankton biomass in various chemotaxonomic groups using spectral fluorescence data.

In the spectroscopic studies of natural waters, like in this thesis, the number of analytes (n) present in the samples is typically larger than one. It is seldom possible to find specific wavelengths for each analyte where there is no overlap with other analytes. For this reason, univariate linear models cannot be used to reliably predict analyte concentrations from the optical signal at one wavelength.

In multivariate calibration, several measured variables are used simultaneously to quantify an unknown variable. In spectroscopy, this translates to using spectral responses of analytes to estimate their concentrations. There are two different linear models of Beer's law, given here in matrix notation:

$$\mathbf{R} = \mathbf{C}\,\mathbf{K} + \mathbf{E}_k \tag{13a}$$

$$\mathbf{C} = \mathbf{R} \, \mathbf{P} + \mathbf{E_r} \tag{13b}$$

where $\mathbf{R}$ is a (l by m) matrix of spectral responses, $\mathbf{C}$ is a (l by n) matrix of analyte concentrations, and $\mathbf{K}$ and $\mathbf{P}$ are (n by m and m by n) matrices of calibration constants. In these matrices, the number of samples is l, the number of wavelengths is m, and the number of analytes is n. Error matrices are presented by $\mathbf{E_k}$ and $\mathbf{E_r}$. Eq. 13a is referred to as the $\mathbf{K}$-matrix approach (also: classical least squares, or reverse calibration) while Eq. 13b is called the $\mathbf{P}$-matrix approach (also: inverse or forward calibration, or multiple linear regression). Though both approaches are used to express Beer's law, they are computationally different (Kalivas & Lang 1994).

The $\mathbf{K}$-matrix approach can represent a basic form of Beer's law. It is a causal physical model where the spectral response ($\mathbf{R}$-matrix) is related to analyte concentrations ($\mathbf{C}$-matrix). Estimates of the spectral coefficients, $\mathbf{K}$, if unknown, are obtained with calibration samples using e.g. least squares (see eq. 6 in study VII). Then, after measuring spectral response of unknown sample ($\mathbf{R_s}$), concentrations for analytes ($\mathbf{C_s}$) in that sample can be calculated as

$$\mathbf{C_S} = (\mathbf{R_S} \, \mathbf{K'})(\mathbf{K} \, \mathbf{K'})^{-1} \tag{14}$$

where $\mathbf{K'}$ is transpose of $\mathbf{K}$. $\mathbf{K}$-matrix method can be used if the number of wavelengths, m, is equal or larger than the number of analytes, n. Including large number of wavelengths may be beneficial in the case of noisy spectral data or when spectrally overlapping analytes are included.

If spectra for pure analytes are not available beforehand, the first critical step in the $\mathbf{K}$-matrix method is calculation of the spectral coefficients, $\mathbf{K}$. This requires careful design of the calibration set to avoid collinearity. Sometimes, like in study VI, there is no possibility for real experimental design to yield a fully orthogonal calibration set, and consequently the goodness of calibration design may be rather fortuitous. The most critical disadvantage for $\mathbf{K}$-matrix method is that all the optically important analytes present in the samples must be included in the analysis. In the presence of unknown analytes (including baseline effects) $\mathbf{K}$-matrix method will give biased results, as spectral responses are considered to take place only due to the analytes included in the calibration phase (Kalivas & Lang 1994).

The use of whole spectra in $\mathbf{K}$-matrix method smoothes out noise and thereby improves precision. As another advantage, matrix $\mathbf{K}$ represents biomass or molar specific optical responses with physical units, and their relevance can be assessed. Further, problems in the fitting can be visualized by plotting residual spectra between the modelled and measured spectra.

In the $\mathbf{P}$-matrix approach Beer's law is rearranged and it is considered that the concentrations of analytes ($\mathbf{C}$ matrix) are function of the spectral response ($\mathbf{R}$ matrix). When concentrations of calibration data set, $\mathbf{C}$, and related spectral responses, $\mathbf{R}$, are determined, calibration coefficients, $\mathbf{P}$, can be calculated e.g. using least squares method. After this, responses for unknown samples ($\mathbf{R_s}$) are measured at the wavelengths used in calibration and concentrations of analytes ($\mathbf{C_s}$) are obtained by multiplication:

$$\mathbf{C_S} = \mathbf{R_S} \, \mathbf{P} \tag{15}$$

The advantage of the $\mathbf{P}$-matrix method, compared to the $\mathbf{K}$-matrix method, is that it does not require information of all the analytes. The major disadvantage of the $\mathbf{P}$-matrix method is that, due to computational reasons, the number of wavelengths m cannot be larger than the number of calibration samples. Consequently, a very important step in the $\mathbf{P}$-matrix approach is to select wavelengths that carry information related to analyte concentrations. In the case that spectral signals of different analytes are largely overlapping, it may occur that there exists no single wavelength where the spectral response and analytes concentration are linearly related. More wavelengths are required in

that case, which may result in collinearity of the spectral data. Further problems appear if spectral responses of analytes and their interferences are poorly known. Instead of the original spectra, latent variables can be used in the **P**-matrix method (Kalivas & Lang 1994). These factor-based methods are described next.

3.6.1.2 Factor based regression methods

When the number of analytes is much less than the number of wavelengths, the spectral responses are typically collinear, thus spectral responses at different wavelengths are linearly related. In such cases the spectra can be compressed. In the method of Principal Components Analysis (PCA) spectral data are reduced to a few linearly independent factors (a.k.a. eigenvector, principal component), represented by matrix **F** (f by m, where f is the number of factors). In PCA solution, score matrix **S** (l by f) reflects the concentrations of different analytes and the original spectral response can be written as:

$$\mathbf{R} = \mathbf{S}\,\mathbf{F} \tag{16}$$

Depending on the number of selected factors and the amount of noise in the data, this solution should describe most of the spectral variations in the original data. Consequently, the number of factors must be optimized, so that they contain most of the information related to analytes, and discard those factors that contain merely noise. Typically it is assumed that the analytes under study have major influence on the spectral variability and the factors are selected using top-down selection (like in study VII). Thus, in PCA the spectral noise is allocated to those factors not used in the final model. Principal Component Regression (PCR) is a two-step process, where PCA is followed by regression step. Normally, this is done using the **P**-matrix approach, where the score matrix (**S**) is used instead of **P**. Thus, like **P**-matrix approach, PCR can be performed for a subset of analytes present in samples. As the spectral compression and regression steps are separated, there is no guarantee that the PCA factors retained are related to the analytes under study.

  Partial Least Squares (PLS) is another method for spectral compression and quantitative analysis. Unlike in PCR, in PLS the steps of spectral reduction and prediction of concentrations of analytes are not separated. Essentially, PLS utilises the correlation between spectral data and concentrations of analytes. In PLS, it is assumed that the changes in the detected signal are due to (few) variables, called latent variables. Their number or contribution is typically not known. The concentrations of analytes are related to these latent variables, and effects of irrelevant spectral variations in the resulting model are reduced.

  First, it is selected whether PLS is run using one or several Y variables (PLS1 and PLS2, respectively). Orthogonalized PLS starts with centering X and Y variables. Then, the maximum number of retained factors is selected larger than number of analytes expected to be present in samples, allowing unexpected phenomena to be modelled. Stepwise, separate scores ($\mathbf{S_R}$, $\mathbf{S_C}$) and factors ($\mathbf{F_R}$, $\mathbf{F_C}$) are computed for both X (**R**-matrix) and Y (**C**-matrix) variables (Martens & Næs 1989, Wold et al. 2001):

$$\mathbf{R} = \mathbf{S_R}\,\mathbf{F_R} \tag{17a}$$

$$\mathbf{C} = \mathbf{S_C}\,\mathbf{F_C} \tag{17b}$$

There are different methods to calculate PLS solution, and orthogonalised PLS algorithms (as given in Martens & Næs 1989) were used in study VII. The key problems in PCR and PLS are that the models and spectral factors are sometimes difficult to interpret, and collection of good calibration set may be difficult, especially if natural samples are used.

3.7 Methods for unpublished studies.

Besides results from the published studies I-VII, this thesis includes results from three unpublished studies, referred as UP-I, UP-II and UP-III.

3.7.1 UP-I: The effects of light intensity and nitrogen deficiency on pigmentation, *in vivo* light absorption, and fluorescence of *Nannochloris* sp. (Chlorophyta) (J. Seppälä, G. Johnsen)

Batch cultures of *Nannochloris* sp. (strain TV1b1) were grown in a modified Erd-Schreiber medium under continuous light at 30 (LL) or 380 (HL) μmol q m^{-2} s^{-1} (PAR). The cultures were acclimated for two weeks. Subsequently, 3-L Erlenmeyer flasks containing 900 mL of nutrient replete medium (HL+N and LL+N) or medium lacking nitrogen (HL-N and LL-N) received 75 mL inoculations. The cultures were kept at 15°C and stirred daily to keep the cells in suspension. Samples for biomass and optical measurements were taken at the time of inoculation (day 0) and at days 1, 2, 4, 7, 11, and 15 (no samples at the last day for HL+N and HL-N). Samples were taken always at the same time of the day, between 9:00 - 12:00 h.

   Samples for cell counts were fixed with Lugols solution. Cell number and size distribution (yielding the biovolume of the cell population) were determined with an Elzone particle counter (Particle Data Europe). Mean cell diameter was calculated according to Stramski and Reynolds (1993). Particulate carbon (POC) and nitrogen (PON) were analysed with a LECA CHN analyser.

   Pigments were quantified with HPLC (SPHERI-5 RP-18 reverse phase C-18 column, detection by absorption at 440 nm and by fluorescence excitation 420 nm, emission 685 nm). *In vivo* fluorescence spectra of DCMU-treated samples were measured using the far-red fluorescence technique with a spectrofluorometer (Hitachi F-3000). Fluorescence spectra were quantum corrected with Basic Blue 3 according to Kopf and Heinze (1984). *In vivo* light absorption spectra were measured from 800 to 350 nm with a dual beam spectrophotometer (Hitachi U-2000) using a wet GF/F filter as a reference. Pathlength amplification factor for *Nannochloris* sp. was determined as in Cleveland and Weidemann (1993).

3.7.2 UP-II: LED fluorometers for phytoplankton studies in the Baltic Sea (J. Seppälä, E. Bauerfeind, F. Pollehne)

Several unialgal cultures were grown at 15°C with light/dark cycle of 16/8 h. Cultures were kept at high white (HL; 400 μmol q m^{-2} s^{-1}) or at low green irradiance (40 μmol q m^{-2} s^{-1}). Samples for fluorescence measurements were taken while cultures were in the exponential phase of their growth curve, and while in the declined phase of growth. *In vivo* fluorescence was measured with LED field fluorometers: (1) Cyclops-7 for Chl*a*, (2) Cyclops-7 for phycoerythrin, (3) Cyclops-7 for phycocyanin (Turner Designs Inc), (4) double-channel fluorometer TwinFlu (TriOS GmbH, channels for Chl*a* and phycocyanin), and (5) double-channel fluorometer miniBackScat SII (Dr. Haardt Optik-Mikroelektronik, channels for Chl*a* and phycobilins). Samples were diluted with culture media so that the readings were in the linear range for each instrument. Background fluorescence was measured from filtrate that was obtained by filtration through Whatman GF/F glassfibre filters. Extracted Chl*a* was measured with a fluorometer (10-AU, Turner Designs Inc).

3.7.3 UP-III: FRR fluorometry to assess nutrient limitation in the Baltic Sea (J. Seppälä, E. Le Floc'h, R. Lignell, R. Geider)

During a mesocosm experiment in Tvärminne (9 units, 50 m³, 30 June-21 July 2003), the natural phytoplankton community was enriched with nutrients (N+P added) for 5 days, in order to induce blooms. After this boosting period, nutrient stress was created by different combinations of daily nutrient treatments (N, P). The mesocosms were sampled daily for variable fluorescence measurements (Fast[tracka], Chelsea Instruments Ltd), which were carried out in the laboratory after 30 min dark acclimation. Chl*a*, inorganic N and P, particulate phosphorus (POP), nitrogen (PON) and carbon (POC) were measured as described in Kangro et al. (2007).

To evaluate various nutrient limitation indicators, non-replicated 24-hour bioassays with factorial 2^2 design, using nutrient additions (NP, N, P), and without additions (Ctrl), were carried out for selected units. Responses of phytoplankton to nutrient additions were measured as change in Chl*a*, and in photosynthetic efficiency, F_V/F_M, by FRRF (as above). Different nutrient sources (internal, external, recycled) supporting phytoplankton growth were analysed using modified dilution experiments as described in Lignell et al. (2003).

4 Results and discussion

4.1 Variability in the bio-optical properties of phytoplankton

Phytoplankton cells can adjust the amount of light energy entering photosystems, and thus optimize resources for growth, by regulating their photosynthetic apparatus qualitatively, quantitatively, as well as functionally. The optical properties of phytoplankton cells are sensitive to changes in temperature, light intensity and spectral quality, and to nutrient stress. The effects of different environmental conditions on cell pigmentation, light absorption, and fluorescence properties were studied in II and UP-I. In both studies a chlorophyte was used as a model organism. The main emphasis was on the detection of responses to nitrogen limitation, and on the effects of photoacclimation. The natural variability in light absorption and fluorescence was studied in I, II, III, V, VI and VII.

In nutrient limited growth conditions, cellular nutrient reserves generally decline, light harvesting and photosynthesis are down-regulated, and consequently growth decreases as a response to decreased nutrient supply (Geider et al. 1998). While several nutrients are required to maintain phytoplankton growth, nitrogen (N), phosphorus (P) and iron are the major nutrients considered limiting in the natural waters. Changes in the photobiology of cells are nutrient-specific (Geider et al. 1993). In the phytoplankton cell, the photosynthetic apparatus is the major reservoir of iron, which plays an important role in several proteins that are essential in the photosynthetic processes (Davey & Geider 2001). Lack of phosphorus may limit the synthesis of nucleic acids and decrease the rate of processes in the Calvin cycle, thereby decreasing the efficiency of light utilization for carbon fixation (Falkowski & Raven 2007). N-stress affects PSII more than PSI, due to the rapid turnover of the N-rich PSII reaction centre proteins, compared to the more stable proteins of the PSI centre (Berges et al. 1996).

Adjustment of cell physiology to changes in irradiance may occur at several temporal scales (Falkowski & LaRoche 1991, Falkowski & Raven 2007). Processes at the short time scale (seconds-minutes) include state transitions, where the distribution of the excitation energy between PSI and PSII is changed, and the xanthophyll-cycle, where specific xanthophylls are de-epoxidated in high light and used to quench excess excitation energy. At longer time scales (hours-days), quantitative and qualitative changes in photoprotective pigments, light harvesting antennas, and stoichiometry

of photosystems may take place (photoacclimation). Photoinhibition occurs at supraoptimal irradiances, when even the photoprotective mechanisms fail. Depending on the duration and intensity of this supraoptimal irradiance, PSII reaction centres are damaged reversibly or irreversibly.

4.1.1 Pigments

In study II, after the onset of N starvation of *Chlorella* sp. culture (after day 2 in N- culture), the synthesis of new pigments ceased (Fig. 3a, b). Eventually, pigments degraded, cellular pigment concentrations decreased, and cells became chlorotic. During this N starvation, the decline was faster in Chl*a* and Chl*b* than in carotenoids, and the amount of carotenoids relative to Chl*a* increased (Fig. 3c). Chl*b*/Chl*a* ratios were comparable in both N-starved and N-replete conditions (range from 0.17 to 0.25 (w:w), average 0.19). A similar decrease in cellular Chl*a* content and increase in carotenoid/Chl*a* ratio was observed for *Nannochloris* sp. in study UP-I (Fig. 4). For *Nannochloris* sp., N limitation took place between days 2 and 4 or between days 4 and 7 for HL-N and LL-N, respectively, as confirmed by time-series of cellular N relative to fresh weight, cellular carbon (C) and Chl*a* (not shown). Clearly, N-limited cells of *Nannochloris* sp., with high C/N ratio, had a lower Chl*a* content (Fig. 5a). C/N ratio was also related to Chl*b*/Chl*a* ratio (r=0.63, n=15), but differences between cultures were not observed, partly because for *Nannochloris* sp. the Chl*b* content was very low (Chl*b*/Chl*a* <0.09 (w:w), see also Raateoja & Seppälä 2001) and no reliable Chl*b* results were obtained in all cases.

The observed decrease in the pigment content of cells and increase in the carotenoids/Chl*a* ratio in N-limited conditions are consistent with previous studies (Sosik & Mitchell 1991, Geider et al. 1998). The relative increase of photoprotective carotenoids may be related to the increased need for thermal dissipation of absorbed light energy, as photosynthesis is decreased during N stress (Geider et al. 1998). Additionally, it must be noted that all chlorophylls, including the common degradation products, contain N, while carotenoids do not.
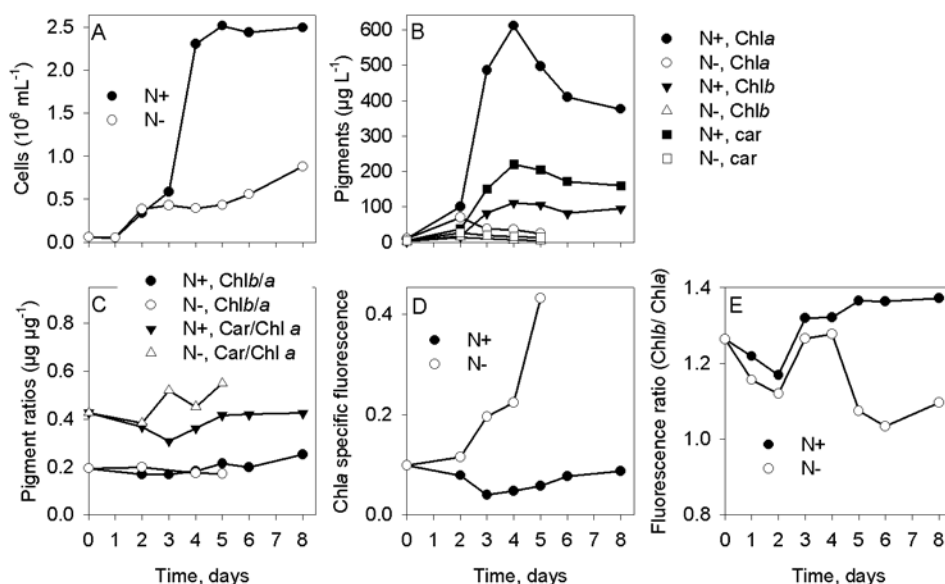

Figure 3. Development of batch cultures of *Chlorella* sp. with (closed symbols) or without (open symbols) nitrogen addition in study II: (A) cell densities, (B) pigment concentrations, (C) pigment ratios, (D) Chl*a*-specific fluorescence, and (E) ratio of fluorescence intensities (emission at 680 nm) after excitation at 480 nm (Chl*b*) to 440 nm (Chl*a*).

Figure 4. Development of batch cultures of *Nannochloris* sp. (study UP-I) grown with media of full nutrients (N+), without nitrogen addition (N-) and in high (HL) or low (LL) light conditions: (A) fresh weight of cells, (B) ratio of Chl*a* to fresh weight, (C) ratio of carotenoids to Chl*a* and (D) relative quantum yield of fluorescence.
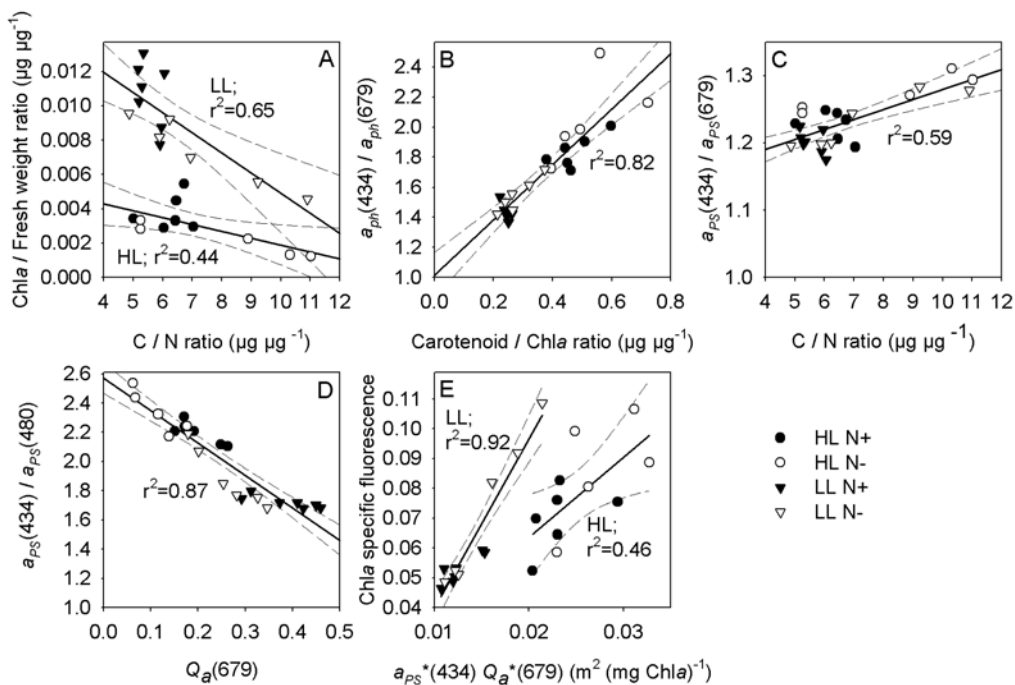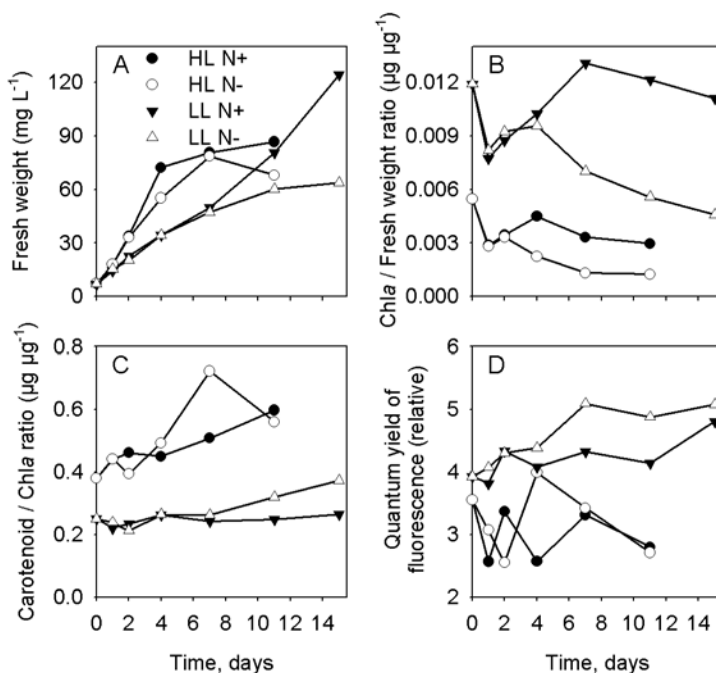

Figure 5. (A) Relationship between carbon to nitrogen ratio and Chl*a* to fresh weight ratio for *Nannochloris* sp. in the study UP-I. (B) Relationship between carotenoids to Chl*a* ratio and blue (a_{ph} (434)) to red (a_{ph}(679)) absorption ratio. (C) Relationship between carbon to nitrogen ratio and blue (a_{PS} (434)) to red (a_{PS}(679)) absorption ratio for photosynthetic pigments. (D) Relationship between efficiency factor for light absorption (Q_a) and (a_{PS} (434)) to (a_{PS}(480)) ratio for photosynthetic pigments. (E) Relationship between the variables in Eq. 12 related to light absorption and Chl*a* specific fluorescence. Linear regression (continuous line, with 95% confidence intervals in dashed lines) are shown for each panel. For A and E, lines are shown separately for two light treatments.

Besides N, irradiance levels affected the pigmentation of *Nannochloris* sp. (UP-I). As a typical photoacclimation response, cells grown in low light had a higher Chl*a* content (Figs. 4b, 5a) because the amount of light harvesting pigments is increased to compensate for lower excitation levels. In high light, the amount of photoprotective carotenoids increased relative to light harvesting pigments (Figs. 4c and 6) to minimize the damage of photosystems due to high irradiance (Falkowski & LaRoche 1991, Geider et al. 1998, MacIntyre et al. 2002). In study II, an additional need for photoprotection may have risen in the N- culture, as the light level inside the culture was relatively high due to low cell densities and chlorosis.
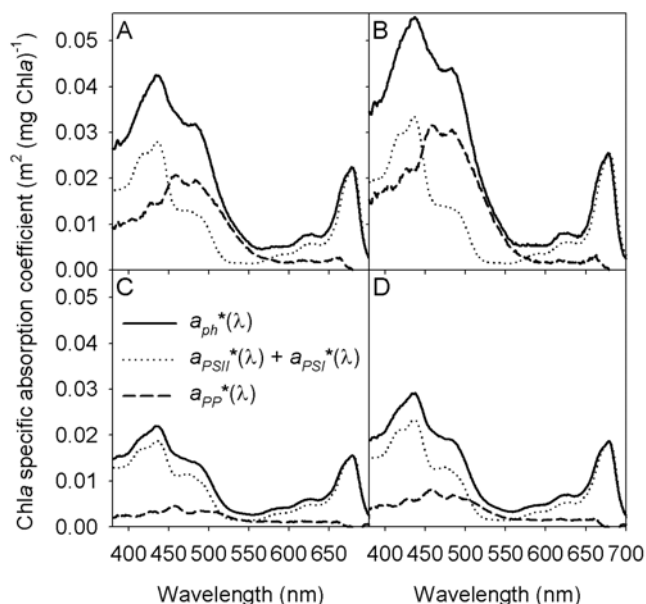

Figure 6. Spectral light absorption of *Nannochloris* sp. (UP-I) grown in (A) high light and nutrients replete conditions, (B) high light and nitrogen depleted conditions, (C) low light and nutrients replete conditions, (D) low light and nitrogen depleted conditions. Chl*a* specific absorption spectra of the whole cells, ($a_{ph}^{*}(\lambda)$), are shown in continuous lines, absorption by photosynthetic pigments, ($a_{PSII}^{*}(\lambda)+a_{PSI}^{*}(\lambda)$), as estimated by no-overshoot method are shown in dotted lines, and their difference, representing absorption by photoprotective pigments, ($a_{PP}^{*}(\lambda)$), are shown in dashed lines.

4.1.2 Light absorption

4.1.2.1 Methods for determining light absorption

In this thesis, the filter-pad method was used to determine light absorption by particulate matter (Yentsch 1962). Using this technique for natural samples, total light absorption by particulate matter can be decomposed into components of phytoplankton pigments and non-algal particulate matter using chemical (extraction or bleaching) or modelling approaches. In studies III and V, the original model of Bricaud and Stramski (1990) was modified, so that one of their assumptions on the normalised shape of phytoplankton absorption was ignored. That assumption, constraining a ratio between $a_{ph}(580)$ and $a_{ph}(692.5)$ (see eq. 3 in the study V), is obviously not valid for situations where PE containing phytoplankton species are present with high absorption in the green spectral region. Instead, a reasonable assumption that $a_{ph}(750) = 0$ was applied, as already suggested by Bricaud and Stramski (1990). Currently, bleaching with NaOCl is applied more often than modelling (Tassan & Ferrari 2002). The two methods provide, however, comparable results (P. Ylöstalo, K. Kallio, J. Seppälä, unpublished).

To obtain an estimate of absorption of photosynthetically usable light, $a_{PS}(\lambda)$ (m^{-1}), Sakshaug et al. (1991) suggested scaling the quantum corrected far-red fluorescence spectra, $F(\lambda)$. They

matched the red Chl*a* fluorescence peak $F(676/730)$ to the corresponding peak in phytoplankton absorption spectra, $a_{ph}(676)$:

$$a_{PS}(\lambda) = F(\lambda)\, a_{ph}(676)\, F(676/730)^{-1} \tag{18a}$$

Because often relatively more photosynthetic accessory pigments are associated with PSII than with PSI, $a_{PS}(\lambda)$, when calculated with Eq.18a, may overshoot $a_{ph}(\lambda)$ at some spectral region (Johnsen & Sakshaug 1993). Subsequently, it was proposed that the scaling at the red peak should be carried out using the proportion of Chl*a* associated with PSII, yielding absorption by PSII, $a_{PSII}(\lambda)$. It was noted that an approximation of $a_{PSII}(\lambda)$ is obtained when spectra are scaled one-to-one at a matchpoint wavelength ($\lambda = mp$), so that $a_{PSII}(\lambda)$ does not overshoot $a_{ph}(\lambda)$ at 540-650 nm (Johnsen et al. 1997, Johnsen & Sakshaug 2007):

$$a_{PSII}(\lambda) = F(\lambda)\, a_{ph}(mp)\, F(mp)^{-1} \tag{18b}$$

The no-overshoot method has been successfully applied to several phytoplankton cultures from various pigment groups (Johnsen & Sakshaug 2007). In study IV, the matchpoint wavelengths between $a_{ph}(\lambda)$ and $F(\lambda)$ were between 570 and 660 nm for cyanobacteria and a prymnesiophyte (fig. 2 in study IV), i.e. in the absorption range for photosynthetic accessory pigments, and similar to the findings of Johnsen & Sakshaug (2007).

Absorption by the photoprotective pigments, $a_{PP}(\lambda)$, is negligible at longer wavelengths (~540-700 nm) (Johnsen & Sakshaug 2007). Therefore, for this spectral range $a_{PS}(\lambda)$ is equal to $a_{ph}(\lambda)$ and is the sum of $a_{PSII}(\lambda)$ and absorption by PSI, $a_{PSI}(\lambda)$ (ignoring absorption by Chl degradation products):

$$a_{PS}(\sim 540-700) = a_{PSII}(\sim 540-700) + a_{PSI}(\sim 540-700) \tag{19a}$$

In the no-overshoot scaling method, a matchpoint is found where $a_{PS}(mp)$ and $a_{PSII}(mp)$ are defined equal, and thus $a_{PSI}(mp)$ is zero. However, it is not so realistic to assume that $a_{PSI}(\lambda)$ always equals zero somewhere in this range. As an example, the matchpoint for green algae *Nannochloris* sp. was at the red peak in all growth conditions (IV, UP-I and Raateoja & Seppälä (2001), see Fig. 6), and there is no reason to conclude that PSI does not contribute to the absorption at the red peak (Culver & Perry 1999).

By allowing an unknown amount of absorption for $a_{PSI}(mp)$, a scaling factor, *sf*, may be introduced,

$$a_{PS}(mp) = sf\, a_{PSII}(mp) \tag{19b}$$

After combining Eqs. 19a and 19b, scaling factor can be expressed as:

$$sf = 1 + a_{PSI}(mp)\, a_{PSII}(mp)^{-1} \tag{19c}$$

If $a_{PSI}(mp)$ is zero (*sf* = 1), $a_{PS}(\lambda)$ obtained with the no-overshoot method yields $a_{PSII}(\lambda)$. In case $a_{PSI}(mp) > 0$, (thus, *sf* > 1), $a_{PS}(\lambda)$ is larger than $a_{PSII}(\lambda)$, but has the shape of $a_{PSII}(\lambda)$. Only in the special case when $a_{PSII}(\lambda)$ and $a_{PSI}(\lambda)$ have a similar shape (e.g. when the same proportions of light harvesting pigments serve PSI and PSII), $a_{PS}(\lambda)$ by the no-overshoot method yields $a_{PSII}(\lambda) + a_{PSI}(\lambda)$ (Culver & Perry 1999). The value of *sf* typically remains unknown. As the matchpoint varies for different species (Johnsen & Sakshaug 2007), it is clear that for natural samples there is no spectral position where PSI absorption can be neglected. Consequently, $a_{PS}(\lambda)$ for natural samples

obtained by spectral scaling (like in III and V) represents something between $a_{PSII}(\lambda)$ and $a_{PSII}(\lambda)$ $+ a_{PSI}(\lambda)$. Suggett et al. (2004) provide a modification of scaling approach to estimate proportion of light absorbed by PSII. They also noted that transfer efficiency is considerably less than 100% for some accessory pigments.

Determined with the no-overshoot method, $a_{ph}(\lambda)$ and $a_{PS}(\lambda)$ for *Nannochloris* sp. were alike at ~540- 700 nm (study UP-I, Fig. 6), and consequently there was a close match in the shapes of absorption by PSI and PSII. Thus, the difference spectra between $a_{ph}(\lambda)$ and $a_{PS}(\lambda)$ approximates $a_{PP}(\lambda)$. To obtain an estimate of $a_{PS}*(\lambda)$ for natural samples, the no-overshoot scaling was used in studies III and V. The resulting scaling factor at the red peak ($a_{PS}*(676) : a_{ph}*(676)$) varied from 0.41 to 1 (with average value 0.85) in study III and from 0.85 to 1 (with average value 0.92) in study V.

An alternative method to reconstruct absorption by photosynthetic pigments includes estimation of pigments by HPLC, discrimination of pigments into photosynthetic and photoprotective ones, and multiplication of concentrations of photosynthetic pigments by their specific *in vivo* absorption coefficients (Bidigare et al. 1989). The error sources in such reconstruction include the inaccuracy in the pigment specific *in vivo* absorption coefficients, problems in determining the amount of package effect (see below), and the variations in the energy transfer efficiencies that are included in fluorescence spectra but not in absorption (Sosik & Mitchell 1995).

4.1.2.2 Package effect and reabsorption

It must be noted that the centre wavelength of the red absorption peak differs slightly between observations, partly due to differences in instrumentation, but mainly due to different protein-bonds among dominant species (Johnsen & Sakshaug 2007). In the subsequent discussion of natural samples, peak wavelengths as determined in study V are used (red peak at 676 nm), and these differ slightly from the peak wavelengths for *Nannochloris* sp. in study UP-I (red peak at 679 nm).

Light absorption of phytoplankton cells is controlled by the pigment composition and the amount of package effect. The package effect is a reduction of light absorption due to self-shading of pigments, compared to the same quantity of pigments in solution (Johnsen & Sakshaug 1996). It is mainly a function of cell size and pigment organization in the cell. An index of package effect, specific absorption efficiency, Q_a* (dimensionless, see Eq. 8), is calculated as the ratio of the Chl$a$-specific *in vivo* absorption coefficient, $a_{ph}*(\lambda)$, to the Chl$a$-specific absorption coefficient of the same material in aqueous solution, $a_{sol}*(\lambda)$,

$$Q_a*(\lambda) = a_{ph}*(\lambda)\, a_{sol}*(\lambda)^{-1} \tag{20}$$

The magnitude of the package effect is typically estimated in the spectral range where only Chl$a$ absorbs and contributions of the other pigments are minimal (i.e. at the red peak around 673-679 nm, though even there absorption by phycobilins and Chl$b$ may have some influence). Determination of $a_{sol}*(\lambda)$ is not trivial, however, and several methods for its determination have been suggested. One assumption is that $a_{sol}*(\lambda)$ is close to the absorption coefficient of pigments in organic solvent, e.g. in acetone, giving a value of 0.0203 m^2 (mg Chl$a$)$^{-1}$ for $a_{sol}*(676)$. Lower values have been reported e.g. by Haardt and Maske (1987), while measurements of unpackaged absorption using dispersed thylakoid fragments yielded a maximum value of 0.027 m^2 (mg Chl$a$) $^{-1}$ (Johnsen et al. 1994a). Differences in the values for *in vivo* and *in vitro* coefficients are, in addition to pigment packaging, due to solvent effects, protein-bonds in intact cells, and absorption by the other cellular material (Johnsen et al. 1994a, Bissett et al. 1997). Recently, Johnsen and Sakshaug (2007) suggested a value for $a_{sol}*(676)$ of 0.033 m^2 (mg Chl$a$) $^{-1}$, as the maximum value they recorded for small-sized cells.

The efficiency factor for light absorption, $Q_a(\lambda)$ (dimensionless) is related to Chl$a$-specific light absorption, $a_{ph}*$, by the following equation:

$$Q_a(\lambda) = (2/3)\, a_{ph}*(\lambda)\, d\, c_i \tag{21}$$

where d (μm) is the diameter of a spherical cell, and c_i (kg m^{-3}) is the intracellular Chl$a$ concentration (Morel & Bricaud 1986). (2/3) d describes the ratio of cell volume to geometrical cross-section. $Q_a(679)$ was calculated in study UP-I. For *Nannochloris* sp., the share of Chl$a$ degradation products and Chl$b$ in total Chl was low, and the absorption at 679 nm is practically due to Chl$a$ only. In theory, the package effect may be considered negligible for very small cells with low Chl$a$ content: the product $d\, c_i$ approaches zero, Q_a approaches zero, Q_a* approaches one, and $a_{ph}*(\lambda)$ approaches $a_{sol}*(\lambda)$. By plotting the experimental results of the product $d\, c_i$ vs. $a_{ph}*(679)$, an intercept value 0.027 m^2 (mg Chl$a$)$^{-1}$ of the linear least-squares fit is obtained (Fig. 7a). As the relation was not linear for the whole range, the highest values of $d\, c_i$ (> 30 mg m^{-2}) were excluded from the analysis. The estimated value for $a_{sol}*(679)$ equals the measured value by Johnsen et al. (1994a) and it is used in the following calculations. The resulting values of $Q_a(679)$ and $Q_a*(679)$ for *Nannochloris* sp. show a nonlinear relationship against $d\, c_i$, with intercepts fixed at 0 and 1, respectively (Morel & Bricaud 1986) (Fig. 7b).
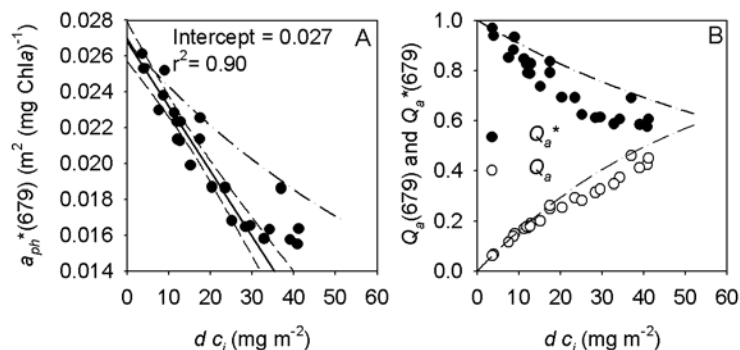

Figure 7. (A) Chl$a$-specific absorption coefficient $a_{ph}*(679)$ as a function of the product of cell diameter (d) and intracellular Chl$a$ concentration (c_i) as measured for *Nannochloris* sp. in the study UP-I. Linear regression (continuous line, with 95% confidence intervals, dashed lines) is calculated for d c_i values < 30 mg m^{-2}. (B) Efficiency factor for light absorption, $Q_a(679)$, and specific absorption efficiency, $Q_a*(679)$, for *Nannochloris* sp. In both figures, dash-dot lines show theoretical fits (Eq. 20-21) when $a_{sol}*(679)$ is 0.027 m^2 (mg Chl$a$)$^{-1}$.

For homogenous spherical particles, Q_a can be modelled as (Morel & Bricaud 1986):

$$Q_a(\lambda) = 1 + 2e^{-\rho'(\lambda)}\rho'(\lambda)^{-1} + 2(e^{-\rho'(\lambda)} - 1)\,\rho'(\lambda)^{-2} \tag{22}$$

where the absorption index $\rho'(\lambda)$ (dimensionless) is defined by

$$\rho'(\lambda) = a_{sol}*(\lambda)\, d\, c_i \tag{23}$$

Using Eq. 20-23, theoretical values for $Q_a(679)$, Q_a* (679) and $a_{ph}*(679)$ can be calculated, as a function of $d\, c_i$. A value of 0.027 m^2 (mg Chl$a$)$^{-1}$ for $a_{sol}*(679)$ does not fully agree with the experimental data (Fig. 7). Actually, the slopes of the experimental data and theoretical model differ clearly regardless of the value chosen for $a_{sol}*(679)$ (not shown). Geider and Osborne (1992) and Lohrenz et al. (2003) show very similar differences when pooling data from several studies. There are several reasons for such a discrepancy. First, the theoretical model is strictly valid for spherical

cells only, and does not take internal cell structure into account. Secondly, absorption measurement errors due to scattering are expected especially if an integrating sphere is not used (as it was not in study UP-I). Further, uncertainties in the pathlength amplification factor in the filter pad-method may bias the absorption coefficients. Thirdly, measurement error in phytoplankton size may occur due to instrumental reasons, or due to fixing of cells (Lugol's solution was used in UP-I). Finally, extraction of pigments may be inefficient and can vary between samples. Unfortunately, it is not possible to identify the most important uncertainties for study UP-I.

Theoretically, $Q_a^*(679)$ varies from 0 to 1, and reported values larger than 1 (e.g. Lohrenz et al. 2003, Bricaud et al. 2004, Babin 2008) are either due to measurement error, error in selection of $a_{sol}^*(\lambda)$ or due to the presence of other pigments/compounds in addition to Chl$a$ that absorb at the red peak. Babin (2008) shows a frequency distribution for Q_a^* with extreme values of 0.2 and 2.1. To estimate the variability of Q_a^* in the Baltic Sea, data in studies III and V was used (Fig. 8a). On average, $Q_a^*(676)$ was 0.64 (corresponding to an $a_{ph}^*(676)$ value of 0.017 m^2 (mg Chl$a$)$^{-1}$) with a range from 0.37 to 0.88 ($a_{ph}^*(676)$ 0.010 to 0.024 m^2 (mg Chl$a$)$^{-1}$).

In studies III and V, the variability in the Chl$a$ specific fluorescence signal (Eq. 12) may be two-fold due to variability in reabsorption, assuming that $Q_a^*(676)$ describes the reabsorption at the emission band of Chl$a$ (around 682nm). It is likely that $Q_a^*(682)$ is slightly higher than $Q_a^*(676)$, as the package effect is less in regions of low absorption (for studies III and V, phytoplankton absorption at 682 nm is approx. 10% lower than absorption at 676nm).

For natural samples, nonlinear relationships have been presented between Chl$a$ concentration and $a_{ph}^*(\lambda)$ (e.g. Bricaud et al. 1995), suggesting that package effect varies predictably with Chl$a$ concentration. Such a global average relationship is not, however, useful for regional or seasonal studies, and large deviations have indeed been observed (Babin et al. 2003). For the pooled data of studies III and V, it is clear that variability in this relationship is large (Fig. 9a). Bricaud et al. (2004) noted that such deviations are related to variations in the package effect due to the size structure of phytoplankton community.
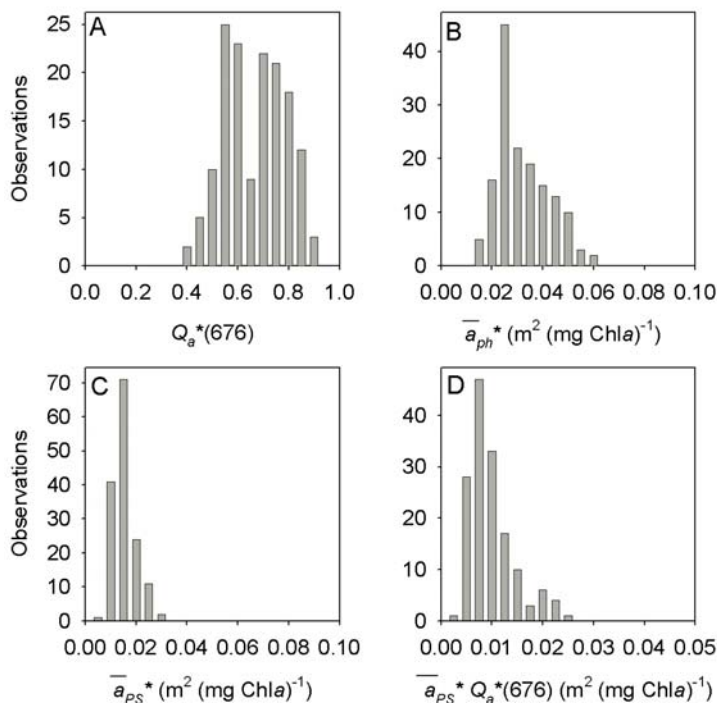

Figure 8. Frequency distributions for (A) specific absorption efficiency, $Q_a^*(679)$, (B) spectrally averaged absorption coefficient of phytoplankton, $\bar{a}_{ph}^*$ (weighted using excitation spectra of Cyclops Chl$a$ fluorometer, Turner Designs Inc.), (C) spectrally averaged absorption coefficient of photosynthetic pigments, $\bar{a}_{PS}^*$ (weighted using excitation spectra of Cyclops Chl$a$ fluorometer, Turner Designs Inc.), and (D) product of $\bar{a}_{PS}^*$ and $Q_a^*(676)$ describing the variation in the fluorescence model (Eq. 12) due to phytoplankton light absorption characteristics. Data is for the natural phytoplankton in the Baltic Sea and is compiled from the studies III and V.
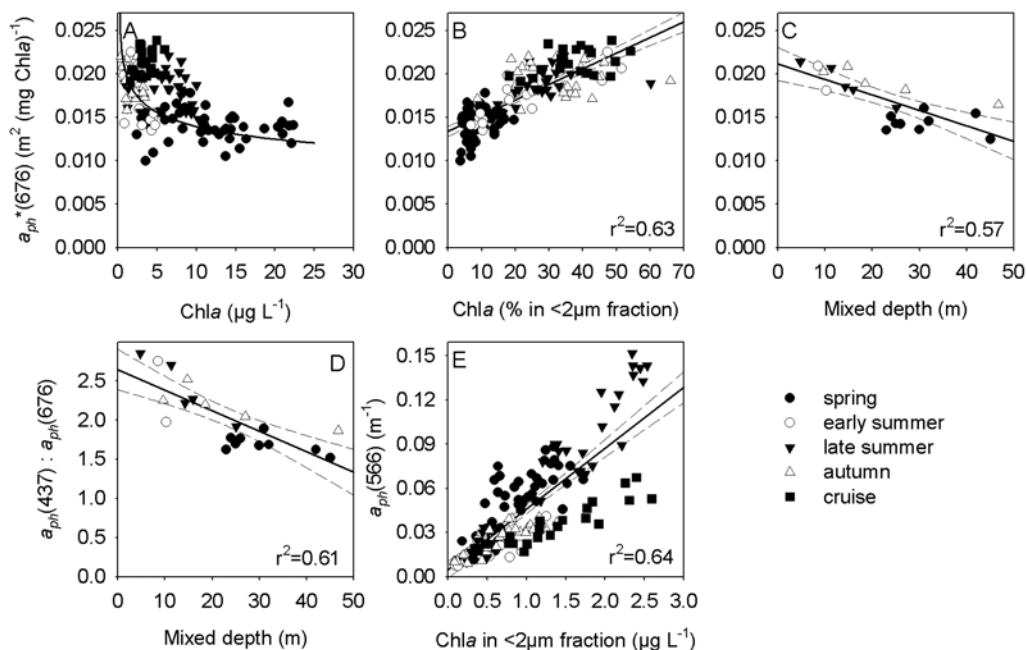
Figure 9. Relationship between (A) Chl$a$ and $a_{ph}*(676)$, (B) fraction of Chl$a$ in picophytoplankton and $a_{ph}*(676)$, (C) depth of mixed surface layer and $a_{ph}*(676)$, (D) depth of mixed surface layer and blue ($a_{ph}(434)$) to red ($a_{ph}(679)$) absorption ratio, and (E) Chl$a$ in picophytoplankton and $a_{ph}(566)$. Data is pooled from studies III and V. Different symbols indicate data collected during different seasons (III), or during a cruise (V). In (A) a power law fit by Bricaud et al. (1995) is shown. In other figures, continuous line shows a linear least squares regression fit (95% confidence intervals with dashed lines).

As a simple index of the size structure, the proportion of Chl$a$ in picophytoplankton (<2µm) explained 63% of the variability in $a_{ph}*(676)$ in my data set (Fig. 9b, n=149). In study V (table 1 and fig. 6d in V), it was shown that $a_{ph}*(\lambda)$ was larger for small cells. Further, the mean diameter of the cells described 71% and 78% of the variability in $a_{ph}*(679)$ of *Nannochloris* sp. HL (n=11) and LL (n=13) cells (study UP-I), respectively (not shown). The slopes between $a_{ph}*(679)$ and cell size for different light treatments were very different (not shown), however, indicating that the overall variability in $a_{ph}*(679)$ is a product of cell size and cellular pigment content (Fig. 7a).

In study III, seasonal variations in the mixing depth explained 57% of the variations in $a_{ph}*(676)$ (averaged over the mixed depth, n=21) and the observed relationship is consistent for various seasons as well (Fig. 9c). This indicates that during periods of deep mixing phytoplankton cells increased their Chl$a$ content to acclimate to lower average light levels (though mixing depth alone does not adequately describe underwater light climate). In the Baltic Sea, the succession of the phytoplankton community is related to seasonality in mixing depth. In spring, with deep mixing, dinoflagellates and diatoms are dominating and these low-light acclimated organisms, with large cells display high pigment packaging. Picophytoplankton that are more abundant in the summer months, with reduced mixing, have very low packaging (Ciotti et al. 2002).

Together, mixing depth and the proportion of Chl$a$ in picophytoplankton explained 87% of the variations in $a_{ph}*(676)$ (n=21) in study III, while the inclusion of Chl$a$ concentration or cumulative daily irradiance in the analysis does not make a significant increase in the coefficient of determination. Temperature explained 49% of the variability in $a_{ph}*(676)$ for >1000 samples collected in various oceanographic regions (Bouman et al. 2003). The mechanism behind such a relationship

is regulation of phytoplankton community structure (species composition and size distribution) by physical processes. Temperature then acts as a proxy for these processes. A similar relation was observed for the data collected in study III, as temperature explained 64% of the variability in a_{ph}*(676) (only samples from the upper mixed layer included, n = 81). Indeed, temperature correlated closely with mixed depth (r=0.67, n=21), and with the proportion of Chl$a$ in picophytoplankton (r=0.74, n=21).

Spatial variability of a_{ph}*(676) in study V was not related to picophytoplankton abundance but rather to the proportion of filamentous cyanobacteria from the total nano- and microphytoplankton biomass (r=0.62, n=22). A possible explanation is that phycocyanin in filamentous cyanobacteria caused elevated absorption at the red peak. a_{ph}*(676) was also positively correlated with salinity (r=0.64, n=22) (fig. 8 in V). This may be related to the change in community structure, change in light conditions (less saline waters are more turbid), or both.

4.1.2.3 Spectral absorption

In addition to Chl$a$, accessory pigments contribute to the spectral shape of a_{ph}*(λ). The simplest way to analyse the spectral variability of a_{ph}*(λ) is the ratio of detected peaks. Typically only the ratio of the blue to the red peak is considered, but as phycoerythrin absorption in the green is an important feature in the Baltic Sea, the variations in the green to red peak are considered here as well.

High values in the blue to red ratio are typical for phytoplankton cells acclimated in high irradiance. Along the increasing irradiance, the concentration of photoprotective carotenoids, absorbing at the blue, increases, while the concentration of Chl$a$ decreases (Falkowski & Raven 2007). Experimental nutrient and light conditions in UP-I affected the pigmentation of *Nannochloris* sp., and the amount of carotenoid pigments relative to Chl$a$ explained most of the variability in the a_{ph}(434) : a_{ph}(679) ratio (Fig. 5b), like in the study of Geider et al. (1998). Such a correlation has been found for natural samples as well (e.g. Lutz et al. 2003).

Roughly, the range for the blue to red peak ratio for natural phytoplankton is from 1 to 5 (Sosik & Mitchell 1995, Babin et al. 2003, Lutz et al. 2003). Generally, the values published for the Baltic Sea are lower than for many other sea areas (studies III, V, Babin et al. 2003), owing to relatively high light attenuation, and thus lower overall requirements for photoprotection. The blue to red ratio of a_{ph}(λ) measured in studies III and V was larger than previously observed in the southern Baltic Sea (Konovalov et al. 1990, Babin et al. 2003). The comparison is limited, however, because in these studies data was collected only during a few days in spring and autumn.

The seasonal changes in the spectral absorption of Baltic Sea phytoplankton are mainly determined by phytoplankton succession, physical forcing of the water column, and the light field. In the seasonal study (III), the mean a_{ph}(437) : a_{ph}(676) was 2.0, with a range from 1.4 to 3.2 (for two typical spectra see fig. 2 in study III). During the spring the ratio was low (on average 1.7), while the highest values, reflecting a high concentration of photoprotective carotenoids, were observed during the summer at times with low mixing depth (Fig. 9d).

Decrease of a_{ph}(437) : a_{ph}(676) with increasing depth was noted only during summer at times of low mixing (III, not shown, two occasions with mixing depth <9m and wind 2-3 m s^{-1}). During other times, the blue to red ratio was vertically uniform throughout the mixed layer. Mixing depth and the amount of picophytoplankton, together explained 82% of the variability in a_{ph}(437) : a_{ph}(676) (n=21). Temperature, which covaries with mixed depth, picoplankton density, and with light, explained a large fraction (71%, n=81) of the variations in a_{ph}(437) : a_{ph}(676). In study V, a_{ph}(437) : a_{ph}(676) had an average value 2.2 (range from 1.7 to 2.5), and no differences were found between different phytoplankton size-groups (for spectra see figs. 5 and 6 in V). In the same study, a spatial pattern of a_{ph}(437) : a_{ph}(676) was found, related to salinity (r=0.70, n=22, see fig. 7 in V).

Because the absorption by photoprotective carotenoids is not included in a_{PS}*(λ), the blue to red ratio is typically smaller and less variable for a_{PS}*(λ) than for a_{ph}*(λ) (Sosik & Mitchell 1995,

Culver & Perry 1999). This was obvious in study UP-I, where the ratio a_{ph}*(434) : a_{ph}*(679) for *Nannochloris* sp. varied from 1.37 to 2.49 (on average 1.69), while the ratio a_{PS}*(434) : a_{PS}*(679) varied from 1.18 to 1.31 (on average 1.23).

Nannochloris sp. (UP-I) had a distinct shoulder in a_{PS}*(λ) around 480 nm in all experimental treatments (Fig. 6), and a_{PS}*(434) : a_{PS}*(480) varied from 1.68 to 2.53 (on average 2.01). Overall, a_{PS}*(434) and a_{PS}*(679) were higher at HL conditions and under nitrogen limitation, while a_{PS}*(480) was rather stable (Fig. 6). To analyse whether the contributions by individual pigments to a_{PS}*(λ) can be resolved, principal component analysis of a_{PS}*(λ) was conducted. The first principal component explained 98% of the spectral variability (not shown) and had a spectral shape resembling closely that of Chl*a*. The second component explained additional 1.2% of the spectral variability and had peaks at 470-480 nm and at 650 nm, marking Chl*b in vivo* absorption. This component covaried with cellular Chl*b* content in the LL-N unit (r=0.84, n=7), but no relation was observed when all the data was pooled. The third component was noisier and explained only 0.3% of the overall spectral variability. However, it could be related to the photosynthetic carotenoids abundant in low light cultures, as it explained 27% and 90% of the variability in a_{PS}*(434) : a_{PS}*(679) ratio in HL and LL cultures, respectively.

In study UP-I, the variations in a_{PS}*(λ) were mainly due to the changes in pigmentation, driven by N availability and light conditions. The ratio a_{PS}*(434) : a_{PS}*(679) correlates with carotenoid/Chl*a* ratio (r = 0.62, n = 24), Chl*b*/Chl*a* ratio (r = -0.61, n = 17), C/N ratio (r = 0.77, n = 24) (Fig. 5c), and Q_a(679) (r = 0.77, n = 24). Similarly, a_{PS}*(434) : a_{PS}*(480) was related to carotenoid/Chl*a* ratio (r = 0.92, n = 24), Chl*b*/Chl*a* ratio (r = -0.75, n = 17), C/N ratio (r = 0.63, n = 24), and Q_a(679) (r = -0.93, n = 24) (Fig. 5d). Thus, N-limitation (high C/N ratio) and acclimation to high light (low Q_a(679)) increase a_{PS}*(434) relative to a_{PS}*(679) or a_{PS}*(480) due to increase of photosynthetic carotenoids relative to Chl*a* and Chl*b*. Fluorescence spectra measured for *Chlorella* sp. in study II were not scaled to absorption, but the relative fluorescence intensity ratio F(480/680) : F(440/680) also shows that during nitrogen limited conditions, relative excitation through Chl*b* diminished (Fig. 3e).

The relative increase of light absorption by PSII accessory pigments, compared to Chl*a*, as a response to low light conditions has been observed for several species from various pigment groups (e.g. SooHoo et al. 1986, Lutz et al. 2001, Johnsen & Sakshaug 2007). Such changes in the shape of a_{PS}*(λ) as a function of decreasing light may occur as light harvesting complexes are increased in number relative to reaction centre Chl*a* (Anderson & Barrett 1986).

The effect of nutrient deficiency on a_{PS}*(λ) has been less studied, but Loftus and Seliger (1975) showed that for various species the spectral fluorescence is identical for cultures in exponential and stationary (potentially nutrient limited) growth phases. Sciandra et al. (2000) showed that shifts in nitrogen conditions affect the spectral fluorescence of *Cryptomonas* sp. at the spectral region where PE (which contains plenty of N and may act as N storage) is absorbing, but other regions were not altered. In their study, the shift from high light conditions to low light conditions, however, increased the share of light absorption by photosynthetic accessory pigments, other than PE. Nitrogen limitation affects similarly fucoxanthin/Chl*a* ratio and spectral fluorescence (ratio of excitation through 550 nm and 440 nm) in *Thalassiosira weissflogii*, but not in *Prorocentrum donghaiense* (Hou et al. 2007). Thus, the effect of nutrient limitation on photosynthetic pigments and spectral properties is not straightforward, and different species may show different responses (Geider et al. 1993).

The observed variations in a_{PS}*(λ) due to light and nutrients in study UP-I are, however, minor when the variability between the phytoplankton groups is considered (fig. 2 in IV, fig. 2 in VI, fig. 4 in VII). These results show clearly that PSII absorption is very low for cyanobacteria at regions of Chl*a* absorption. In eukaryotic phytoplankton groups, >50% of Chl*a* is associated with PSII, while for cyanobacteria this fraction is only 10-20%. The major part of cyanobacterial Chl*a* is located

in non-fluorescing PSI (Johnsen & Sakshaug 2007).Growth conditions affect the cellular content of phycobiliproteins, and their relative abundances. These variations are directly reflected in the shape of $a_{ph}(\lambda)$ and $a_{PS}(\lambda)$. PE containing cyanobacteria may perform complementary chromatic adaptation, by modifying their PE to PC ratio (Tandeau de Marsac 1977) or phycourobilin to phycoerythrobilin ratio (Palenik 2001), while PEC content is regulated by light intensity (Bryant 1982). For some cyanobacteria species phycobilins can serve as a supply of nitrogen, and thus nitrogen deficiency may alter $a_{ph}(\lambda)$ and $a_{PS}(\lambda)$ a lot.

There are not many reported $a_{PS}(\lambda)$ values for natural samples, especially when considering the whole spectral range including the red Chl$a$ peak. Culver and Perry (1999) observed the blue to red ratio of $a_{PS}(\lambda)$ in the Puget Sound to vary from 0.78 to 1.78 (on average 1.26), while the measurements from the Californian Current System (Sosik & Mitchell 1995) had a more narrow range, typically from 1.5 to 2.0. On average, $a_{PS}(437) : a_{PS}(676)$ was 1.4 (range from 0.8 to 2.2) in study III and 1.6 (range from 0.9 to 2.1) in study V. Reasons for these variations are not conclusive based on the data collected in these two studies. Unlike for total phytoplankton absorption, the blue to red absorption ratio for photosynthetic pigments was not related to water mixing depth or changes in the community size structure (studies III and V, not shown). It was pointed out by Sosik and Mitchell (1995) that $a_{PS}{}^*(\lambda)$ has more noise than $a_{ph}{}^*(\lambda)$, because fluorescence is measured using discrete unconcentrated (and sometimes very dilute) water samples, while absorption is measured after concentration of samples onto filters. Another factor complicating the interpretation of $a_{PS}{}^*(\lambda)$ variations in nature is related to the problems in the no-overshoot scaling described in 4.1.2.1.

For study III, $a_{PS}{}^*(\lambda)$ and $a_{ph}{}^*(\lambda)$ were closely related to each other at the green and red peaks, as at these regions the photosynthetic pigments contribute similarly to both spectra (Fig. 10b, c). In the blue, the spectra differed more due to the contribution of photoprotective carotenoids to $a_{ph}{}^*(\lambda)$ (Fig. 10a). The green to red absorption ratio of both $a_{PS}{}^*(\lambda)$ and $a_{ph}{}^*(\lambda)$ varied seasonally, obviously due to phycobiliproteins absorbing at the green spectral region, indicating the presence of cyanobacteria and cryptomonads during the summer months (fig. 2c in III).

The amount of picophytoplankton (measured as Chl$a$ in cells < 2µm) in the natural samples (III and V) correlated with $a_{ph}(566)$ (r=0.80, n=149, Fig. 9e) and with $a_{PS}(566)$ (r=0.79, n=138). Picocyanobacteria often dominate this size-class in the Baltic Sea (Kuparinen & Kuosa 1993), and based on study V, PE is their major pigment. The relationship between picophytoplankton and $a_{ph}(566)$ varied slightly between seasons. The reasons explaining this seasonal variability include the presence of larger PE containing organisms, the presence of picoeukaryotes (which contribute to Chl$a$ but do not contain PE), variable PE to Chl$a$ ratio in picocyanobacteria, and the presence
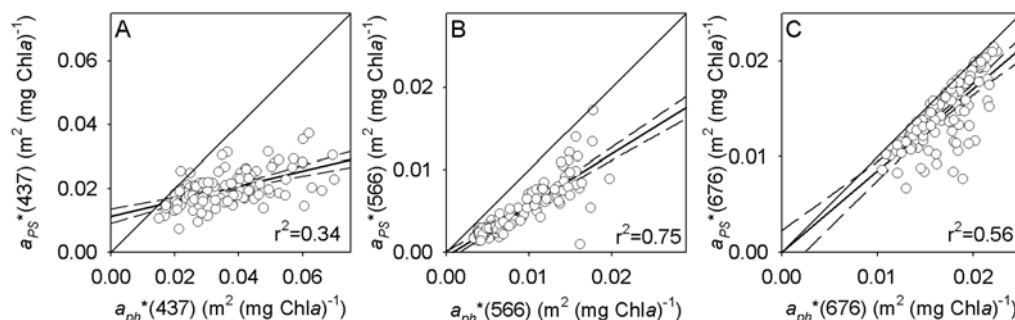

Figure 10. Relationship between (A) $a_{ph}{}^*(437)$ and $a_{PS}{}^*(437)$, (B) $a_{ph}{}^*(566)$ and $a_{PS}{}^*(566)$ and (C) $a_{ph}{}^*(676)$ and $a_{PS}{}^*(676)$ for the natural Baltic Sea phytoplankton during a seasonal study III. In each figure, a bold continuous line shows a linear least squares regression fit (95% confidence intervals with dashed lines) and a thin continuous line shows one-to-one relation.

of other pigments contributing to the absorption in the green. In study V, $a_{ph}(566) : a_{ph}(676)$ and $a_{PS}(566) : a_{PS}(676)$ were higher for picophytoplankton than for larger phytoplankton (fig. 6d and table 1 in V), indicating high content of PE in picophytoplankton.

Models of phytoplankton fluorescence (e.g. Eq. 8-12) include light absorption at the blue peak, because the excitation beam of field instruments is typically centred at 440-470 nm. In the model of Mitchell and Kiefer (1988), $a_{ph}*(435)$ was used to represent light absorption and they note that this varies at least 4-fold between phytoplankton cultures depending on the growth conditions. In a more recent model (eq. 7.1 in Babin 2008), light absorption is weighted by the intensity of fluorometer excitation beam. Babin (2008) shows 10-fold variability in the spectrally averaged absorption coefficient of phytoplankton when weighted by natural irradiance spectra ($\bar{a}_{ph}*$; (m^2 mg Chl$a$)$^{-1}$). For the Baltic Sea, 4-fold variability in $\bar{a}_{ph}*$ was observed in study III (Fig. 11a, table 2 in III). As noted also by Babin (2008), to be relevant for fluorescence modelling (when using an active fluorometer, not natural fluorescence) the weighting must be done using a constant excitation spectrum of fluorometer. Such a scaling was done using the absorption spectra collected in studies III and V, and the spectra of Cyclops 7 Chl$a$ fluorometer (Turner Designs Inc) with a peak wavelength at 460 nm and 20 nm half-width of full–maximum. The observed variability in $\bar{a}_{ph}*$ was 4-fold (on average 0.030 m^2 (mg Chl$a$)$^{-1}$, range from 0.013 to 0.057, Fig. 8b). This parameter describes the total phytoplankton absorption, while only the absorption by PSII should be considered in fluorescence modelling (Eq. 12, or eq. 7.9 in Babin 2008).

When the absorption spectra (from study III) were weighted by natural irradiance spectra, $\bar{a}_{ph}*$ was on average 2 times higher than $\bar{a}_{PS}*$ (Fig. 11a). Both showed similar seasonality with lowest values during spring bloom and highest values during late summer. $\bar{a}_{ph}*$ and $\bar{a}_{PS}*$ decreased towards deeper layers, because the spectral composition of the irradiance changed with depth (figs. 2 and 5a in III). The difference between $\bar{a}_{ph}*$ and $\bar{a}_{PS}*$ was approximately 2-fold when calculated with spectra of Cyclops 7 Chl$a$ fluorometer, in agreement what was found for natural irradiance (Fig. 11a). The resulting overall variation of $\bar{a}_{PS}*$ calculated with the fluorometer spectra was 7-fold (on average 0.013 m^2 (mg Chl$a$)$^{-1}$, range from 0.004 to 0.029, Fig. 8c). When the absorption characteristics of natural phytoplankton included in models of fluorescence ($Q_a*(679)$ and $\bar{a}_{PS}*$, Eq 8-12) were pooled together, they exhibited 15-fold variability (on average 0.0086 m^2 (mg Chl$a$)$^{-1}$; range from 0.0015 to 0.0230, Fig. 8d).
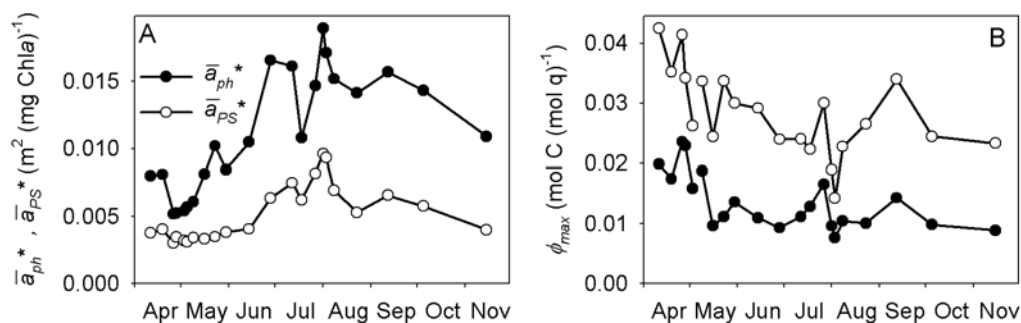

Figure 11. (A) Seasonality of the spectrally averaged absorption coefficient of total ($\bar{a}_{ph}*$) and photosynthetic ($\bar{a}_{PS}*$) phytoplankton absorption when weighted by natural irradiance spectra. (B) Seasonality in the maximum quantum yield for C fixation, calculated using of $\bar{a}_{ph}*$ or $\bar{a}_{PS}*$. Data is from study III.

4.1.3 Chl*a* specific fluorescence and quantum yield of fluorescence

In the various studies included in this thesis, Chl*a in vivo* fluorescence intensity and Chl*a* concentration were overall linearly related (Table 6). This linearity, however, stems from a wide range of Chl*a* concentrations in each study, and the variations in Chl*a* specific fluorescence, *R*, were notable. As presented in Eq. 7-12, *R* includes variables related to light absorption, light reabsorption and quantum yield of fluorescence. Consequently, the variations in *R* take place due to photoinhibition, photoacclimation, nutrient stress, diel rhythm, and the group-specific pigmentation of photosystems (Falkowski & Kiefer 1985). Additionally, instrument properties (the energy of excitation, the spectra of excitation light and emission detection) influence whether F_0, F_M, or something in between is measured (Babin 2008). Moreover, the spectral settings of fluorometer determine the contributions of various photosynthetic pigments, not Chl*a* alone, to the measured signal. The magnitude and importance of these various sources of variation may be studied separately with cultures, but in nature the variations in *R* are more difficult to interpret.

In the N+ culture of *Chlorella* sp. (II), *R* (fluorescence measured with spectrofluorometry at 440 nm) decreased during the start of the exponential growth phase (Fig. 3d). The minimum value was observed during the highest growth rate at day 3, and *R* increased slowly after that. In the nitrogen-depleted culture, *R*-values increased throughout the experiment. The overall variability in *R* was 2.5- and 4.4-fold for N+ and N- cultures, respectively, while the variability was 10-fold when both cultures are considered. A similar pattern was noted when fluorescence was normalized to absorption (fig. 7 in II), but these values were biased by the absorption of photoprotective carotenoids that overlap with Chl*a* and Chl*b* absorption in the blue region. In the mesocosm

Table 6. Variability in Chla specific fluorescence, *R*, during different studies, correlation between Chla concentration and fluorescence intensity, and correlation between *R* and $Q_a^*(676)$, $a_{PS}^*(437)$,phytoplankton community size structure and abundance of cyanobacteria. Correlation coefficients are given when P<0.05. n.a= not available, n.s. = not significant.

Study	Measurement	Variability in R	Correlation coefficients				
			[Chla] vs. Fluores-cence	$Q_a^*(676)$ vs. R	$a_{PS}^*(437)$ vs. R	Size structure [a] vs. R	Cyano-bacteria abundance [b] vs. R
I	In situ CTD fluor-ometer	2.6-fold	0.87	n.a.	n.a.	0.71[a]	-0.52
I	Spectrofluorometry (exc438/em680)	2.5-fold	0.72	n.a.	n.a.	0.60[a]	-0.58
III	In situ CTD fluor-ometer	3.8-fold	0.96	0.33	n.s.	0.47	n.s.
III	Spectrofluorometry (exc 440/ em 730), DCMU	3.5-fold	0.94	n.s.	n.s.	n.s.	n.s.
V	Spectrofluorometry (exc 439/ em 680), DCMU	2.0-fold	0.87	0.54	0.72	n.s.	n.s.
VI	Flow-through fluor-ometry	9.9-fold	0.63	n.a.	n.a.	n.a.	n.a.

[a] % of Chl*a* in <2µm size fraction
[b] % of cyanobacteria from total phytoplankton biomass

experiment (II), the phytoplankton community was manipulated by nutrient additions creating a series of phytoplankton blooms. R varied 5-fold, as a response to the growth stage of the phytoplankton community, the lowest values being observed during intensive growth stage (fig. 8 in II). In these experiments, the increase in R can be related to the decline in photosynthetic activity and the declined quantum yield of PSII photochemistry during the nutrient limitation and the reduced growth of cells. The increase in R may partly be a result of the increase in absorption efficiency, due to the lower package effect of less pigmented cells (Cleveland & Perry 1987).

Variability in R (using DCMU treated samples, thus $R=F_M$ [Chl$a$]$^{-1}$) was 2.3 –fold for *Nannochloris* sp. (UP-I). As photochemical fluorescence quenching was zero when using DCMU, the variation in R should be related to light absorption and non-photochemical quenching. At the exponential growth phase of *Nannochloris* sp., R was higher in high light conditions than in low light conditions. This was explained by the higher a_{PSII}*(440) and higher Q_a* under high light, and together their product explained 55% of the variability in R (n=24). This relationship had different slopes for HL and LL samples, and the fit was more significant for LL (r^2=0.92, n=13) than for HL (r^2=0.46, n=11) (Fig. 5e). Thus, the light absorption properties of phytoplankton controlled the magnitude of R (when photochemical quenching is ignored), especially under the low light conditions. Importantly, as nitrogen availability largely controlled the light absorption, R was also related to the nutritional status of the cells and the C/N ratio explained 69% of the variability in R (n=24).

The variability in R, not explained by light absorption or photochemical quenching, is related to non-photochemical quenching. Based on the scatter in Fig. 5e it is evident that non-photochemical fluorescence quenching was more pronounced in HL cultures. However, non-photochemical quenching cannot be quantified by the measurements conducted in UP-I. To estimate non-photochemical quenching by fluorescence methods require dark-adapted value of F_M using unstressed cells with maximum photochemical efficiency and minimum heat dissipation (Maxwell & Johnson 2000). Short-term non-photochemical quenching related to high energy state quenching and state transitions were obviously relaxed in UP-I, as the samples were kept in a dim light for a relatively long period (minutes-some hours), but relaxation of possible photo-inhibition (damage of PSII) may take several hours (Maxwell & Johnson 2000). As an index of nonphotochemical quenching, a pool of specific photoprotective carotenoids, like zeaxanthin in higher plants and green algae may be used, but zeaxanthin was not reliably detected in UP-I as it co-eluted with lutein in the HPLC column.

To determine the relative importance of various factors affecting R, requires simultaneous measurement of several variables, including variable fluorescence parameters, amount of xanthophyll cycle pigments, a_{PS}*(λ), and Q_a*. Besides these, also the diel cycles of Chl$a$ synthesis and circadian rhythms in the physiological processes modify Φ_F, and thus R (Dandonneau & Neveux 1997). Mitchell and Kiefer (1988) concluded that R is largely determined by the absorption properties of cells, and less by the variations in the quantum yield.

Some previous studies included the absorption of non-photosynthetic pigments in the calculation of fluorescence efficiency (division of R by $\bar{a}_{ph}$*, calculated for fluorometer excitation light) (Cleveland & Perry 1987, Mitchell & Kiefer 1988, Geider et al. 1993, also in study I) mainly because $\bar{a}_{PSII}$* is not easily obtained (but see e.g. Geider et al. 1998). In that case, the calculated fluorescence efficiency does not describe Φ_F for PSII, but it is largely determined by the presence of photoprotective pigments that have high absorption at the typical excitation range of Chl$a$ fluorometers.

In theory, Φ_F can be calculated if all other terms in Eq. 12 are known. Typically, fluorescence measurements (including instrumental factors) use relative units, and consequently only relative values for Φ_F are obtained. For *Nannochloris* sp. (UP-I), relative Φ_F was calculated from spectrofluorometric measurement of maximum fluorescence (after DCMU treatment) with excitation at 440 nm (Eq. 12). In this calculation, the main error source is a_{PSII}*(440) as the obtained value

includes unknown contribution from a_{PSI} (see 4.1.2.1. and Fig. 6). The resulting Φ_F varied 2-fold, and was larger for the cells grown in the low light (Fig. 4d). The difference most likely reflects the variation in non-photochemical quenching.

Recently, Serra et al. (2009) considered nonphotochemical fluorescence quenching as the only source of diel variability in R in natural samples, thus ignoring shifts in package effect and species structure. Diel variability in fluorescence variables has been shown by Dandonneau & Neveux (1997) and observed also in the Baltic Sea during the spring bloom (M. Raateoja, unpublished). Contrary, in study I, R was similar in daytime and nighttime samples though the weather was very sunny. In study VI, R showed slight diel variations in early summer, with maximum R at night and decreased values during the day (not shown). At best, the time of day explained 48% of the variations in R (transect 19.-21. July 2005; second order polynomial, n=12). Later in the summer this diel variability was not significant.

Small cells with a low package effect have high R-values (Alpine & Cloern 1985). Similarly, in the Gulf of Riga (I), higher R-values were observed in the northern Gulf where small cells were more abundant (Table 6, and figs 8b and 11 in I). At the same time, R correlated with the share of filamentous cyanobacteria of the total phytoplankton biomass (r = -0.52, n = 18), and the amount of PE fluorescence (indicating the presence of cyanobacteria, r = -0.77, n = 18). It is known that cyanobacteria have a very low R (IV and VI).

In study III, R (when fluorescence was measured *in situ* with submersible fluorometer) was to some extent related to the package effect (indicated by $Q_a^*(676)$) and size structure of the phytoplankton community (Table 6). Especially in spring, when small picophytoplankton was not abundant (<2 µm share of the total Chl*a* was <20%), R decreased with the increasing abundance of large cells (as >20 µm share of the total Chl*a*, r = -0.69, n = 40). At the seasonal scale, R was related to the relative abundance of picophytoplankton (Table 6), and this relationship was more significant when the spring season was not included (r=0.56, n=44). Although *in situ* Chl*a* fluorescence and Chl*a* fluorescence measured in laboratory (excitation 440 nm, emission 730 nm, DCMU treated samples) were correlated (r=0.95, n=104), R measured with the latter method was not significantly related to the variability in light absorption or phytoplankton community structure. In study V, R (excitation 440 nm, emission 680 nm, DCMU treated samples with) varied 2-fold in the northern Baltic Sea (fig. 10a in V) and was related to the package effect ($Q_a^*(676)$) and $a_{PS}^*(437)$ (Table 6). A combination of the later two variables did not explain the variation in R any better than $a_{PS}^*(437)$ did alone. R-values recorded for size-fractions <2 µm and 2-20 µm were comparable, while the values for >20 µm fraction, containing filamentous cyanobacteria, were rather noisy, and sometimes very low (see fig. 14 in V).

The species-specific variability in R, using various types of commercial LED field fluorometers, was studied in UP-II. Excitation spectra of these instruments are shown in Fig. 12. By comparing these spectra and $a_{PS}^*(\lambda)$ for different phytoplankton pigment groups, it is evident that for cyanobacteria, with very low $a_{PS}^*(\lambda)$ in the blue, R-values will be low (see also fig. 2 in VI). As shown in study IV, LEDs with a maximum around 460-470 nm poorly match $a_{PSII}^*(\lambda)$ of cyanobacteria. Using an instrument with excitation maximum at 460 nm (Cyclops Chl*a*, Turner Designs Inc.), R for cyanobacteria was 4-25 times smaller than for eukaryotic species (Fig. 13a). It is thus clear that in natural samples even slight changes in the biomass of eukaryotic species mask the larger changes in the abundance of cyanobacteria, when measured with Chl*a* fluorescence. One possibility to decrease the group specific variations in R is to increase the spectral bandwidth of excitation light. In another Chl*a* fluorometer tested (miniBackScat SII, Dr. Haardt Optik Mikroelectronic), a blue LED with a very wide spectrum was used. Consequently, the signal from cyanobacteria increased and was now only 2-9 -times smaller relative to eukaryotes (Fig. 13a). Thus, fluorescence and R-values are highly dependent on the spectral settings of the instrument.

Figure 12. Excitation spectra of commercial field fluorometers used in study UP-II. 1. Chl*a* channel of miniBackScat SII (Dr.Haardt Optik Mikroelectronic), 2. Cyclops-7 for Chl*a* 3. Cyclops-7 for PE 4. Cyclops-7 for PC (Turner Designs Inc.) and 5. PC channel of TwinFlu (TriOS GmbH). Each spectrum is scaled to maximum intensity.
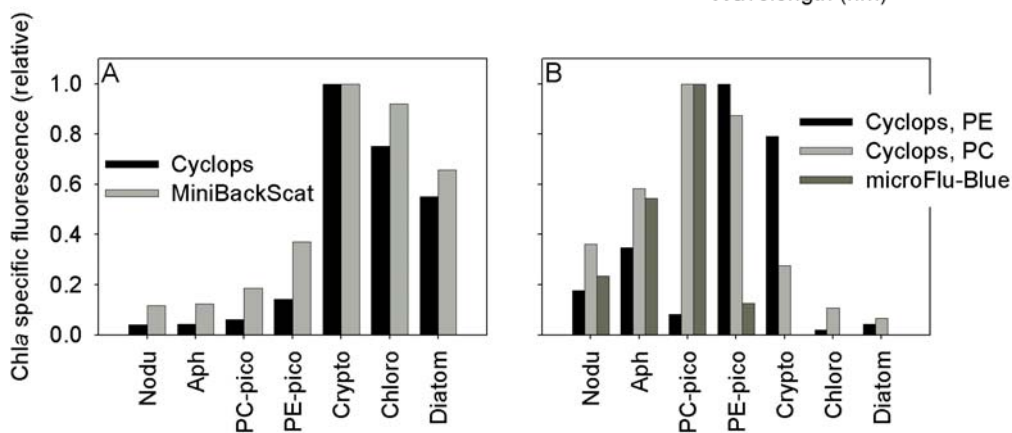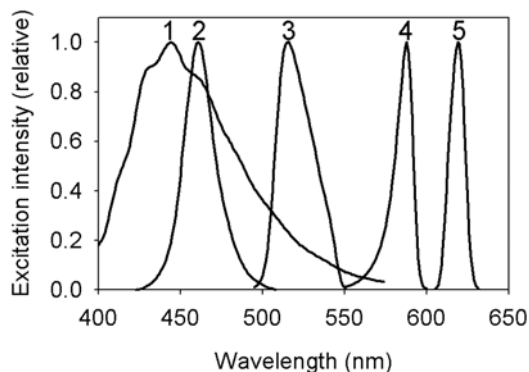

Figure 13. (A) Chl*a* specific fluorescence responses of various algal species as measured with Chl*a* channel of miniBackScat SII and Cyclops-7 for Chl*a* (UP-II). (B) Corresponding phycobilin fluorescence responses, relative to Chl*a* concentrations, measured with Cyclops-7 for PE, Cyclops-7 for PC, and PC channel of TwinFlu. Results are averages for several samples obtained at different growth conditions. Nodu=*Nodularia spumigena*, Aph=*Aphanizomenon* sp., PC-pico=PC rich strain of *Synechococcus* sp., PE-pico = PE rich strain of *Synechococcus* sp., Crypto=cryptomonad *Rhodomonas* sp., Chloro = chlorophyte *Chlamydomonas* sp., Diatom = *Skeletonema costatum*.

During the spring bloom in the Baltic Sea, Chl*a* fluorescence and extracted Chl*a* measurements are typically linearly related, while during the summer months they are not (Kaitala et al. 2008). One obvious reason for the poor fit during summer months is the lower absolute range of concentrations. The first-order source of variation between Chl*a* concentration and fluorescence is the actual phytoplanton biomass, and when the range of concentrations used in the comparison is relatively large, even large variations in *R* seem not to affect the goodness of the regression fit. Using the continuous measurements of Chl*a* fluorescence during summer months (VI), *R* varied 10-fold. The lowest R-values were recorded when filamentous cyanobacteria were most abundant. It was evident that in the Baltic Sea, at times of cyanobacterial blooms, *R* was largely determined by the relative abundance of cyanobacteria.

Summary of major results in 4.1

- Determining absorption by photosynthetic pigments using spectral scaling with the no-over-shoot method represented something between $a_{PSII}(\lambda)$ and $a_{PSII}(\lambda) + a_{PSI}(\lambda)$.
- In the Baltic Sea, seasonality in the phytoplankton spectral absorption and in the package effect was related to physical forcing of the water column and phytoplankton succession. Mixing depth and (related) abundance of picophytoplankton, together explained 87% and 82% of the variability in $a_{ph}*(676)$ and $a_{ph}(437) : a_{ph}(676)$, respectively.
- In cultures, the variations in $a_{PS}*(\lambda)$ were mainly due to changes in pigmentation, driven by nitrogen availability and light conditions, while the variations in nature were more complex and included the variability among the phytoplankton groups.
- Natural variability of the variables included in the fluorescence model (Eq. 12) was large (2.4-fold for $Q_a*(676)$ and 7-fold, for $\bar{a}_{PS}*$).
- In the Baltic Sea, the natural variability in Chl$a$ specific fluorescence was 2-10 fold, and related to the abundance of cyanobacteria, the size structure of the phytoplankton community, package effect, and $a_{PS}*(437)$.

4.2 Calibration of field fluorometers

Fluorescence is measured in arbitrary units, based on an instrument output that is typically a voltage, generated by a photomultiplier tube or photodiode. For field Chl$a$ fluorometers, however, the preferred output is Chl$a$ concentration. Field fluorometers can be calibrated with algal cultures or with water samples taken from the study area. The first approach assumes that the fluorescence properties of the material used for calibration, e.g. an algal culture or a chlorophyll extract, are comparable to those in natural populations. The second approach makes the assumption that fluorescence characteristics of the natural populations do not largely vary during the study period, or geographically. Often it is feasible to carry out both approaches. For operational use, it is very important that the fluorometer is pre-calibrated using a constant secondary standard and this calibration is frequently checked (see study VI). This is the only way to ensure that fluorescence records obtained at different transects or times are comparable.

Both the *in vivo* fluorescence measurement, and the measurement of extracted Chl$a$ concentration are accurate (if instructions for pigment analysis are followed, Wright & Mantoura 1997), and typically the deviations from the linear relationship between these two do not arise from measurement errors. The most common way of relating these two quantities is linear regression. In terms of Eq. (7), this is setting R as a constant (often an intercept term is included, considered as a background fluorescence). As discussed in the previous section, such linearity assumes that terms related to light harvesting, fluorescence yield, and light re-absorption are constants. This is hardly valid for any natural situations.

Linear calibration typically yields a reasonable prediction if samples are collected over a wide range of concentrations, and in a situation where the phytoplankton community structure is not highly variable, e.g. during spring bloom conditions in the Baltic Sea (Kaitala et al. 2008). A linear calibration may lead to biased results when the variability in concentration of Chl$a$ is low or during the changes in the phytoplankton community. Coefficient of determination (r^2) is often used as a measure of the goodness of fit of linear calibration. However, poor linear fit between Chl$a$ concentration and fluorescence does not, as such, mean that R–values vary more than during a good fit. An alternative approach for calibration is a constant R (e.g. average of observations, not slope), Additionally, it is possible to parameterize variations in R due to depth, distance, time of day, or irradiance (e.g. Strass 1990, Dandonneau & Neveux 1997). For example, the horizontal

variations in R in studies I and V (fig. 8b in I and fig. 10a in V) would have allowed a construction of a spatial model.

The match between the excitation light of the fluorometer and $a_{PSII}^*(\lambda)$ of different species affect R (Fig. 13a). Following this, there are two possibilities to increase the prediction ability of Chl$a$ concentration. First, a wider spectral excitation (approaching white light, Figs. 12 and 13) covers the absorption range of most PSII antenna pigments (Babin 2008). The second approach includes separate spectral channel, which allow the user to adjust relative weight of the channels in the validation (e.g. by using multivariate regression).

In Lake Tanganyika, the variations in Chl$a$ concentrations were better explained with both Chl$a$ and PE fluorescence than Chl$a$ fluorescence alone (Salonen et al. 1999). PE fluorescence was required, because PE containing cyanobacteria with low Chl$a$ fluorescence, and obviously with relatively constant PE/Chl$a$ ratio was abundant. Similarly, in the Baltic Sea (VI) the variability in Chl$a$ concentrations was explained more by PC fluorescence than by Chl$a$ fluorescence because PC containing filamentous cyanobacteria was abundant. During the early- and mid-phases of the cyanobacterial bloom, PC alone explained most of the variability in Chl$a$ concentrations, while in the later phases the best prediction was obtained with both PC and Chl$a$ fluorescence (table 1 and figs. 4 and 5 in VI). For the whole summer, using both Chl$a$ and PC fluorescence explained 82% of the variability in Chl$a$ concentration, while Chl$a$ fluorescence alone explained only 39%. Based on study VI, it is clear that during summer months in the Baltic Sea, with high cyanobacterial abundance, PC fluorescence must be recorded along with Chl$a$ fluorescence in order to quantify Chl$a$.

Additional wavebands may be useful for phytoplankton communities with diverse PSII pigmentation (see below 4.4). However, there is no reason to expect a fixed wavelength combination that will give a good prediction in all cases, as in several occasions other terms affecting R are more important. Using the data collected in study III, a stepwise regression analysis with forward selection was performed, to add wavebands to complement the Chl$a$ band in the regression model so that the coefficient of determination was maximised (J. Seppälä, unpublished). After 440 nm, the next most important wavelength was 575 nm, followed by 645 nm. Similarly, using a dataset for Finnish lakes, the best additional wavelengths were 643 nm and 469 nm (J. Seppälä, unpublished).

Chl$a$ concentration can be derived from fluorescence intensity in various ways. The selected method should be described in detail, and for further use, the relation between raw instrument data and a secondary standard must be stored. Whether it is worthwhile to test all possible transformations depends on the application. Moreover, it must be emphasized that processes affecting R are mostly not random, but have predictable seasonal, diel, or spatial patterns. During monitoring activities (e.g. ship-of-opportunity monitoring described in VI) it may be beneficial to improve the knowledge on the variations in R by pooling data from several transects and even several years together (assuming proper referencing and blanking of the fluorometers).

Field fluorometers may supply data to parameterize remote sensing Chl$a$ algorithms. Vepsäläinen et al. (2005) demonstrated the combined use of remote sensing data and flow-through fluorometry during the spring bloom in the Baltic Sea. To match these two data is problematic during cyanobacterial blooms, however. First, Chl$a$ fluorometry is not able to resolve Chl$a$ concentrations during mass occurrence of cyanobacteria, as discussed above. Secondly, bloom forming filamentous cyanobacteria are not uniformly distributed in the water column, but may form surface scums and horizontal patches (Kutser et al. 2004).

Summary of major results in 4.2

- Chl*a* fluorescence cannot be used for detection of cyanobacteria in mixed phytoplankton populations, as the cyanobacteria have very low Chl*a*-specific fluorescence.
- Additional wavebands may improve the fluorescence detection of Chl*a*. During summer in the Baltic Sea, phycocyanin *in vivo* fluorescence must be studied along with Chl*a in vivo* fluorescence to quantify Chl*a*.

4.3 Phycobilin fluorescence in the detection of cyanobacteria

4.3.1 Phycobilins in the Baltic Sea

In the Baltic Sea, the blooms of N_2-fixing filamentous cyanobacteria (mainly *Nodularia spumigena*, *Aphanizomenon* sp., and *Anabaena* spp.) occur frequently during summer months. These blooms may cover large areas and their dynamics and extent cannot be efficiently studied with traditional sampling and microscopy. Satellite images can be used to detect surface accumulations, but the detection limit for PC is high with the current ocean colour sensors (e.g. MERIS; Kutser et al. 2006, Metsamaa et al. 2006).

As phycobilins are specific to cyanobacteria, phycobilin fluorescence may be used to assess the abundance of cyanobacteria (Yentsch & Yentsch 1979). Phycobilin rich phytoplankton species are abundant in the Baltic Sea, and cells benefit especially from PE and PEC, which absorb light at the maximum transmission, 550 to 570 nm (fig. 2 in III and fig. 1 in IV, Table 3). Babichenko et al. (1993) and Poryvkina et al. (1994) suggested that the natural variability in PC fluorescence in the coastal Gulf of Finland, using LIDAR and excitation–emission matrix techniques, was due to filamentous cyanobacteria. They also noted that the phycobilin content of cyanobacteria may be low in surface blooms, as high light acclimated cells downregulate pigmentation. Similarly, in the Gulf of Riga, during intense surface bloom of *Aphanizomenon flos-aquae* very low PC fluorescence was observed (I).

The abundance of various cyanobacterial groups, including single-celled picocyanobacteria, spherical gomphosphaerioid colonies, mucilaginous colonies of pico-sized cells, N_2-fixing filamentous species, and other filamentous species, varies seasonally and in response to environmental factors (Laamanen 1997, Stal et al. 2003). In summer, picocyanobacteria may contribute up to 50% of total phytoplankton biomass in the Baltic Sea (Kuparinen & Kuosa 1993, Stal et al. 2003). In the open Baltic Sea, most of the picocyanobacterial cells are rich in PE according to epifluorescence microscopy (Kuparinen & Kuosa 1993, Niiranen 2008, study V). In study V, the proportion of PC-rich cells varied from 0 to 9% of the total picocyanobacterial cell abundance, and the proportion increased towards low-saline areas (r=-0.63, n=22). Kuparinen and Kuosa (1993) suggested that PC-rich picocyanobacteria are common only in low-saline waters. Contrary to these findings, Stomp et al. (2007) reported that at the entrance to the Gulf of Finland PC-rich picocyanobacterial cells make up 23 - 61% of the all picocyanobacterial cells. Whether this contradiction in the relative abundance of PC-rich picocyanobacteria is due to methodological differences (flow-cytometry in Stomp et al. 2007, epifluorescence microscopy in others) or represents natural variability, is not known. Globally, the abundance of various picocyanobacterial colour-types is related to the spectral light attenuation (Pick 1991, Stomp et al. 2007), PE-rich red picocyanobacteria being most abundant in waters where green light penetrates deepest. In waters where coloured dissolved organic matter efficiently absorbs blue and green light PC-rich green picocyanobacteria are abundant.

Despite the high diversity of the cyanobacteria found in the Baltic Sea, open sea blooms are composed of N_2-fixing filamentous cyanobacteria, while in the coastal areas also other cyanobac-

teria species (e.g. *Microcystis aeruginosa* and *Planktothrix agardhii*, Schiewer 2008) may form blooms. Filamentous *Pseudanabaena* spp. is often abundant in the Baltic Sea (Helcom 2004), like in the samples of study VI. *Pseudanabaena* has two pigmentation phenotypes; PC-rich and another containing both PE and PC (Acinas et al. 2009). In the Baltic Sea, colony-forming picocyanobacteria may occasionally be abundant (Hajdu et al. 2007), but their pigmentation is poorly known.

Study VI showed, based on fluorescence, that *Nodularia spumigena* and *Aphanizomenon* sp. do not contain PE. The lack of PE has been confirmed for several *Nodularia* spp. strains isolated from the Baltic Sea, and grown in various irradiance and nutritional conditions (J. Seppälä, unpublished). PE was also absent in *Aphanizomenon* sp. and *Anabaena* sp. isolated from the Baltic Sea (J. Seppälä & P. Ylöstalo, unpublished). Contrary to these findings, based on immunogold localisation, PE was present in the *Aphanizomenon* sp. cells during a bloom at the central Baltic Sea (Janson et al. 1994). However, several heterocyst-forming species, including all studied *Anabaena* and *Aphanizomenon* strains, contain PEC instead of PE (Bryant 1982). PE or PEC was absent in the *Nodularia* strains studied by Bryant (1982). These strains originated from soil and thermal spring and were phylogeneticly different from Baltic planktonic *Nodularia* strains (Laamanen et al. 2001). Thus, whether Baltic *Nodularia* contains PEC or not, or not always, remains unknown. At the deeper greenish water layers in the Baltic Sea, the green absorbing PEC or PE increases the utilization of light and can promote growth of phytoplankton. The presence (*Aphanizomenon* sp.) or absence (*N. spumigena*) of PEC may explain in part why *N. spumigena* prefers surface waters and *Aphanizomenon* sp. often shows the maximum at deeper layers (Hajdu et al. 2007).

Although the majority of phycobilins can be attributed to cyanobacteria, other phytoplankton groups in the Baltic Sea do contain phycobilins. In the Baltic Sea, cryptomonads contain mainly PE (see fig. 2e in VI and fig. 4 in VII), though their phycobilin content has not been extensively studied, and PC-containing species/strains may occur in coastal areas. The phototrophic ciliate *Mesodinium rubrum*, sometimes very abundant in the Baltic Sea, contains PE (Lindholm & Mörk 1989). Some dinoflagellate species may as well contain PE (Vesk et al. 1996).

During 1994, an extensive cyanobacterial surface bloom, dominated by *Aphanizomenon flos-aquae*, took place in the Gulf of Riga (I). A strong and clear phycoerythrin signal was observed using 560 nm excitation and 570 nm emission, with a secondary emission centered at 650 nm (figs 6 and 7 in I). Such a fluorescence signal is typical for cyanobacteria, which transfer energy from PE to PC to APC (see Table 3). In the areas with the strongest PE signal, cryptomonads were almost totally lacking. In the northern parts where cryptomonads were abundant, PE fluorescence was low. PE fluorescence was not associated with the picophytoplankton either (measured as fractionated Chl*a*, thus picocyanobacteria not separated from the other picophytoplankton), but it correlated with Chl*a* in >10μm cells. Based on this correlation it was hypothesised that the PE signal derived from large cyanobacteria (fig. 12 in I). This contradicts with the pigmentation of *Aphanizomenon* and *Nodularia* discussed above. Further, the EEMs show low noise PE spectra for all stations (fig. 6 in I), while filamentous species often produce noisy signals as they are not evenly distributed in the samples and they are moving inside the cuvette during measurement (it took 30 min to record one EEM).

In study V, spectral studies showed, coincident with the epifluorescence microscopy, that the size-fraction <2 μm does not have notable fluorescence or absorption due to PC (figs 6d, 13a, and 14c in V). Picophytoplankton contributed to PE fluorescence (range 35-100%, average 74%) and picophytoplanktonic PE fluorescence and Chl*a* were correlated (r=0.83, n=22, fig. 15a in V). In turn, PE fluorescence was not related to the cell number of PE-containing picocyanobacteria. This may be due to site-specific variations in the cell size and pigmentation. PE fluorescence was observed for 2-20 μm size-fraction as well, but without the shoulder around 650 nm (observed in the <2 μm fraction), indicating the absence of PC and eukaryotic origin of PE. The highest PE fluorescence for 2-20 μm size-fraction was observed at station LL17 (for location see fig. 1 in V),

where cyanobacterium *Cyanonepheron styloides* and ciliate *Mesodinium rubrum* were most abundant. At a few stations, low PE fluorescence peaks were observed for >20 μm size fraction (this is estimated by difference from measurements of total and <20 μm fractions), but they could not be related to phytoplankton community structure. Like in studies with cultures (see fig. 2 in VI), sample of concentrated filamentous cyanobacteria showed no PE fluorescence. PC fluorescence was generally low relative to the Chl*a* peak (fig. 13 in V). Only the >20 μm size-fraction had a PC-peak at 655 nm (this peak may contain APC fluorescence as well) (figs. 12 and 14c in V). PC fluorescence (excitation 630 nm, emission 650 nm) correlated with the abundance of filamentous cyanobacteria (r=0.76, n=20), or even better with the biomass of the main filamentous species, *Aphanizomenon* sp. (r=0.88, n=20). In samples with a high proportion of *Aphanizomenon* sp., PC fluorescence relative to Chl*a* fluorescence was high (fig. 15b in V).

4.3.2 Detection of phycobilin fluorescence

Commercial field fluorometers are available for *in situ* PE and PC detection, but the waveband settings vary from one manufacturer to another (see Fig. 12). A specific problem for phycobilin detection is that their excitation and emission maxima are typically very close to each other but in order to reject stray light a reasonable separation between excitation and detection wavelengths is required.

The PE fluorescence peak is clearly separated from the other pigments (fig. 2 in VI), and fluorometer wavebands can be slightly adjusted (e.g. to reject stray light, or based on available optical components) without losing specificity. However, detection should not be extended to PC or Chl*a* emission bands (>620 nm). Brief examination of the available LED fluorometers (based on the information the manufacturers provide at their web-pages, spring 2009) reveals that the PE sensors have excitation peak at 525 – 565 nm, while detection is typically at 570-585 nm (though in some instruments detection is done using Chl*a* band at 680 nm). With the original optical kit for PE detection in the common 10-AU fluorometer (Turner Designs Inc.) fluorescence is detected at >570 nm, and Chl*a* emission is included (Niiranen 2008). The natural variability in the fluorescence properties of various PE-forms (Neveux et al. 2006) should be taken into account when selecting wavelengths for PE detection.

PE containing strains of picocyanobacteria *Synechococcus* sp. and cryptophyte *Rhodomonas* sp. showed high response when measured with a PE fluorometer (Cyclops-7 for PE, Turner Designs Inc, UP-II), while the PE-lacking eukaryotic species and picocyanobacteria *Synechococcus* sp. showed negligible PE signal (Fig. 13b) and the PE-lacking filamentous cyanobacteria had intermediate values (PE fluorescence is normalized to Chl*a* content, and thus results are weighted by PE:Chl*a* concentration ratios). Thus there was a slight interference from filamentous cyanobacteria to the PE signal detected with this instrument. This interference was higher with *Aphanizomenon* sp., than with *Nodularia spumigena* and may be due to PEC in the cells

In the commercial PC fluorometers the excitation peaks varies from 585 to 620 nm, and emission is detected either using a narrow (20nm FWHM) window at 645-655 nm or wide window extending from 620 nm above 700 nm (web-survey, spring 2009). Instruments with excitation below 600 nm excite also PE. As an example, the detected PC fluorescence signal was high for species lacking PC or with very low PC content (*Rhodomonas* sp. and PC-poor *Synechococcus* sp., respectively, Fig. 13b) when using an instrument with excitation at 590 nm (Cyclops-7 for PC, Turner Designs Inc., Fig. 12). Those instruments, which detect fluorescence above 660 nm, may receive considerable bias from Chl*a* fluorescence. The interference of PE and Chl*a* was low for an instrument with excitation centred at 630 nm and emission at 655 nm (TwinFlu, Trios Gmbh, Figs. 12, 13b). Brient et al. (2008) discussed the advantages and limitations of this instrument in detail. In a PC-specific fluorometer, the wavebands match the actual PC fluorescence peak well.

The exact location of PC peak varies slightly between species (fig. 2 in VI), and it overlaps largely with APC (which may be important source of fluorescence for some species).

Variability between Chl*a* concentration and *in vivo* fluorescence is widely studied, but for phycobilins such studies are scarce (Wyman 1992), mainly because reliable routine methods for quantitative phycobilin analyses from natural samples have not been reported. Phycobilin fluorescence yield depends on the rates of excitation energy transfer between various phycobilins and from phycobilins to Chl*a* in PSII. Therefore variation in the pigment-specific fluorescence of phycobilins is likely similar to that of Chl*a*.

When phycobilin fluorometers are used in monitoring of cyanobacterial abundance, phycobilin fluorescence is often referenced against biomass or cell number of cyanobacteria (Izydorczyk et al. 2005, Brient et al. 2008, and studies I, V, and VI). Study VI shows linear relation between PC fluorescence and biomass of filamentous cyanobacteria in the Baltic Sea, with no seasonal variability in the relationship (fig. 4a in VI). Ruiz-Verdú et al. (2008) observed that ratio of PC to cyanobacterial Chl*a* was nearly constant in Spanish lakes covering gradient of various trophic states. However, cyanobacteria regulate their phycobilin-content as a response to light and nutrient conditions (Bryant 1986). It can be expected that cyanobacterial populations staying at different water depths are differently pigmented. For example, during sunny and calm conditions filamentous cyanobacteria floating near surface may become phycobilin-poor. In addition, phycobilins can be used as nitrogen supply for growth during nitrogen deficient conditions (Wyman et al. 1985). Therefore the relation between cyanobacterial biomass and phycobilin fluorescence may not be linear.

The results from study VI show that PC fluorescence can be used to detect blooms of filamentous cyanobacteria in the Baltic Sea, at the spatial and temporal scales not available with other methods (see fig. 3 in VI). Recently, new ship lines have been included in the phycobilin fluorescence monitoring in the Baltic Sea, allowing more detailed studies on the development of the blooms. Pooling these fluorescence records with available phytoplankton counts should now be carried out.

Summary of major results in 4.3.

- The specificity of various commercial field fluorometers for phycobilin detection was assessed. It was shown that for reliable phycocyanin detection, instrument wavebands must match the actual phycocyanin fluorescence peak well.
- In the Baltic Sea, phycoerythrin and phycocyanin fluorescence were relevant indicators for abundance of picocyanobacteria and filamentous cyanobacteria, respectively.
- Phycocyanin fluorescence was noted suitable for ship-of-opportunity monitoring of filamentous cyanobacteria in the Baltic Sea.

4.4 Discrimination of phytoplankton pigment groups using spectral fluorescence

Yentsch and Yentsch (1979) suggested that *in vivo* spectral fluorescence signatures may be used to characterise phytoplankton communities. There are several advantages of fluorescence over other phytoplankton detection methods. The detection limit for *in vivo* fluorescence is lower than for many other phytoplankton detection methods and therefore phytoplankton *in vivo* fluorescence can be detected *in situ* without manipulation of samples. Furthermore, the fluorescence of living phytoplankton takes place at wavelengths not disturbed much by the other compounds (Millie et al. 2002) and non-photosynthetic carotenoids with low taxonomic specificity, which modify spectral absorption and reflectance, do not influence the spectral fluorescence (Johnsen & Sakshaug 1996).

Detecting other fluorescence excitation-emission- pairs, in addition to Chl*a* fluorescence (excitation at blue, emission at red), may be useful to obtain better validation of Chl*a* concentration, or to infer some information related to phycobilin-containing organisms of the phytoplankton community, as discussed in the previous sections. In study I, 5 excitation-emission wavelength pairs were selected for the rapid screening of natural phytoplankton, and the results were analysed against phytoplankton counts. Though variability in the fluorescence ratios was evident (fig. 8 in I), only phycoerythrin-related fluorescence correlated with the taxonomic information. This and a parallel study (Babichenko et al. 1999) indicated that simple correlation methods are not able to retrieve high-quality information on phytoplankton community structure.

Instruments with 3-5 wavelength pairs have been made to separate the corresponding amount of taxonomic groups (Beutler et al. 2002, Gaevsky et al 2005). The separation is based on spectral libraries, which contain so-called norm or reference spectra for each taxonomic group. Such a spectral library method is accurate when the reference spectra are constant, like for the extracted pigments (Neveux & Lantoine 1993). For living phytoplankton, however, the biomass-specific fluorescence coefficients (i.e. reference spectra, $\mathbf{K}$ in Eq. 13a) are not constant. These methods with few wavelengths are very sensitive to changes in the reference spectra, but also to variations in the background signal, and they rely on the assumption that all components contributing to fluorescence are included. Despite these limitations, the 5-wavelength method has been noted suitable for cyanobacterial bloom monitoring (Leboulanger et al. 2002), though the added value of various wavelengths was not demonstrated.

Discrimination of various phytoplankton species using fluorescence spectra has been demonstrated for cultures (e.g. Oldham et al. 1985, Gerhardt & Bodemer 2000, Zhang et al. 2006). Typically, the taxonomic groups which contribute 5-10% to the fluorescence signal are resolved reliably. Most such studies describe new instruments, or calculation methods, and usability for natural samples is rarely confirmed.

Spectral libraries with classical least squares regression analysis (e.g. $\mathbf{K}$-matrix method in Eq. 13a) decompose spectral data in straightforward way into the taxonomic groups found in the library. The discrimination may be poor for groups with highly variable spectral properties, and reference spectra does not exist for uncultured phytoplankton groups. Optical properties of natural populations are very dynamic (see section 4.1.) and may be hard to reproduce in laboratory conditions. As an alternative to spectral libraries, biomass-specific fluorescence coefficients may be calculated with a separate calibration step using natural samples with known taxonomical composition (eq. 6 in study VII). This may reduce problems caused by pigment acclimation in nature relative to cultures and by the fact that some species abundant in nature are difficult to culture. Biomass-specific fluorescence coefficients for different taxonomic groups, determined during the mesocosm experiment, were compared with spectra of cultures (VII). For most groups the spectral shapes were comparable but the spectrum estimated for cyanobacteria differed from the one obtained using cultures. Obviously, the cultured cyanobacteria was not representative for the experiment, emphasizing the problems that spectral libraries may encounter.

The least squares regression method used in study VII to separate phytoplankton groups is based on the $\mathbf{K}$-matrix approach of Beer's law (see section 3.6.1.). The model is simple to compute, but sometimes negative concentrations may be obtained. In those cases a method of non negative least squares should be preferred (Lawson & Hanson 1974). Residuals between the observed and the predicted spectra evaluate the spectral fit. Problems in the least squares methods arise when noise or background signals are significant, when spectra of different analytes (here, taxonomic phytoplankton groups) are collinear, or when not all analytes are included in the least squares model. In these cases factorial regression methods perform better, as shown in study VII.

In the PCR method, spectra are first reduced to few independent factors that explain most of the spectral variability. For the application considered here, it may be assumed that these factors

represent reference spectra for various phytoplankton pigment groups (though they do not necessarily do that). In study VII, the two first factors were related to chlorophytes and cryptophytes, respectively, while the additional factors were not explicitly related to any single group. PCR is a two-step process, where spectral reduction is followed by regression step. Therefore, there is no guarantee that factors obtained during the first step, describing spectral data, are related to the concentrations. In PLS both concentration data and spectra are used to build up a model, so that the predictive power is optimised. Consequently, PLS can be used to predict only preferred components (e.g. only one spectral phytoplankton group, if desired). To determine which method gives the most accurate prediction, the model outcomes should be compared analytically, as in study VII. In several cases of spectral analysis using multivariate methods, PLS has been superior (Stæhr & Cullen 2003, Trygg 2004).

Overall, PLS performed better than PCR or least squares methods in the detection of phytoplankton groups in study VII. PLS predicted 79% of the cases correctly, when accepting biomass errors < 0.1 mg L^{-1} or the residuals < ± 20% of the observed biomass. Further restricting these constraints down to 0.05 mg L^{-1} and ± 10% reduced the acceptable predictions down to 57%.

In study VII, biomass of cyanobacteria was poorly predicted with least squares (**K**-matrix approach) and PCR, while prediction was slightly better using PLS (fig. 7 and table 1 in VII). Biomass estimate of picocyanobacteria was the reason for relatively poor prediction of cyanobacteria. PLS for one variable (PLS1) predicted biomass of filamentous cyanobacteria and picoplanktonic Chl*a* (picocyanobacteria dominated this size-fraction in the experiment) accurately, but failed to predict biomass of picocyanobacteria (fig. 9 in VII). This is surprising, considering that picocyanobacteria were more abundant than filamentous cyanobacteria in the experiment, and due to their smaller size they should have been evenly distributed in samples with sufficiently high biomass levels. The obvious reason is that biomass of picocyanobacteria was not accurately calculated, as it was based on fixed cell diameter, though picocyanobacteria is a non-homogeneous group with variable cell sizes and colony types (Kuparinen & Kuosa 1993). Further, phycobilin pigmentation of picocyanobacteria may be dynamic, reflecting light and nutrient availability. The biomass of cryptophytes was sometimes very low, and their absence was predicted in some occasions when using least squares method. The abundance of chromophytes was also low, and they were best predicted by PLS. For the main phytoplankton group, Chlorophyta, the estimates by each method were quite comparable, though PLS performed best.

PLS method (as well as other methods described in VII) requires a careful taxonomic examination of calibration samples, followed by a grouping based on the pigmentation of the various taxonomic classes. The calibration dataset must be created separately for each case, where different spectral groups, or differences in phytoplankton acclimation are expected. PLS is a statistical tool, and may not provide physically meaningful spectral loadings. Therefore the interpretation of the results may be sometimes difficult. Further problems may evolve, if the number of eigenvectors is not optimised, causing over- or underfitting (Martens & Næs 1989). On the positive side, unknown components are not a problem in PLS. Noise and background signals are rejected by factor analysis. Additionally, spectral vectors are directly related to concentrations in a true single step analysis.

Study III provided additional data to evaluate PLS performance with natural communities, and to compare whether absorption or fluorescence spectra (excitation 380-700 nm, emission 730 nm) provides better prediction. Prediction of bulk Chl*a* using the spectra and PLS model was not much different when using a single wavelength at Chl*a* absorption or fluorescence peaks (comparison not shown, but see Fig. 14a & c). PLS predictions were better with absorption than fluorescence spectra. Obviously Chl*a*-specific absorption is much less variable than Chl*a*-specific fluorescence (that includes Chl*a*-specific absorption as one of several terms, Eq. 12). Picophytoplankton, often dominated by PE-containing picocyanobacteria, was related to absorption at green or to PE fluo-

rescence (Fig. 9e). Consequently, PLS model, using the whole absorption or fluorescence spectra, predicted picoplanktonic Chl*a* very accurately (Figs. 14 b & d).

It is clear that absorption and fluorescence spectra of various phytoplankton groups vary seasonally, as a response to environmental conditions and due to changes in species structure. Therefore, methods to discriminate phytoplankton spectral groups should be optimised separately for each study site and season. To test the generality of the approach, I used PLS method to estimate phytoplankton seasonal succession in the Baltic Sea using absorption and fluorescence spectra collected in study III. The predictions using fluorescence spectra were slightly better for cyanobacteria, while the absorption data allowed better predictions for diatoms and dinoflagellates (Fig. 15). In the low concentration range the predicted biomass was higher than observed, while at higher concentrations, the observed and the predicted biomass were quite similar for all groups. Minor phytoplankton groups had a low and noisy contribution to the total optical signal, challenging a reliable prediction. However, biomass estimates from microscopy may also be poor for groups with low abundance.

PLS predictions reproduced the seasonal dynamics of phytoplankton correctly (Fig. 16), especially for total Chl*a* and Chl*a* in <2μm phytoplankton. Both absorption and fluorescence data predict cyanobacterial abundance in spring, not seen in the microscopy, while the actual bloom at July-August was correctly identified. In the autumn, again, optical data predicted the presence of cyanobacteria, which was not observed. Spring bloom of diatoms and dinoflagellates was predicted well, while during summer predictions and observations differed slightly.

The spectral fluorescence methods for the discrimination of phytoplankton groups included three main sources of error. These are 1) diversity of pigmentation inside each pigment group, 2) acclimation of pigments to environmental conditions and 3) variable fluorescence. The latter may be reduced by using an inhibitor of electron transport, such as DCMU (like in study III). For these reasons no single constant spectra exist for any group, making the all-purpose solution unattainable. Absorption spectra performed better than fluorescence (Figs. 14, 15). It must be noted, however, that collection of absorption spectra (here, with filter pad method) is more time-consuming than measuring fluorescence spectra that can be measured directly from water samples, and can be automated.

Spectral methods to discriminate phytoplankton groups may assist the detection of blooms, and provide taxonomic information of dominant species or groups. These methods support but
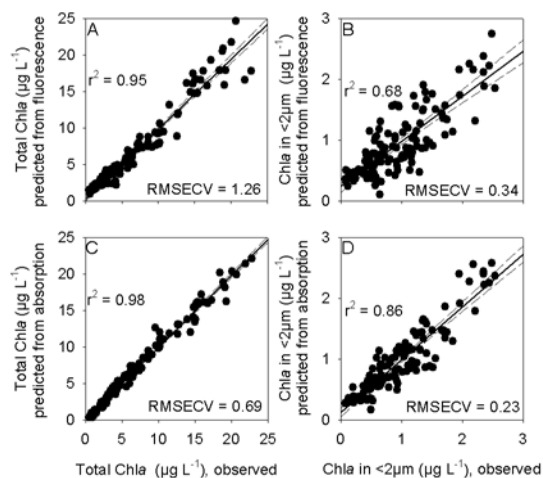

Figure 14. Relationship between observed and PLS predicted Chl*a* concentration in total and <2 μm size fractions when using (A and B) spectral fluorescence and (C and D) spectral absorption collected during study III. Predictions are carried out using full cross validation. Solid line shows linear least squares regression fit (95% confidence limits by dashed line). Values for root mean square error in cross validation (RMSECV), calculated as in VII, are shown.

cannot replace accurate taxonomic methods such as microscopy. Once instruments with sensitivity and robustness suitable for field use are available, these methods can be used to detect more detailed spatio-temporal phytoplankton dynamics. The performance of spectral fluorescence in the discrimination of spectral groups may be further enhanced using EEMs, or including direct emission or excitation lines of phycobilin pigments.
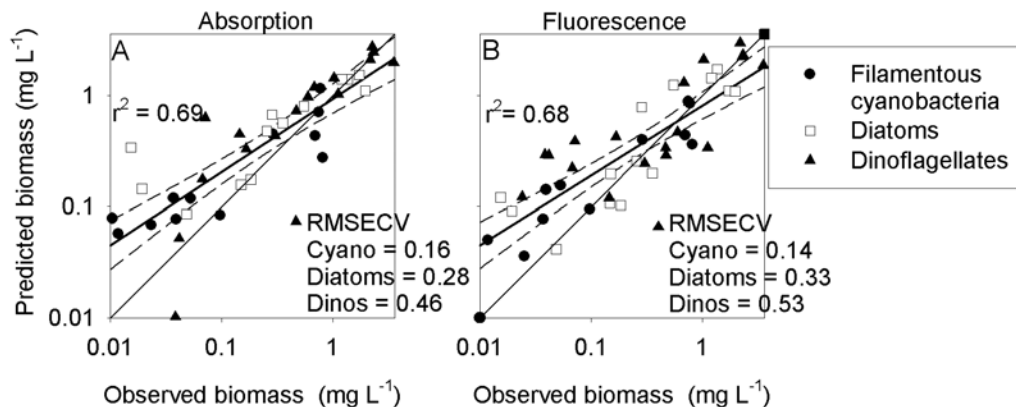

Figure 15. Relationship between observed and PLS predicted phytoplankton biomass in different groups using (A) spectral absorption and (B) spectral fluorescence collected during study III. Predictions are carried out using full cross validation. Bold solid line shows linear least squares regression fit (95% confidence limits by dashed line), thin solid line shows 1:1 relationship. Values for root mean square error in cross validation (RMSECV), calculated as in VII, are shown.
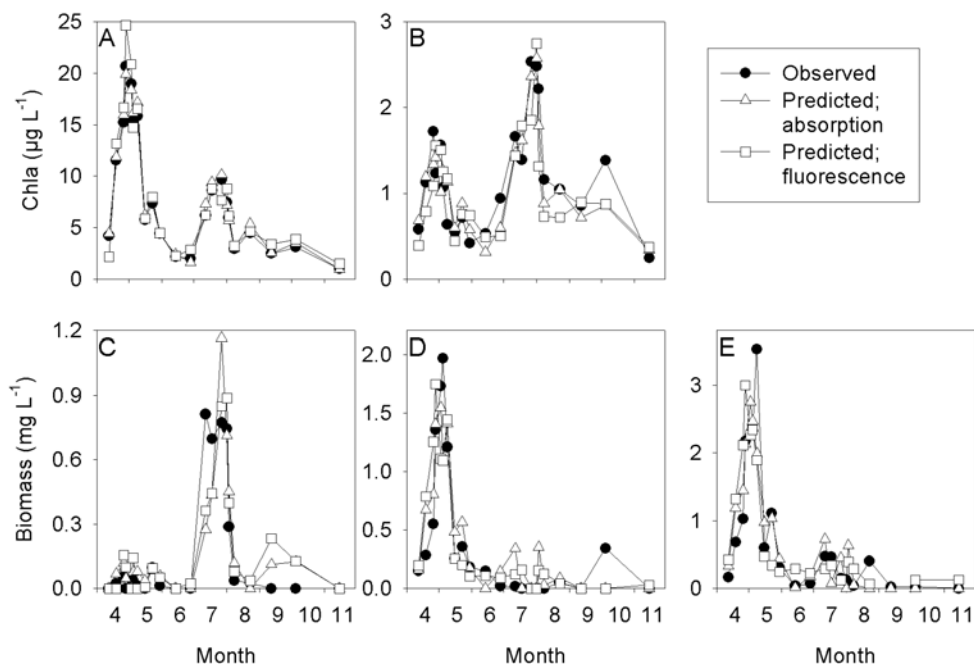

Figure 16. Seasonality in (A) total Chl*a* and (B) Chl*a* in <2 µm fraction, and in biomass of (C) cyanobacteria (not including picocyanobacteria), (D) diatoms, and (E) dinoflagellates in study III, as measured with traditional Chl*a* extraction and microscopy, and when predicted using PLS and spectral absorption and fluorescence (full cross-validation).

Summary of major results in 4.4.

- When multivariate calibration methods to discriminate phytoplankton spectral groups were compared, the partial least squares (PLS) method gave the closest predictions for all taxonomic groups and with the accuracy needed for phytoplankton bloom detection.
- PLS was especially suitable when spectra from different constituents were overlapping, the background noise was high and variable, and not all of the optically active compounds were known.
- PLS required a good calibration data set, with no collinearity of constituent concentrations.

4.5 Fluorescence methods to detect phytoplankton physiology

4.5.1 Photosynthetic efficiency of filamentous cyanobacteria measured by FRR fluorometry

For healthy cells the maximum F_V/F_M is considered to be close to 0.65 (Kromkamp & Forster 2003, Suggett et al. 2003). However, for filamentous N_2-fixing cyanobacteria *Nodularia spumigena* and *Aphanizomenon* sp. F_V/F_M varied from 0.02 to 0.20 and was rather insensitive to variations in nutrient status of cells or growth stages, when measured with commercial Fast Repetition Rate fluorometer (FRRF) (IV). The principle of FRRF is a cumulative closure of reaction centres using short intense flashes of blue light. For PE-lacking N_2-fixing filamentous cyanobacteria PSII absorption was very low in the wavelength region of FRRF excitation (fig. 2 in IV). Consequently, FRRF excitation light did not saturate PSII of these cyanobacteria during a measurement cycle, and the resulting F_V/F_M were much lower than for eukaryotes (table 1 in IV). An increase of flash duration did not give any improvement (not shown). The addition of DCMU into dark acclimated sample increased F_V/F_M, but still the electron transport chain was not totally saturated. When additional green background light (that was absorbed by PSII pigments) was supplied, F_V/F_M increased remarkably and was close to 0.65, indicating healthy and active cells (table 1 in IV).

Another possibility considered for low F_V/F_M is the elevated F_0 levels due to phycobilin and PSI fluorescence. However, in that case both DCMU induced and spectrofluorometric methods should give low values for F_V/F_M, which was not observed (table 1 in IV). Phycobilin content of cyanobacteria determines whether excitation light (95% of light is between 458 to 514 nm for commercial FRRF Fast[tracka]) is absorbed efficiently enough to yield unbiased F_V/F_M values. The bulk of oceanic cyanobacteria contain a phycourobilin-rich form of PE (absorption at 495-500 nm, Wood et al. 1998, Neveux et al. 2006) and obviously in healthy growth stages show high F_V/F_M values. Potentially the inapplicability of FRRF fluorometry is limited to only those cyanobacteria species lacking PE (see Bryant 1982). Using other type of instruments, like multiple turnover fluorometers, or yellow-red excitation light, also N_2-fixing filamentous cyanobacteria show high F_V/F_M values.

During study III, filamentous cyanobacteria comprised up to 60% of the total biomass of the nano- and microphytoplankton community in late summer but this seemed to have no effect on *in situ* F_V/F_M values (Fig. 17). Because of the low Chl*a* specific fluorescence response of all cyanobacteria, FRRF method measures mainly the eukaryotic part of the phytoplankton community. Even at times of cyanobacterial blooms, eukaryotic species are abundant, apart from the dense surface accumulations of cyanobacteria. By selecting appropriate wavebands for excitation (e.g. specific for phycocyanin), PSII saturation for cyanobacteria should be obtained and cyanobacterial response could be separated from eukaryotic species.

Figure 17. Seasonality in (A) Chl*a* and the share of filamentous cyanobacteria out of the total nano- and microphytoplankton in study III and (B) photochemical efficiency, $(F_M'-F_S)/F_M'$ and effective absorption cross section, σ_{PSII}', measured under ambient natural light in the SW Finnish coastal zone, northern Baltic Sea. Fluorescence measurements are averages from 6, 9 and 15 m, and standard deviations are shown as errorbars. Times of potential nitrogen (N) and phosphorus (P) limitation are shown (where concentrations were below 1 and 0.1 µmol of inorganic N and P L^{-1}, respectively).
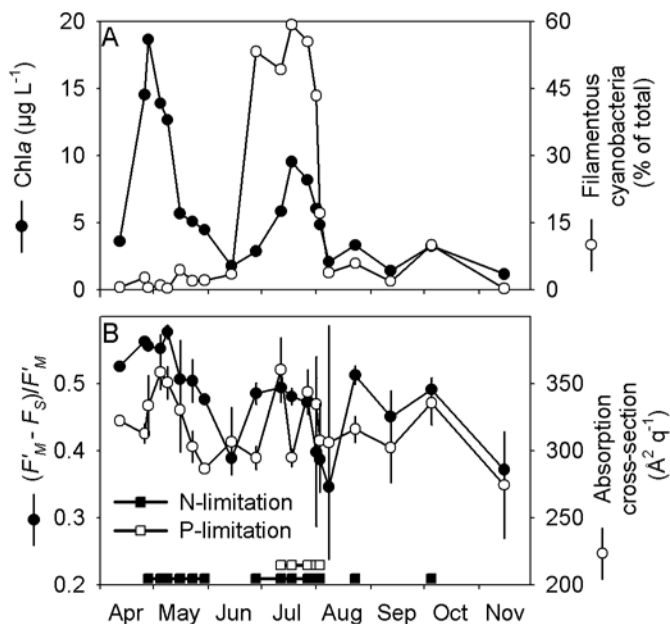
4.5.2 Spectral light absorption by photosynthetic pigments

The maximum quantum yield of photosynthesis, Φ_{max}, is the rate of CO_2 fixed per absorbed photon, with a theoretical maximum of 0.125 mol C (mol q)$^{-1}$ (Falkowski & Raven 2007). Φ_{max} is calculated as

$$\Phi_{\max} = \alpha \, \bar{a}_{ph}*^{-1} \tag{24}$$

where α is the initial slope of the photosynthesis-irradiance curve, and $\bar{a}_{ph}*$ is calculated for the experimental light conditions (Falkowski & Raven 2007). In study III, Φ_{max} varied 3-fold, from 0.0076 to 0.024 mol C (mol q)$^{-1}$ (Fig. 11b), while both smaller and higher values have been obtained in other studies (reviewed by Babin et al. 1996, MacIntyre et al. 2002). There are several reasons why the observed Φ_{max} is considerably lower than the theoretical maximum, including the increased absorption by photoprotective pigments, the decrease of competent reaction centres due to irradiance or nutrient stress, and electron sinks other than CO_2 during the light reactions (Sakshaug et al. 1997, MacIntyre et al. 2002). Importantly, the calculation of Φ_{max} as above includes absorption of light by photoprotective pigments that do not transfer the energy to photosystems.

To separate variability of Φ_{max} due to photoprotective and photosynthetic pigments, $\bar{a}_{PS}*$ may be used instead of $\bar{a}_{ph}*$ in the calculation of Φ_{max} (Sakshaug et al. 1991). Then, Φ_{max} in study III varied from 0.014 to 0.042 mol C (mol q)$^{-1}$, 2.2 times higher than values calculated with $\bar{a}_{ph}*$ (Fig. 11b). The difference was smallest during spring, with the lowest amounts of photoprotective pigments. Most of the Φ_{max} values presented in the literature are still based on $\bar{a}_{ph}*$.

Phytoplankton primary production may be modelled using the variable fluorescence technique (e.g. Kromkamp & Forster 2003, Suggett et al. 2003, III). In FRRF, the functional cross-section of PSII is measured. In contrast, with the pulsed amplitude modulation (PAM) technique, quantification of the light absorbed by PSII has been traditionally estimated to equal 50% of total absorption, to achieve an equal light absorption between PSI and PSII. This, however, neglects the presence of photoprotective pigments, and the fact that PSII:PSI ratio is often above unity (Johnsen & Sakshaug

2007). Consequently, the most reliable prediction of oxygenic photosynthesis is obtained with PSII absorption, $\bar{a}_{PSII}$*, estimated using the no-overshoot method (Hancke et al. 2008).

The examples above underline the value of correct $\bar{a}_{PSII}$* measurements. As stated in section 4.1.2.1, the existing measuring techniques are valid for cultures, but not strictly for natural phytoplankton samples where various species, with variable PSII and PSI spectra, are present. $\bar{a}_{PSII}$* for natural phytoplankton communities are not often reported, and to my knowledge, potential methodological errors have not been studied.

4.5.3 Variable fluorescence to assess nutrient limitation

Eutrophication, due to anthropogenic load of nutrients, is a severe threat to many coastal seas like the Baltic Sea (Elmgren 2001). For the management of these ecosystems, the identification of the limiting nutrient is important when deciding on nutrient load reductions. For the determination of phytoplankton nutrient limitation various indicators are available, including nutrient concentrations and ratios, nutrient uptake and turnover rates, responses of biomass and productivity in bioassays, and enzyme activity (e.g. Beardall et al. 2001). As phytoplankton photochemistry is sensitive to nutrient stress, the efficiency of photochemistry, measured with variable fluorescence techniques, is among the methods used in the detection of nutrient limitation of natural phytoplankton populations (Graziano et al. 1996, Behrenfeld et al. 2006). Generally, nutrient limitation is considered to lower the efficiency of PSII photochemistry, F_V/F_M, and increase the effective PSII absorption cross section, σ_{PSII} (Kolber et al. 1988, Berges et al. 1996). Each of the abovementioned methods has limitations and often the combined use of several techniques/parameters is required to correctly identify nutrient limitation.

Study III estimated *in situ* variable fluorescence for the northern Gulf of Finland. The measured photochemical efficiency under natural light was represented by $(F_M'-F_S)/F_M'$, where F_M' is maximum fluorescence measured under natural light, and F_S is steady state fluorescence. The spectrally unscaled PSII absorption cross-section under ambient light, σ_{PSII}', was used to obtain comparable results from various depths (see study III). To avoid the effects of high irradiance at the surface, only the values measured between 6 and 15 m were used. High $(F_M'-F_S)/F_M'$ values (>0.5) persisted throughout the spring bloom, even though inorganic N depleted and the bloom declined (Fig. 17). Thereafter, slightly lower values were observed, while both inorganic N and P were low. The times of possible nutrient limitation were estimated using concentrations of inorganic nutrients, as shown in Fig. 17. There is no indication that $(F_M'-F_S)/F_M'$ was especially low, or σ_{PSII}' especially high at these times. The exceptional drops in $(F_M'-F_S)/F_M'$ in mid-June (0.39) and beginning of August (0.35) were recorded during upwelling events, and thus at the times of high inorganic nutrient concentrations. The low photosynthetic competence during upwelling could be related to photoinhibition or the uplift of physiologically incompetent cells. For the whole study, $(F_M'-F_S)/F_M'$ was related to Chl$a$ (r=0.68, n=58), and thus the high $(F_M'-F_S)/F_M'$ values were observed during bloom peaks. This relationship was not, however, fully linear (not shown). σ_{PSII}' varied from 210 to 380 Å^2 q^{-1} (average 318 Å^2 q^{-1}) (Fig. 17b), and was not related to package effect, absorption coefficients, nutrient situation nor community structure. Suggett et al. (2004) concluded that *in situ* variability in σ_{PSII} is related to both physiological and taxonomical information.

In a mesocosm experiment with a natural phytoplankton community (UP-III), combined addition of N and P (balanced addition in Redfield ratio) resulted in a phytoplankton bloom and Chl$a$ increased from 3.5 to 20 μg Chl$a$ L^{-1}. During this nutrient replete boosting period, F_V/F_M varied from 0.52 to 0.58 (Fig. 18). After day 5, the daily nutrient treatments of different units were split to create either N or P deficiency. Thereafter F_V/F_M declined in all units down to values 0.42-0.49 towards the end of the experiment (see Fig. 18).

Figure 18. Dynamics of F_V/F_M and inorganic nutrient concentrations in two mesocosms during an experiment in Tvärminne, July 2003 (UP-III). Both units received balanced N and P additions (1 µmol NH$_4$-N L^{-1} d^{-1}, N:P = 16:1 mol/mol) for 5 days (vertical lines in panels). After this boosting period units were manipulated with daily N (A) or P –additions (B).
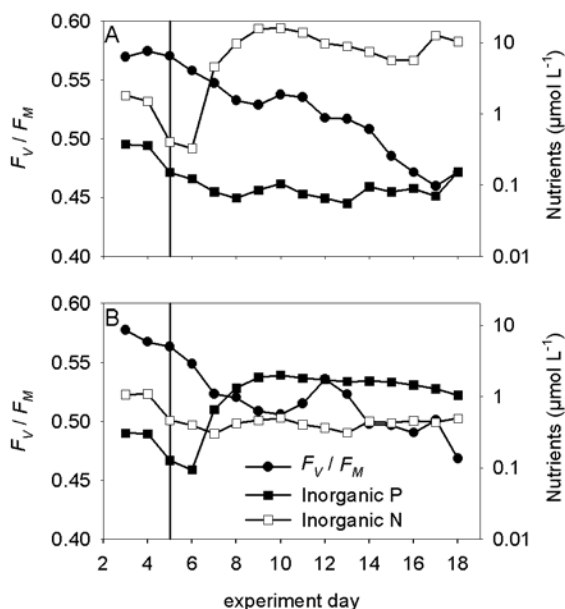
Though F_V/F_M in the different treatments did not differ significantly, it was related to other indices of nutrient limitation like particulate nutrient ratios, and the highest F_V/F_M values were found in nutrient replete samples (with nutrient ratios close to the Redfield ratio) (Fig. 19). Clearly, for P deficient cases, represented as high PON:POP and POC:POP ratios, low F_V/F_M values were observed, while N deficiency (i.e. low PON:POP and high POC:PON ratios) was not as closely related to F_V/F_M. During the experiment, N$_2$-fixing filamentous cyanobacteria dominated phytoplankton biomass, and they provided new N to the system (determined as an increase of total N in the units without N additions) (Kangro et al. 2007). This new N may leak from cyanobacteria, and thereby directly reduce N limitation of the phytoplankton community.

The interpretation of F_V/F_M during a field campaign (III) or in a mesocosm experiment (UP-III) is complex and the values alone cannot be used to predict nutrient limitation of samples. In similar manner, Parkhill et al. (2001) and Kruskopf and Flynn (2006) found that the use of variable fluo-
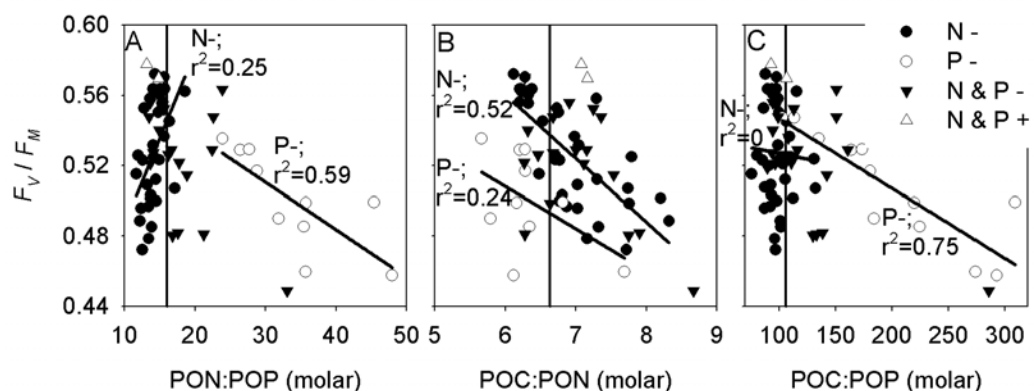

Figure 19. Relationship between F_V/F_M and particulate nutrient ratios in the different N depleted (N-, <1 µmol L^{-1}), P depleted (P-, <0.1 µmol L^{-1}), N & P depleted (N & P -)or N & P replete (N & P +) samples during a mesocosm experiment in Tvärminne, July 2003 (UP-III). Results from all 9 mesocosms are pooled. Redfield ratios are shown with vertical lines. Regression fits for N or P depleted samples are shown.

rescence as a proxy of nutrient limitation is not straightforward. Decline in F_V/F_M occurs during nutrient starvation, but not necessarily during low concentrations of nutrients when the cells have acclimated to the reduced supply of nutrients (Parkhill et al. 2001). In batch cultures, low F_V/F_M values may be obtained when nutrients are fully depleted (and internal stores are consumed), but this may not be relevant for natural systems with continuous (though sometimes low) supply of nutrients through recycling (Parkhill et al. 2001). Further, species-specific differences in the responses and effect of irradiance make the use of natural F_V/F_M variations as a measure of nutrient limitation even more challenging.

In nutrient-starved conditions, a resupply of limiting nutrient may enhance F_V/F_M. Such responses of F_V/F_M to the supply of limiting nutrient have been observed during some experiments (e.g. station 8 in Graziano et al. 1996; spring 1998 in Bergmann et al. 2002). Moore et al. (2008) found lack of response to nutrient stress relief, which may reflect a balanced nutrient-limited growth or efficient nutrient cycling.

To study physiological (F_V/F_M) and biomass (Chl*a*) responses to resupply of limiting nutrient, nutrient addition bioassays were carried out during a mesocosm study (UP-III). Simultaneous dilution experiments resolved the sources of nutrients supporting phytoplankton growth at the onset of each bioassay. During the boosting period, when mesocosm units received both N and P, we carried out two bioassays. In days 3 and 5, Chl*a* increased due to N-additions, while F_V/F_M increased only in the latter bioassay (Fig. 20). Internal N stores, supporting phytoplankton growth, were available in day 3, but not in day 5 (Fig. 21), and may explain the different patterns in the systemic Liebig-type biomass limitation (Chl*a* response) and physiological Blackman-type limitation (F_V/F_M response). After boosting period, one of the mesocosm units was enriched daily with N. Nevertheless, Chl*a* response in the bioassay at day 7 indicated N limitation for this unit, but F_V/F_M did not respond to any nutrient treatment (Fig. 20). Again, internal N stores were high during this experiment (Fig. 21). Later (days 9, 11, 14) this unit became P-limited, as indicated by positive Chl*a* and F_V/F_M responses to resupply of P (Fig. 20). In another mesocosm unit, the initial N limitation of phytoplankton community was enhanced by P additions. Bioassays indicated consistent N limitation based on Chl*a* responses (Fig. 20). Positive responses of F_V/F_M to N resupply were observed for days 7 and 11. At the onset of these bioassays there were no sources of N supporting phytoplankton growth (Fig. 21). In day 9, N sources for phytoplankton growth were not available either, and the lack of F_V/F_M response to N resupply cannot be explained. In day 14, nutrient recycling by zooplankton made N available for phytoplankton growth, which may explain the lack of F_V/F_M response (Figs. 20, 21). Overall, biomass and F_V/F_M responses to nutrient additions were similar in 7 bioassays out of 12 conducted (Fig. 20). In a similar experiment conducted in the Odense Fjord, biomass N limitation was observed in 6 cases, and 5 out of them were identified as N-limited using F_V/F_M responses, while both of the 2 P-limited situations were similarly diagnosed by biomass and F_V/F_M responses (J. Seppälä, E. Le Floc'h, R. Lignell, unpublished). To summarize the results from bioassays, the observed differences between biomass and physiological limitation were in most cases explained by the available internal nutrient sources or by nutrient recycling.

The use of variable fluorescence in probing phytoplankton physiology and nutrient limitation is not straightforward, though the results obtained here, using bioassays, are more promising than in many other sea areas (e.g. Moore et al. 2008). Variable fluorescence can provide rapid and valuable physiological information about nutrient limitation when combined with other methods (e.g. biomass responses during bioassays).
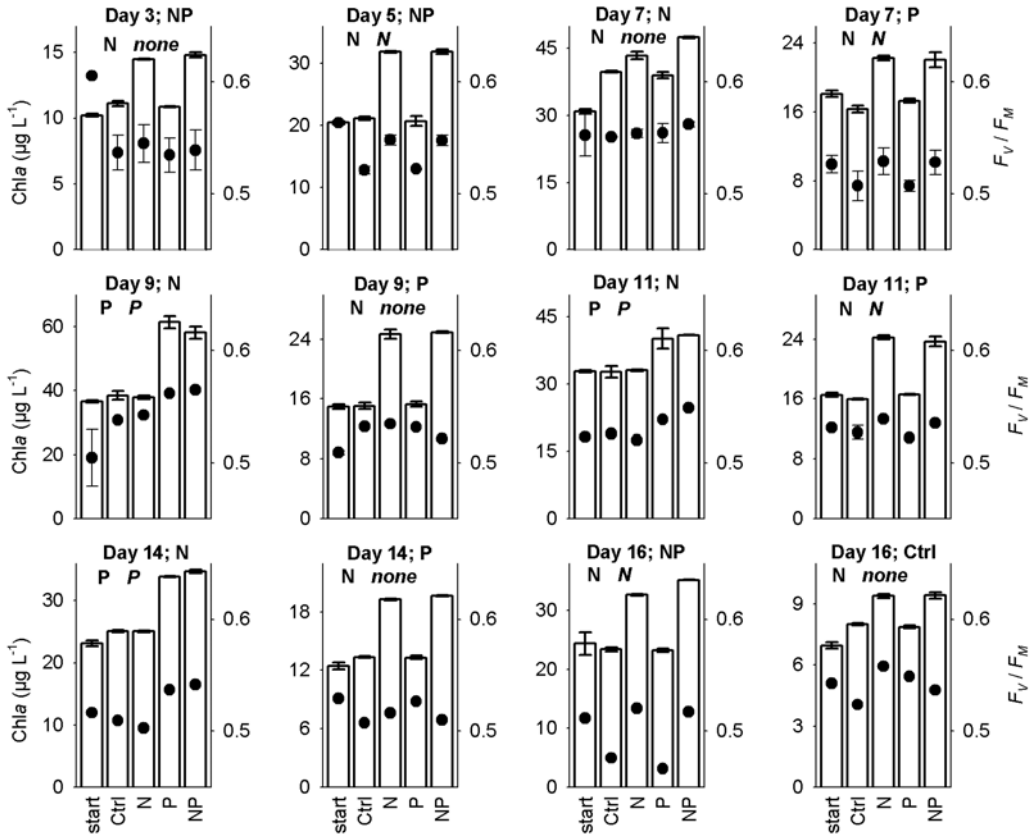
Figure 20. Nutrient addition bioassays during Tvärminne mesocosm experiment, July 2003 (UP-III). In each panel, the title gives starting day for 24-h bioassay, followed by nutrient treatment of the experimental meso-cosm unit sampled for that particular bioassay. Chl*a* (bars) and F_V/F_M (circles) were measured from initial water sample (start), and from differently manipulated (Ctrl = Control, N = addition of N, P = addition of P, NP = addition of N and P) bioassay units after 24-h incubation period. Errorbars are for standard deviation of replicate measurements. Below the title, in each panel the limiting nutrient is given in normal (Chl*a*, biomass-limitation) and italicised text (F_V/F_M, physiological limitation).

Figure 21. Different nitrogen sources (external, internal, recycled) that supported phytoplankton growth during Tvärminne mesocosm experiment, July 2003 (UP-III). The relative contributions of N supplies were estimated with dilution experiments using methods described in Lignell et al. (2003). The absence of N sources (days 7, 9 and 11 for experimental unit enriched by P) indicates strong N limitation of phytoplankton. X-labels describe the day for experiment, and nutrient treatment of the experimental mesocosm unit sampled.
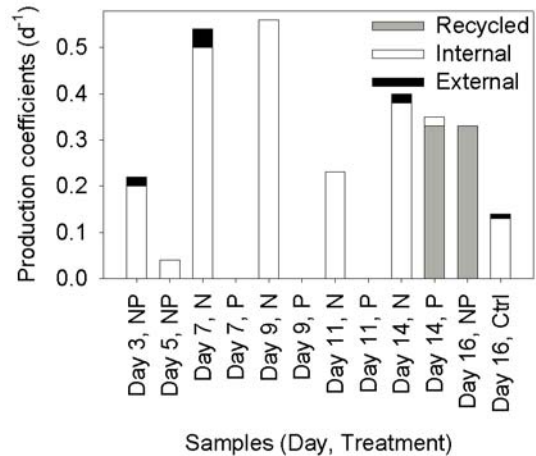
Summary of major results in 4.5

- Fast Repetition Rate fluorometry with blue excitation light was found inadequate for the detection of variable fluorescence of phycoerythrin-lacking cyanobacteria.
- Properly determined PSII absorption spectra were valuable for estimation of the maximum quantum yield of photosynthesis, without effect of photoprotective pigments.
- Seasonal changes in *in situ* variable fluorescence did not directly reflect the nutrient limitation pattern of phytoplankton, while the results from controlled environments (mesocosms) showed that during bloom events variable fluorescence changed along with other nutrient limitation indicators.
- The detection of limiting nutrient using variable fluorescence was possible during an active nutrient manipulation of phytoplankton community. In such bioassays, biomass (Chl*a*) and variable fluorescence increased in response to resupply of limiting nutrient.

5 Conclusions and future perspectives

Fluorescence-based detection of phytoplankton has become as a significant method to monitor phytoplankton in the Baltic Sea. Project Alg@line collects annually >million fluorescence records at the different subbasins of the Baltic Sea, and many research vessels are equipped with flow-through fluorometers. New field fluorometers for phycocyanin detection have been applied for the assessment of distribution of filamentous cyanobacteria in the Baltic Sea during recent years (VI). While flow-through spectral fluorometry for chemotaxonomic studies has been tested (Babichenko et al. 1999, 2000), the methold has not been used in operational monitoring. Variable fluorescence methods can be used to estimate phytoplankton production (III) and to detect phytoplankton nutrient stress, but until now these methods are still at the exploratory phase and have not been a part of Baltic Sea monitoring programmes. Fluorescence monitoring of living phytoplankton has a central role to play in future approaches to detect, monitor and forecast phytoplankton dynamics, including bloom events, in the Baltic Sea. This thesis provides some basic understanding of the state-of-the-art for these various methods, and is hopefully useful when different fluorescence techniques are used, evaluated or developed further.

Light absorption properties of PSII, reabsorption of fluoresced light, and quantum yield of fluorescence determine phytoplankton fluorescence. Each of these variables is affected by environmental factors, as shown with cultures (II, UP-I). In nature, the factors determining light absorption and fluorescence are more difficult to distinguish and quantify. In the Baltic Sea, phytoplankton absorption characteristics were related to the water column dynamics and phytoplankton community structure (III, V). Variations in the Chl*a* specific fluorescence were much more complex due to the additional effects of quantum yield of fluorescence and phytoplankton group specific differences in the photosystems (I, II, III, V, VI, UP-I).

Chl*a* fluorometers can be used for easy and quick qualitative or semiquantitative survey, to detect areas or layers with higher-than-average phytoplankton accumulations, which can be subsequently studied by other methods. Regularly, however, the desired end-product is Chl*a* concentration, derived from fluorescence signal of online instruments calibrated with known samples. The conversion from Chl*a* fluorescence intensity to Chl*a* concentration is not straightforward, and linear least squares regression could be replaced by methods, which account for the variability of Chl*a* specific fluorescence diurnally, spatially, or related to environmental factors.

During the bloom of filamentous cyanobacteria in summer in the Baltic Sea, Chl*a* fluorescence and concentration were not related, but rather fluorescence of phycocyanin explained most of the variability in Chl*a* concentrations (VI). This is explained by the very low Chl*a* specific fluorescence

of cyanobacteria, and by the relatively high share of total Chl*a* in that phytoplankton group. Thus, in summer phycocyanin fluorescence should be used as a predictor, in addition to Chl*a* fluorescence, to estimate Chl*a* concentration.

In the open Baltic Sea, phycocyanin fluorescence intensity and biomass of filamentous cyanobacteria were linearly related (VI). A successful phycocyanin monitoring should be accompanied by frequent validation with microscopy, and, if possible at some point, by measurements of phycobilin concentrations. The instrument selection is yet another concern when monitoring filamentous cyanobacteria, as several manufacturers provide fluorometers for phycocyanin detection using wavelengths shifted away from the actual fluorescence peak of phycocyanin (UP-II). The best instrument match closely to the excitation (620-630 nm) and emission (650 nm) of phycocyanin (VI).

The currently available instruments for chemotaxonomic studies have 3-5 excitation-emission wavelength-pairs. The number of wavelength-pairs should be, however, greater than the number of chemotaxonomic groups of phytoplankton to be separated. The methods based on few wavelengths are sensitive to errors from background signal, unknown fluorophores, and spectral collinearity of chemotaxonomic groups. Using spectral fluorescence can improve chemotaxonomic separation of phytoplankton. The success of spectral fluorescence to provide chemotaxonomic information, when combined with advanced chemometric method of partial least squares, was demonstrated in study VII, and in additional analysis of spectral data of natural phytoplankton community.

Derivation of phytoplankton primary production from variable fluorescence measurements requires several assumptions to be made (III). The most widespread oceanographic application of variable fluorescence, utilizing commercial FRRF, was noted inapplicable to studies of filamentous cyanobacteria from the Baltic Sea. The excitation light of this instrument does not match with the PSII absorption of PE lacking cyanobacteria (VI). Variable fluorescence provides information of the physiological state of phytoplankton community. The method can be used to detect physiological nutrient limitation, when combined with nutrient addition bioassays (UP-III).

Regardless which fluorescence approach is used, the basic requirements include frequent measurements of the instrument stability and response (using secondary standard), the subtraction of background fluorescence of particle free water collected at study site, and the prevention of biofouling. These are easily realised for instruments in laboratory, while the task is more demanding for instruments in profiling or flow-through systems. Another important requirement for successful fluorescence detection of phytoplankton is to understand the principles of fluorescence arising from living cells, which is much more complicated than fluorescence from pure pigments. After such a lesson, one realizes that interpretation of phytoplankton fluorescence signal in terms of biomass, taxonomy, physiology, or production must be done with caution. Unquestionably, this implicates that *in vivo* fluorescence based detection of phytoplankton should not be considered as an alternative for more traditional methods of pigment determinations, microscopy, or ^{14}C-based productivity. Rather, fluorescence methods should be utilized in obtaining complementary data, at very low cost, with higher temporal and spatial coverage.

6 Acknowledgements

Most of all, I wish to thank my supervisor Timo Tamminen for all the support, scientific visions, friendship, mentoring as well as trust and patience (!) during the years on the road. I thank Dr. Hugh MacIntyre for accepting the invitation to act as an opponent in the public defence of my thesis. I greatly acknowledge the comments on the thesis by reviewers Anssi Vähätalo and Tiit Kutser. Prof. Jukka Horppila guided me smoothly through university bureaucracy, thanks! The manuscript of the thesis benefited from the additional comments made by Timo, Geir, Falk and, of course by Stefan (with 199 suggestions for changes). The papers and unpublished studies in this thesis include contributions from 18 other scientists; thanks Maija, Sergey, Aina, Larisa, Alexi, Mika, Harri, Pasi, Setsi, Seija, Petri, Kalle, Geir, Edi, Falk, Emilie, Ripa & Richard! Ritvalle kiitos väitöskirjani taitosta!

Once upon a time, Setsi took me along to Tvärminne, asked me to wipe out the dust on Shimadzu and to start measuring. Since that, he has been fuelling me with scientific ideas, and is a great friend to have. In Tvärminne, I suddenly realized to be a part of a larger group, PELAG, guided by Timo. That wonderful bunch of people – Timo, Setsi, Ripa, Ansti, Kaitsu, Tapani, Pirjo, and international fellows Kalle and Tom – happily making science together (parties and football too), welcomed me warmly. I still keep on writing "PELAG" whenever labelling my new lab-gear.

Tvärminne soon became as my home ground, not only because it is a marvellous place to make research, but also due to great staff. Elina and Mervi are really out-of-this-world (hey, positively) and will always have a place in my heart; thanks for all these years in Onnela! Jouko, Raija, Lallu, Ulla, Bebbe, Totti, Svante, Marko and all others, thanks for keeping the big wheel running.

During various mesocosm experiments, when cruising at Seven Seas, or just during other work, I have had a honour of access to several great scientist, great personalities, and great friends. Ripa, my giant-hearted fellow from Onnela (it's place close to esso-bar, if you wonder), thanks for happy hours. Harri, thanks for taking care, despite all that teasing and fighting (I'm happy it was limited to football matches). Thanks to Purjo, Riitta, Sanna, Outsa, Tarja, Sirpa, Laura, Susa, Seija, Susku, Anke, Guy, Magnus, Kristian, Roope, Hermanni, Petri, and many, many others.

I would like to thank Sergey, Larisa and Aina for kindly introducing me the world of fluorescence and for the great time during common experiments and cruises. Geir, thanks for the lessons in Trondheim during the early years. The marvellous period at IOW was kindly hosted by Falk and Edi.

It was a pleasure to start working with Mika, old pal from study years, and seriously begin discovering mysteries of photochemical reactions (and some instruments too…). Mika has an admirable skill of being positive, at the moments when the experiments are failing and sky is black - thanks! Pasi came along a bit later, and was immediately ready to perform the most dedicated optical measurements. Thanks for all the clever thinking and hard work, my friend! Stefan just dropped in, with fresh ideas and clear mind. He deserves 199 thanks, and few more.

Aku, Kari (I hope there is a heaven for hardrock fellows too), Kossu and others, thanks for great times. All the folks at Valkeakoski and Juankoski, thanks for support and care.

Finally, Erika, Lauri and Siiri, my warmest thanks are to you, for love and fun.

Hey ho, lets go!

7 References

Acinas SG, Haverkamp THA, Huisman J, Stal LJ (2009) Phenotypic and genetic diversification of *Pseudanabaena* spp. (cyanobacteria). ISME journal 3: 31-46

Alpine AE, Cloern JE (1985) Differences in in vivo fluorescence yield between three phytoplankton size classes. J Plankton Res 7: 381–390

Anderson JM, Barrett J (1986) Light-harvesting pigment-protein complexes of algae. In: Staehelin LA, Arntzen CJ (eds.) Photosynthesis III. Encl Plant Phys Vol. 19, Springer-Verlag, Berlin, p 269-285

Anderson DM, Glibert PM, Burkholder JM (2002) Harmful algal blooms and eutrophication: Nutrient sources, composition, and consequences. Estuaries 25: 704–726

Babichenko S, Kaitala S, Leeben A, Poryvkina L, Seppälä J (1999) Phytoplankton pigments and dissolved organic matter distribution in the Gulf of Riga. J Mar Syst 23: 69-82

Babichenko S, Leeben A, Poryvkina L, van der Wegt R, de Vos F (2000) Fluorescent screening of phytoplankton and organic compounds in sea water. J Env Monit 2: 378-383

Babichenko S, Poryvkina L, Arikese V, Kaitala S, Kuosa H (1993) Remote sensing of phytoplankton using laser-induced fluorescence. Rem Sens Env 45: 43-50

Babin M (2008) Phytoplankton fluorescence: theory, current literature and in situ measurement. In: Babin M, Roesler CS, Cullen JJ (eds.) Real-time coastal observing systems for marine ecosystem dynamics and harmful algal blooms: Theory, instrumentation and modeling. Unesco, Paris, p 237-280

Babin M, Stramski D (2002) Light absorption by aquatic particles in the near-infrared spectral region. Limnol Oceanogr 47: 911-915

Babin M, Morel A, Claustre H, Bricaud A, Kolber Z, Falkowski PG (1996) Nitrogen- and irradiance-dependent variations of the maximum quantum yield of carbon fixation in eutrophic, mesotrophic and oligotrophic marine systems. Deep-Sea Res 43:1241-1272

Babin M, Stramski D, Ferrari GM, Claustre H, Bricaud A, Obolensky G, Hoepffner N (2003) Variations in the light absorption coefficients of phytoplankton, nonalgal particles, and dissolved organic matter in coastal waters around Europe. J Geophys Res 108: C7 3211 doi: 10.1029/2001JC000882

Babin M, Cullen JJ, Roesler CS, Donaghay PL, Doucette GJ, Kahru M, Lewis MR, Scholin CA, Sieracki ME, Sosik HM (2005) New approaches and technologies for observing harmful algal blooms. Oceanography 18: 210-227

Beardall J, Roberts S, Young E (2001) Approaches for determining phytoplankton nutrient limitation. Aquatic Sciences 63: 44–69

Behrenfeld MJ, Worthington K, Sherrell RM, Chavez FP, Strutton P, McPhaden M, Shea DM (2006) Controls on tropical Pacific Ocean productivity revealed through nutrient stress diagnostics. Nature 442: 1025–1028

Berges JA, Charlebois DO, Mauzerall DC, Falkowski PG (1996) Differential effects of nitrogen limitation on photosynthetic efficiency of photosystems I and II in microalgae. Plant Physiol 110: 689-696

Bergmann T, Richardson TL, Paerl HW, Pinckney JL, Schofield O (2002) Synergy of light and nutrients on the photosynthetic efficiency of phytoplankton populations from the Neuse River Estuary, North Carolina. J Plankton Res 24: 923-933

Beutler M, Wiltshire KH, Meyer B, Moldaenke C, Lüring C, Meyerhöfer M, Hansen U-P, Dau H (2002) A fluorometric method for the differentiation of algal populations in vivo and in situ. Photosynth Res 72: 39–53

Bidigare RR, Schofield O, Prézelin BB (1989) Influence of zeaxanthin on quantum yield of photosynthesis of *Synechococcus* clone WH7803 (DC2). Mar Ecol Prog Ser 56: 177-188

Bissett WP, Patch JS, Carder KL, Ping Lee Z (1997) Pigment packaging and Chl *a*-specific absorption in high-light oceanic waters. Limnol Oceanogr 42: 961-968

Bjørnland T (1982) Chlorophylls and carotenoids of the marine alga *Eutreptiella gymnastica*. Phytochemistry 21: 1715-1719

Bouman HA, Platt T, Sathyendranath S, Li WKW, Stuart V, Fuentes-Yaco C, Maass H, Horne EPW, Ulloa O, Lutz V, Kyewalyanga M (2003) Temperature as indicator of optical properties and community structure of marine phytoplankton: implications for remote sensing. Mar Ecol Prog Ser 258: 19-30

Braslavsky SE (2007) Glossary of terms used in photochemistry, 3rd edition (IUPAC Recommendations 2006). Pure Appl Chem 79 293-465

Bricaud A, Stramski D (1990) Spectral absorption coefficients of living phytoplankton and nonalgal biogenous matter: A comparison between the Peru upwelling area and the Sargasso Sea. Limnol Oceanogr 35: 562-582

Bricaud A, Babin M, Morel A, Claustre H (1995) Variability in the chlorophyll –specific absorption coefficients of natural phytoplankton: Analysis and parameterization. J Geophys Res 100: 13321-13332

Bricaud A, Claustre H, Ras J, Oubelkheir K (2004) Natural variability of phytoplanktonic absorption in oceanic waters: Influence of the size structure of algal populations, J Geophys Res 109: C11010, doi:10.1029/2004JC002419.

Brient L, Lengronne M, Bertrand E, Rolland D, Sipel A, Steinmann D, Baudin I, Legeas M, Le Rouzic B, Bormans M (2008) A phycocyanin probe as a tool for monitoring cyanobacteria in freshwater bodies. J Environ Monit 10: 248-255

Bryant DA (1982) Phycoerythrocyanin and phycoerythrin: properties and occurrence in cyanobacteria. J Gen Microbiol 128: 835-844

Bryant DA (1986) The cyanobacterial photosynthetic apparatus: Comparison to those of higher plants and photosynthetic bacteria. In: Platt T, Li WKW (eds.) Photosynthetic picoplankton. Can Bull Fish Aquat Sci 214: 423-500

Campbell D, Hurry V, Clarke AK, Gustafsson P, Öquist G (1998) Chlorophyll fluorescence analysis of cyanobacterial photosynthesis and acclimation. Microbiol Molec Biol Rev 62: 667-683

Ciotti ÁM, Lewis MR, Cullen JJ (2002) Assessment of the relationships between dominant cell size in natural phytoplankton communities and spectral shape of the absorption coefficient. Limnol Oceanogr 47: 404-417

Clegg RM (2006) Nuts and bolts of excitation energy migration and energy transfer. In: Papageorgiou GC, Govindjee (eds.) Chlorophyll a fluorescence. A signature of photosynthesis: Advances in Photosynthesis and Respiration, Vol.19: 83-105

Cleveland JS, Perry MJ (1987) Quantum yield, relative specific absorption and fluorescence in nitrogen limited *Chaetoceros grasilis*. Mar Biol 94: 489–497

Cleveland JS, Weidemann AD (1993) Quantifying absorption by aquatic particles: A multiple scattering correction for glass-fiber filters. Limnol Oceanogr 38: 1321-1327

Crawford DW, Lindholm T (1997) Some observations on vertical distribution and migration of the phototrophic ciliate *Mesodinium rubrum* (= *Myrionecta rubra*) in a stratified brackish inlet. Aquat Microb Ecol 13: 267-274

Cullen JJ, Ciotti ÁM, Davis RF, Lewis MR (1997) Optical detection and assessment of algal blooms. Limnol Oceanogr 42: 1223-1239

Culver ME, Perry MJ (1999) The response of photosynthetic absorption coefficient to irradiance in culture and in tidally mixed estuarine waters. Limnol Oceanogr 44: 24-36

Dandonneau Y, Neveux J (1997) Diel variations of *in vivo* fluorescence in the eastern equatorial Pacific: an unvarying pattern. Deep-Sea Res II 44:1869–1880

Darecki M, Stramski D (2004) An evaluation of MODIS and SeaWiFS bio-optical algorithms in the Baltic Sea. Rem Sens Env 89: 326-350

Davey M, Geider RJ (2001) Impact of iron limitation on the photosynthetic apparatus of the diatom *Cheatoceros muelleri* (Bacillariophyceae). J Phycol 37: 987-100

Desiderio RA, Moore C, Lantz C, Cowles TJ (1997) Multiple excitation fluorometer for *in situ* oceanographic applications. Appl Opt 36: 1289-1296

Dubelaar GBJ, Geerders PJF, Jonker RR (2004) High frequency monitoring reveals phytoplankton dynamics. J Environ Monit 6: 946–952

Dubelaar GBJ, Gerritzen PL, Beeker AER, Jonker RR, Tangen K (1999) Design and first results of CytoBuoy: A wireless flow cytometer for in situ analysis of marine and fresh waters. Cytometry 37: 247–254

Eker-Develi E, Berthon JF, van der Linde D (2008) Phytoplankton class determination by microscopic and HPLC-CHEMTAX analyses in the southern Baltic Sea. Mar Ecol Prog Ser 359: 69-87

Elmgren R (2001) Understanding human impact on the Baltic ecosystem: changing views in recent decades. Ambio 30: 222-231

Falkowski PG (2006) Tracing oxygen's imprint on Earth's metabolic evolution. Science 311: 1724-1725

Falkowski P, Kiefer DA (1985) Chlorophyll *a* fluorescence in phytoplankton: relationship to photosynthesis and biomass. J Plankton Res 7: 715-731

Falkowski PG, LaRoche J (1991) Acclimation to spectral irradiance in algae. J Phycol 27: 8-14

Falkowski PG, Raven JA (2007). Aquatic Photosynthesis (2nd edition). Princeton University Press, Princeton

Finni T, Kononen K, Olsonen R, Wallström K (2001) The history of cyanobacterial blooms in the Baltic Sea. Ambio 30: 172-178

Flemer DA, (1969) Continuous measurement of *in vivo* chlorophyll of a dinoflagellate bloom in Chesapeake Bay. Chesapeake Science 10: 99-103

Frank HA, Chynwat V, Desamero RZB, Farhoosh R, Erickson J, Bautista J (1997) On the photophysics and photochemical properties of carotenoids and their role as light-harvesting pigments in photosynthesis. Pure Appl Chem 69: 2117-2124

Gaevsky NA, Kolmakov VI, Anishchenko OV, Gorbaneva TB (2005) Using DCMU-fluorescence method for the identification of dominant phytoplankton groups. J Appl Phycol 17: 483–494

Geider RJ, Osborne BA (1992) Algal photosynthesis. Chapman & Hall, New York

Geider RJ, LaRoche J, Greene RM, Olaizola M (1993) Response of the photosynthetic apparatus of *Phaeodactylum tricornutum* (Bacillariophyceae) to nitrate, phosphate, or iron starvation. J Phycol 29: 755-766

Geider RJ, MacIntyre HL, Graziano LM, McKay RML (1998) Responses of the photosynthetic apparatus of *Dunaliella tertiolecta* (Chlorophyceae) to nitrogen and phosphorus limitation. Eur J Phycol 33: 315-332

Gerhardt V, Bodemer U (2000) Delayed fluorescence excitation spectroscopy: a method for determining phytoplankton composition. Arch Hydrobiol Spec Issues Advanc Limnol 55: 101–119

Graziano, LM, Geider RJ. Li WKW, Olaizola M (1996) Nitrogen limitation of North Atlantic phytoplankton: Analysis of physiological condition in nutrient enrichment experiments. Aquat Microb Ecol 11: 53–64

Green BR, Durnford DG (1996) The chlorophyll-carotenoid proteins of oxygenic photosynthesis. Ann Rev Plant Phys Plant Mol Biol 47, 685-714

Haardt H, Maske H (1987) Specific in vivo absorption coefficient of chlorophyll *a*. Limnol Oceanogr 32: 608-619

Hajdu S, Höglander H, Larsson U (2007) Phytoplankton vertical distributions and composition in Baltic Sea cyanobacterial blooms. Harmful Algae 6: 189–205

Hancke TB, Hancke K, Johnsen G, Sakshaug E (2008) Rate of O_2 production derived from pulse-amplitude-modulated fluorescence: testing three biooptical approaches against measured O_2-production rate. J Phycol 44: 803–813

Helcom (2004) Checklist of Baltic Sea phytoplankton species. Baltic Sea Environment Proceedings No. 95

Henrion R, Henrion G, Böhme M, Behrendth (1997) Three-way principal component analysis for fluorescence spectroscopic classification of algal species. Fresenius J Anal Chem 357: 522-526

Hou JJ, Huang BQ, Cao ZR, Chen JX, Hong HS (2007) Effects of nutrient limitation on pigments in *Thalassiosira weissflogii* and *Prorocentrum donghaiense*. J Integr Plant Biol 49: 686−697

Hällfors G, Hällfors S (1992), The Tvärminne collection of algal cultures. Tvärminne Studies 5: 15–17

Izydorczyk K, Tarczynska M, Jurczak T, Mrowczynski J, Zalewski M (2005) Measurement of phycocyanin fluorescence as an online early warning system for cyanobacteria in reservoir intake water. Env Toxicol 20: 425-430

Janson S, Carpenter EJ, Bergman B (1994) Fine structure and immunolocalisation of proteins in *Aphanizomenon* sp. from the Baltic Sea. Eur J Phycol 29: 203-211

Jeffrey SW (1997) Application of pigment methods to oceanography. In: Jeffrey SW, Mantoura RFC, Wright SW (eds.) Phytoplankton Pigments in Oceanography: Guidelines to Modern Methods, UNESCO, Paris, p. 127-166

Jeffrey SW, Humphrey GF (1975) New spectrophotometric equations for determining chlorophylls *a*, *b*, c_1 and c_2 in higher plants, algae and natural populations. Biochem Physiol Pflanzen 167: 191-194

Jeffrey SW, Vesk M (1997) Introduction to marine phytoplankton and their pigment signatures. In: Jeffrey SW, Mantoura RFC, Wright SW (eds.) Phytoplankton Pigments in Oceanography: Guidelines to Modern Methods, UNESCO, Paris, p. 37-84

Jeffrey SW, Welschmeyer NA (1997) Spectrophotometric and fluorometric equations in common use in oceanography. In: Jeffrey SW, Mantoura RFC, Wright SW (eds.) Phytoplankton Pigments in Oceanography: Guidelines to Modern Methods, UNESCO, Paris, p. 597-615

Jerlov NG (1968) Optical oceanography. Elsevier, Amsterdam.

Johnsen G, Sakshaug E (1993) Bio-optical characteristics and photoadaptive responses in the toxic and bloom-forming dinoflagellates *Gyrodinium aureolum*, *Gymnodinium galatheanum*, and two strains of *Prorocentrum minimum*. J Phycol 29: 627-642

Johnsen G, Sakshaug E (1996) Light harvesting in bloom-forming marine phytoplankton: species-specifity and photoacclimation. In: Figueroa FL, Jiménez C, Pérez-Lloréns JL, Niell FX (eds.) Underwater light and algal photobiology, Scientia Marina 60 (Supl. 1): 47-56

Johnsen G, Sakshaug E (2007) Biooptical characteristics of PSII and PSI in 33 species (13 pigment groups) of marine phytoplankton, and the relevance for pulse-amplitude-modulated and fast-repetition-rate fluorometry. J Phycol 43: 1236-1251

Johnsen G, Prézelin BP, Jovine RVM (1997) Fluorescence excitation spectra and light utilization in two red tide dinoflagellates. Limnol Oceanogr 42: 1166-1177

Johnsen G, Nelson NB, Jovine RVM, Prézelin BB (1994a) Chromoprotein- and pigment-dependent modeling of spectral light absorption in two dinoflagellates, *Prorocentrum minimum* and *Heterocapsa pygmaea*. Mar Ecol Prog Ser 114: 245-258

Johnsen G, Samset O, Granskog L, Sakshaug E (1994b) *In vivo* absorption characteristics in 10 classes of bloom-forming phytoplankton: taxonomic characteristics and responses to photoadaptation by means of discriminant and HPLC analysis. Mar Ecol Prog Ser 105: 149-157

Jovine RVM, Johnsen G, Prézelin B (1995) Isolation of membrane bound light-harvesting-complexes from the dinoflagellates *Heterocapsa pygmaea* and *Prorocentrum minimum*. Photosynth Res 44: 127-138

Kahru M, Nômmann S (1990) The phytoplankton spring bloom in the Baltic Sea in 1985, 1986: multitude of spatiotemporal scales. Cont Shelf Res 10: 329-354

Kahru M, Savchuk OP, Elmgren R (2007) Satellite measurements of cyanobacterial bloom frequency in the Baltic Sea: interannual and spatial variability. Mar Ecol Prog Ser 343: 15-23

Kaitala S, Babichenko S, Poryvkina L, Leeben A (1994) Fluorescent analysis of pigment composition of natural phytoplankton. Mar Tech Soc J 28: 50-58

Kaitala S, Seppälä J, Raateoja M, Hällfors S, Fleming-Lehtinen V, Maunula P, Helminen J, Ylöstalo P (2008) Recent advances in ferrybox monitoring on board FINNMAID ferry. US/EU-Baltic International Symposium, 2008 IEEE/OES. Issue, 27-29 May 2008: 1-5.

Kalivas JH, Lang PM (1994) Mathematical analysis of spectral orthogonality. Marcel Dekker Inc., New York.

Kangro K, Olli K, Tamminen T, Lignell R (2007) Species-specific responses of a cyanobacteria-dominated phytoplankton community to artificial nutrient limitation in the Baltic Sea. Mar Ecol Prog Ser 336: 15-27

Kiang NY, Siefert J, Govindjee, Blankenship RE (2007) Spectral signatures of photosynthesis. I. Review of Earth organisms. Astrobiol 7: 222-251

Kiefer DA (1973a) Fluorescence properties of natural phytoplankton populations. Mar Biol 22: 263-269

Kiefer DA (1973b) Chlorophyll *a* fluorescence in marine centric diatoms: responses of chloroplasts to light and nutrient stress. Mar Biol 23: 39-46

Kirk JTO (1994) Light and photosynthesis in aquatic ecosystems (2nd edition) Cambridge University Press, Cambridge

Kolber ZS, Prášil O, Falkowski PG (1998) Measurements of variable chlorophyll fluorescence using fast repetition rate techniques: defining methodology and experimental protocols. Biochim Biophys Acta 1367: 88-106

Kolber, Z, Zehr J, Falkowski P (1988) Effects of growth irradiance and nitrogen limitation on photosynthetic energy conversion in photosystem II. Plant Physiol 88: 923-929

Konovalov BV, Belyayeva GA, Bekasova OD, Kosakowska A (1990) Light-absorbing capacity of phytoplankton in the Gulf of Gdansk in May, 1987. Oceanologia 28: 25-37

Kopf U, Heinze J (1984) 2,7-Bis-(diethylamino) phenazoxonium chloride as a quantum counter for emission measurements between 240 and 700 nm. Anal Chem 56: 1931–1935

Kromkamp JC, Forster RM (2003) The use of variable fluorescence measurements in aquatic ecosystems: differences between multiple and single turnover measuring protocols and suggested terminology. Eur J Phycol 38: 103-112

Kruskopf M, Flynn KJ (2006) Chl content and fluorescence responses cannot be used to gauge reliably phytoplankton biomass, nutrient status or growth rate. New Phytol 169: 525–536

Kuparinen J, Kuosa H (1993) Autotrophic and heterotrophic picoplankton in Baltic Sea. Adv Mar Biol 29: 73-128

Kutser T (2004) Quantitative detection of chlorophyll in cyanobacterial blooms by satellite remote sensing. Limnol Oceanogr 49: 2179-2189

Kutser T, Metsamaa L, Strömbeck N, Vahtmäe E (2006) Monitoring cyanobacterial blooms by satellite remote sensing. Est Coast Shelf Sci 67: 303-312

Küpper H, Seibert S, Parameswaran A (2007). A fast, sensitive and inexpensive alternative to analytical pigment HPLC: quantification of chlorophylls and carotenoids in crude extracts by fitting with Gauss-peak spectra. Anal Chem 79: 7611-7627

Laamanen MJ (1997) Environmental factors affecting the occurrence of different morphological forms of cyanoprokaryotes in the northern Baltic Sea. J Plankton Res 19: 1385-1403

Laamanen MJ, Gugger MF, Lehtimäki JM, Haukka K, Sivonen K (2001) Diversity of toxic and nontoxic *Nodularia* isolates (cyanobacteria) and filaments from the Baltic Sea. Appl Env Microbiol 67: 4638–4647

Lakowicz JR (1999) Principles of fluorescence spectroscopy (2nd edition). Kluwer Academic / Plenum Publishers, New York.

Lawson CL, Hanson BJ (1974) Solving least squares problems. Prentice-Hall, Englewood Cliffs.

Leboulanger C, Dorigo U, Jacquet S, Le Berre B, Paolini G, Humbert JF (2002) Application of a submersible spectrofluorometer for rapid monitoring of freshwater cyanobacterial blooms: a case study. Aquat Microb Ecol 30: 83–89

Lee T, Tsuzuki M, Takeuchi T, Yokoyama K, Karube I (1994) *In vivo* fluorometric method for early detection of cyanobacterial waterblooms. J Appl Phycol 6: 489-495

Lewis MR (2008) Measurement of apparent optical properties for diagnosis of harmful algal blooms In: Babin M, Roesler CS, Cullen JJ (eds.) Real-time coastal observing systems for marine ecosystem dynamics and harmful algal blooms: Theory, instrumentation and modeling. Unesco, Paris, p 207-236

Lignell R, Seppälä J, Kuuppo P, Tamminen T, Andersen T, Gismervik I (2003) Beyond bulk properties: Responses of coastal summer plankton communities to nutrient enrichment in the northern Baltic Sea. Limnol Oceanogr 48: 189-209

Lindholm T, Mörk AC (1989) Symbiontic algae and plastids in planktonic ciliates. Memoranda of Societas pro Fauna et Flora Fennici 65: 17-22

Loftus ME, Seliger HH (1975) Some limitations of the *in vivo* fluorescence technique. Chesapeake Science 16: 79-92

Lohrenz SE, Weidemann AD, Tuel M (2003) Phytoplankton spectral absorption as influenced by community size structure and pigment composition. J Plankton Res 25: 35-61

Lorenzen CJ (1966) A method for continuous measurement of *in vivo* chlorophyll concentration. Deep-Sea Res 13: 223-227

Lotze HK, Lenihan HS, Bourque BJ, Bradbury RH, Cooke RG, Kay MC, Kidwell SM, Kirby MX, Peterson CH, Jackson JBC (2006) Depletion, degradation, and recovery potential of estuaries and coastal seas. Science 312: 1806-1809

Lutz VA, Sathyendranath S, Head EJH, Li WKW (2001) Changes in the *in vivo* absorption and fluorescence excitation spectra with growth irradiance in three species of phytoplankton. J Plankton Res 23: 555-569

Lutz VA, Sathyendranath S, Head EJH, Li WKW (2003) Variability in pigment composition and optical characteristics of phytoplankton in the Labrador Sea and the Central North Atlantic. Mar Ecol Prog Ser 260: 1-18

MacIntyre HL, Kana TM, Anning T, Geider RJ (2002) Photoacclimation of photosynthesis irradiance response curves and photosynthetic pigments in microalgae and cyanobacteria. J Phycol 38:17-38

Mackey MD, Mackey DJ, Higgins HW, Wright SW (1996) CHEMTAX - A program for estimating class abundances from chemical markers: Application to HPLC measurements of phytoplankton. Mar Ecol Prog Ser 144: 265– 283

Martens H, Næs T (1989) Multivariate calibration. John Wiley & Sons, Chichester

Maxwell K, Johnson GN (2000) Chlorophyll fluorescence – a practical guide. J Exp Botany 51: 659-668

Metsamaa L, Kutser T, Strömbeck N (2006) Recognising cyanobacterial blooms based on their optical signature: a modelling study. Boreal Env Res 11: 493–506

Meyer-Harms B, Pollehne F (1998) Alloxanthin in *Dinophysis norvegica* (Dinophysiales, Dinophyceae) from the Baltic Sea. J Phycol 34: 280-285

Millie DF, Schofield OME, Kirkpatrick GJ, Johnsen G, Evens TJ (2002) Using absorbance and fluorescence spectra to discriminate microalgae. Eur J Phycol 37: 313-322

Millie DF, Schofield OM, Kirkpatrick GJ, Johnsen G, Tester PA, Vinyard BT (1997) Detection of harmful algal blooms using photopigments and absorption signatures: A case study of the Florida red tide dinoflagellate, *Gymnodinium breve*. Limnol Oceanogr 45: 1240-1251

Mimuro M (1990) Excitation energy flow in the photosynthetic pigment systems: structure and energy transfer mechanism. Bot Mag Tokyo 103: 233–253

Mitchell BG, Kiefer DA (1988) Chlorophyll *a* specific absorption and fluorescence excitation spectra for light limited phytoplankton. Deep Sea Res 35: 639–663

Moberg L, Karlberg B (2001) Validation of multivariate calibration method for the determination of chlorophyll *a*, *b* and *c* and their corresponding pheopigments. Anal Chim Acta 450: 143-153

Moberg L, Robertson G, Karlberg B (2001) Spectrofluorometric determination of chlorophylls and pheopigments using parallel factor analysis. Talanta 54: 161-170

Moore CM, Mills MM, Langlois R, Milne A, Achterberg EP, La Roche J, Geider RJ (2008) Relative influence of nitrogen and phosphorus availability on phytoplankton physiology and productivity in the oligotrophic sub-tropical North Atlantic Ocean. Limnol Oceanogr 53: 291-305

Morel A, Bricaud A (1986) Inherent optical properties of algal cells including picoplankton: theoretical and experimental results. In: Platt T, Li WKW (eds.) Photosynthetic picoplankton. Canadian Bulletin of Fisheries and Aquatic Sciences 214: 521-559

Mulligan HF, Kingsbury JM (1968) Application of an electronic particle counter in analyzing natural populations of phytoplankton. Limnol Oceanogr 13: 499-506

Müller P, Li XP, Niyogi KK (2001) Non-photochemical quenching. A response to excess light energy. Plant Physiol 125: 1558–1566

Neori A, Vernet M, Holm-Hansen O, Haxo FT (1988) Comparison of chlorophyll far-red fluorescence spectra with photosynthetic oxygen action spectra for photosystem II in algae. Mar Ecol Prog Ser 44: 297-302

Neveux J, Lantoine F (1993) Spectrofluorometric assay of chlorophylls and pheophytins using the least squares approximation technique. Deep-Sea Res 40: 1747-1765

Neveux J, Seppälä J, Dandonneau Y (2009) Recent developments in spectroscopic methods for the analysis of pigment extracts. In Roy S, Egeland ES, Johnsen G, Llewellyn C, Wright S (eds.) Phytoplankton pigments in oceanography – *Vol 2*. submitted.

Neveux J, Tenório MMB, Dupouy C, Villareal TA (2006) Spectral diversity of phycoerythrins and diazotroph abundance in tropical waters. Limnol Oceanogr 51: 1689–1698

Niiranen S (2008) Phycoerythrin fluorescence-based operative monitoring of the Baltic Sea picocyanobacteria. MSc -thesis, University of Helsinki, Aquatic Sciences

Oi VT, Glazer, AN, Stryer L (1982) Fluorescent phycobiliprotein conjugates for analyses of cells and molecules. J Cell Biol 93: 981-986

Oldham PB, Zillioux EJ, Warner IM (1985) Spectral 'fingerprinting' of phytoplankton populations by twodimensional fluorescence and Fourier-transform-based pattern recognition. J Mar Res 43: 893–906

Olli K, Heiskanen AS, Seppälä J (1996) Development and fate of *Eutreptiella gymnastica* bloom in nutrient enriched enclosures in the coastal Baltic Sea. J Plankton Res 18: 1587–1604

Olson RJ, Sosik HM (2007) A submersible imaging-in-flow instrument to analyze nano- and microplankton: Imaging FlowCytobot. Limnol Oceanogr Methods 5:195-203

Owens TG (1991) Energy transformation and fluorescence in photosynthesis. NATO ASI Series G27: 101–137

Owens TG, Gallagher JC, Alberte RS (1987) Photosynthetic light-harvesting function of violaxanthin in *Nannochloropsis* spp. (Eustigmatophyceae). J Phycol 23: 79–85

Palenik B (2001) Chromatic adaptation in marine *Synechococcus* strains. Appl Environ Microbiol 67: 991-994

Parkhill J, Maillet G, Cullen J (2001) Fluorescence-based maximal quantum yield for PSII as a diagnostic of nutrient stress. J Phycol 37: 517–529

Parsons TR, Strickland JDH (1963) Discussion of spectrophotometric determination of marine plant pigments with revised equations for ascertaining chlorophylls and carotenoids. J Mar Res 21:155-163

Pick FR (1991) The abundance and composition of freshwater picocyanobacteria in relation to light penetration. Limnol Oceanogr 36: 1457–1462

Platt T (1972) Local phytoplankton abundance and turbulence. Deep-Sea Res 19: 183-187

Poryvkina L, Babichenko S, Kaitala S, Kuosa H, Shalapjonok A (1994) Spectral fluorescence signatures in the characterization of phytoplankton community composition. J Plankton Res 16: 1315-1327

Raateoja MP (2004) Fast repetition rate fluorometer (FRRF) measuring phytoplankton productivity: A case study at the entrance to the Gulf of Finland, Baltic Sea. Boreal Env Res 9: 263-276

Raateoja MP, Seppälä J (2001) Light utilization and photosynthetic efficiency of *Nannochloris* sp. (Chlorophyceae) approached by spectral absorption characteristics and fast repetition rate fluorometry (FRRF). Boreal Env Res 6: 205-220

Raateoja M, Seppälä J, Kuosa H, Myrberg K (2005) Recent changes in the productive state of the SW Finnish coast in the Baltic Sea. Ambio: 34: 188-191

Rantajärvi E (ed.) (2003) Alg@line in 2003: 10 years of innovative plankton monitoring and research and operational information service in the Baltic Sea. Meri – Report Series of the Finnish Institute of Marine Research No. 48

Raven JA, Falkowski PG (1999) Oceanic sinks for atmospheric CO2. Plant, Cell and Environment 22: 741-755

Reynolds C (2006) The ecology of phytoplankton. Cambridge University Press, Cambridge

Rowan KS (1989) Photosynthetic pigments of algae. Cambridge University Press, New York

Ruiz-Verdú A, Simis SGH, de Hoyos C, Gons HJ, Peña-Martínez R (2008) An evaluation of algorithms for the remote sensing of cyanobacterial biomass. Rem Sens Env 112: 3996-4008

Röttgers R, Häse C, Doerffer R (2007) Determination of the particulate absorption of microalgae using a point-source integrating-cavity absorption meter: verification with a photometric technique, improvements for pigment bleaching, and correction for chlorophyll fluorescence. Limnol Oceanogr Methods 5: 1-12

Sakshaug E, Johnsen G, Andresen K, Vernet M (1991) Modeling of light-dependent algal photosynthesis and growth: experiments with Barents Sea diatoms *Thalassiosira nordenskioeldii* and *Chaetoceros furcellatus*. Deep-Sea Res 38: 415-430

Sakshaug E, Bricaud A, Dandonneau Y, Falkowski PG, Kiefer DA, Legendre L, Morel A, Parslow J, Takahashi M (1997) Parameters of photosynthesis: definitions, theory and interpretation of results. J Plankton Res 19: 1637-1670

Salonen K, Sarvala J, Järvinen M, Langenberg V, Nuottajärvi M, Vuorio K, Chitamwebwa DBR (1999). Phytoplankton in Lake Tanganyika - vertical and horizontal distribution of *in vivo* fluorescence. Hydrobiologia 407: 89-103

Sathyendranath S, Cota G, Stuart V, Maass H, Platt T (2001) Remote sensing of phytoplankton pigments: a comparison of empirical and theoretical approaches. Int J Remote Sensing 22: 249-273

Schiewer U (2008) Ecology of Baltic coastal waters. Springer, Berlin.

Schlüter L, Garde K, Kaas H (2004) Detection of the toxic cyanobacteria *Nodularia spumigena* by means of a 4-keto-myxoxanthophyll-like pigment in the Baltic Sea. Mar Ecol Prog Ser 275: 69–78

Schofield O, Grzymski J, Bissett WP, Kirkpatrick GJ, Millie DF, Moline M, Roesler CS (1999) Optical monitoring and forecasting systems for harmful algal blooms: possibility or pipe dream. J Phycol 35: 1477-1496

Scholin CA, Doucette GJ, Cembella AD (2008) Prospects for developing automated systems for *in situ* detection of harmful algae and their toxins. In: Babin M, Roesler CS, Cullen JJ (eds.) Real-time coastal observing systems for marine ecosystem dynamics and harmful algal blooms: Theory, instrumentation and modeling. Unesco, Paris, p 413-462

Sciandra A, Lazzara L, Claustre H, Babin M (2000) Responses of growth rate, pigment composition and optical properties of *Cryptomonas* sp. to light and nitrogen stresses. Mar Ecol Prog Ser 201: 107–120

Serra T, Borrego C, Quintana X, Calderer L, López R, Colomer J (2009) Quantification of the effect of nonphotochemical quenching on the determination of in vivo Chl a from phytoplankton along the water column of a freshwater reservoir. Photochem Photobiol 85: 321-331

Sidler WA 1994. Phycobilisome and phycobiliprotein structures. In Bryant DA (Ed.), The molecular biology of cyanobacteria. Kluwer, Amsterdam, pp. 139-216

Sieracki CK, Sieracki ME, Yentsch CS (1998) An imaging-in-flow system for automated analysis of marine microplankton. Mar Ecol Prog Ser 168: 285-296

Simis SGH, Peters SWM, Gons HJ (2005). Remote sensing of the cyanobacterial pigment phycocyanin in turbid inland water. Limnol Oceanogr 50: 237-245

SooHoo JB, Kiefer DA, Collins DJ, McDermid IS (1986) *In vivo* fluorescence excitation and absorption spectra of marine phytoplankton: I. Taxonomic characteristics and responses to photoadaptation. J Plankton Res 8: 197–214

Sosik HM (2008) Characterizing seawater constituents from optical properties. In: Babin M, Roesler CS, Cullen JJ (eds.) Real-time coastal observing systems for marine ecosystem dynamics and harmful algal blooms: Theory, instrumentation and modeling. Unesco, Paris, p 281-329

Sosik HM, Mitchell BG (1991) Absorption, fluorescence, and quantum yield for growth in nitrogen-limited *Dunaliella tertiolecta*. Limnol Oceanogr 36: 910-921

Sosik HM, Mitchell BG (1995) Light absorption by phytoplankton pigments and detritus in the California Current System. Deep-Sea Res 42: 1717-1748

Sosik HM, Olson RJ (2007) Automated taxonomic classification of phytoplankton sampled with imaging-in-flow cytometry. Limnol Oceanogr Methods 5: 204-216

Stal LJ, Albertano P, Bergman B, von Bröckel K, Gallon JR, Hayes PK, Sivonen K, Walsby AE (2003) BASIC: Baltic Sea cyanobacteria. An investigation of the structure and dynamics of water blooms of cyanobacteria in the Baltic Sea - responses to a changing environment. Cont Shelf Res 23: 1695-1714

Stomp M, Huisman J, Vörös L, Pick FR, Laamanen M, Haverkamp T, Stal LJ (2007) Colourful coexistence of red and green picocyanobacteria in lakes and seas. Ecol Letters 10: 290–298

Stoń J, Kosakowska A (2000) Qualitative and quantitative analysis of Baltic phytoplankton pigments. Oceanologia 42: 449-471

Stramski D, Reynolds RA (1993) Diel variations in the optical properties of a marine diatom. Limnol Oceanogr 38:1347-1364

Strass V (1990) On the calibration of largescale fluorometric chlorophyll measurements from towed undulating vehicles. Deep Sea Res 37: 525–540

Stæhr PA, Cullen JJ (2003) Detection of *Karenia mikimotoi* by spectral absorption signatures. J Plankton Res 25: 1237-1249

Suggett DJ MacIntyre HL, Geider RJ (2004) Evaluation of biophysical and optical determinations of light absorption by photosystem II in phytoplankton. Limnol Oceanogr Methods 2: 316-332

Suggett DJ, Oxborough K, Baker, NR, MacIntyre HL, Kana, TM, Geider RJ (2003) Fast repetition rate and pulse amplitude modulation chlorophyll *a* fluorescence measurements for assessment of photosynthetic electron transport in marine phytoplankton. Eur J Phycol 38: 371-384

Tandeau de Marsac N (1977) Occurrence and nature of chromatic adaptation in cyanobacteria. J Bacteriol 130: 82-91

Tassan S, Ferrari GM (1995) An alternative approach to absorption measurements of aquatic particles retained on filters. Limnol Oceanogr 40: 1358-1368

Tassan S, Ferrari GM (2002) A sensitivity analysis of the 'Transmittance–Reflectance' method for measuring light absorption by aquatic particles. J Plankton Res 24: 757-774

Ting CS, Rocap G, King J, Chisholm SW (2002) Cyanobacterial photosynthesis in the oceans: the origins and significance of divergent light-harvesting strategies. Trends in Microbiology 10: 134-142

Tikkanen T (1986) Kasviplanktonopas. Suomen Luonnonsuojelun Tuki Oy, Helsinki.

Trygg J (2004) Prediction and spectral profile estimation in multivariate calibration. J Chemom 18: 166–172

Udenfriend S. (1962) Fluorescence assay in biology and medicine. Academic Press, New York.

Utermöhl H (1958) Zur Vervollkommnung der quantitativen Phytoplanktonmethodik. Mitteilungen der Internationale Vereiningung für Theoretische und Angewandte Limnologie 9: 1-38

Vepsäläinen J, Pyhälahti T, Rantajärvi E, Kallio K, Pertola S, Stipa T, Kiirikki M, Pulliainen J, Seppälä J (2005) The combined use of optical remote sensing data and unattended flow-through fluorometer measurements in the Baltic Sea. Int J Remote Sens 26: 261-282

Vesk M, Dibbayawan TP, Vesk PA (1996) Immunogold localization of phycoerythrin in chloroplasts of *Dinophysis acuminata* and *D. fortii* (Dinophysiales, Dinophyta). Phycologia 35: 234-238

Vincent WF (1983) Fluorescence properties of the freshwater phytoplankton: three algal classes compared. Br Phycol. J 18: 5–21

Vitousek PM, Mooney HA, Lubchenco J, Melillo JM (1997) Human domination of Earth's ecosystems. Science 277: 494-499

Watras CJ, Baker AL (1988) Detection of planktonic cyanobacteria by tandem *in vivo* fluorometry. Hydrobiologia 169: 77-84.

Wold S, Sjöström M, Eriksson L (2001). PLS-regression: a basic tool of chemometrics. Chemom Intell Lab Syst 58: 109–130

Wood AM, Phinney DA, Yentsch CS (1998) Water column transparency and the distribution of spectrally distinct forms of phycoerythrin-containing organisms. Mar Ecol Prog Ser 162: 25-31

Wright, SW, Mantoura RFC (1997) Guidelines for collection and pigment analysis of field samples. In: Jeffrey SW, Mantoura RFC, Wright SW (eds.) Phytoplankton Pigments in Oceanography: Guidelines to Modern Methods, UNESCO, Paris, p. 429-445

Wyman M (1992) An in vivo method for the estimation of phycoerythrin concentrations in marine cyanobacteria (*Synechococcus* spp.) Limnol Oceanogr 37: 1300-1306

Wyman M, Gregory RPF, Carr NG (1985) Novel role for phycoerythrin in a marine cyanobacterium, *Synechococcus* Strain DC2. Science 15: 818-820

Wänstrand I, Snoeijs P (2006) Phytoplankton community dynamics assessed by ships-of-opportunity sampling in the northern Baltic Sea: A comparison of HPLC pigment analysis and cell counts. Est Coast Shelf Sci 66: 135-146

Yentsch, CS (1962) Measurement of visible light absorption by particulate matter in the ocean. Limnol Oceanogr 7: 207-217

Yentsch CS, Menzel DW (1963) A method for determination of phytoplankton chlorophyll and phaeophytin by fluorescence. Deep-Sea Res 10: 221-231

Yentsch CS, Phinney DA (1985) Spectral fluorescence: an ataxonomic tool for studying the structure of phytoplankton populations. J Plankton Res 7: 617–632

Yentsch CS, Yentsch CM (1979) Fluorescence spectral signatures: the characterization of phytoplankton populations by the use of excitation and emission spectra. J Mar Res 37: 471-483

Yentsch, CM, Horan PK, Muirhead K, Dortch Q, Haugen E, Legendre L, Murphy LS, Perry MJ, Phinney DA, Pomponi SA, Spinrad RW, Wood M, Yentsch CS, Zahuranec BJ, (1983) Flow cytometry and cell sorting: A technique for analysis and sorting of aquatic particles. Limnol Oceanogr 28: 1275-1280

Zhang QQ, Lei SH, Wang XL, Wang L, Zhu CJ (2006) Discrimination of phytoplankton classes using characteristic spectra of 3D fluorescence spectra. Spectrochimica Acta Part A 63: 361–369